SUSY explanation of lepton g-2 and exotic searches at LHC and beyond

Kazuki Sakurai
(University of Warsaw)

[**arXiv:2001.05980**]: **D.Felea, J.Mamuzic, R.Maselek, N.E.Mavromatos, V.A.Mitsou, J.L.Pinfold, R.Ruiz de Austri, A.Santrai, O.Vives**

JHEP 1912 (2019) 017 [**arXiv:1910.04761**]: **A. Papaefstathiou, S.Plätzer**

JHEP 1910 (2019) 024 [**arXiv:1908.03607**]: **M.Badziak**

20/01/2020 Seminar at IPMU, Kashiwa

Contents

- SUSY explanation for lepton g-2 anomalies
- Novel long-lived particle searches by MoEDAL
- EW sphaleron productions at hadron colliders
- Conclusion

Muon and Electron g-2

- A long standing muon g-2 anomaly:

$$\Delta a_\mu \equiv a_\mu^{\rm exp} - a_\mu^{\rm SM} = (2.74 \pm 0.73) \times 10^{-9}$$

T. Blum, et al ‘18
BNL ‘06

~ 3.7 σ

- The electron g-2 is one of the most precisely measured quantities:

$$a_e^{\rm exp} = 0.00115965218073(28)$$

D.Hanneke, S.Fogwell,
G.Gabrielse ‘08

- The latest theoretical calculation of electron g-2 includes 5-loop QED contributions and the main uncertainty comes from the error on $\alpha_{\rm EM}$

- Recently the most precise measurement for $\alpha_{\rm EM}$ is carried out

$$\alpha_{\rm EM}^{-1} = 137.035999046(27)$$

R.H.Parker, C.Yu, W.Zhong,
B.Estey, H.Müller ‘18

- This leads

$$a_e^{\rm SM} = 0.00115965218161(23)$$

$$\boxed{\Delta a_e \equiv a_e^{\rm exp} - a_e^{\rm SM} = -\,(8.8 \pm 3.6) \times 10^{-13}}$$

~ 2.4 σ

Muon and Electron g-2

- **3.7-σ anomaly in muon g-2**

$$\vec{\mu} = g \left(\frac{e}{2m} \right) \vec{s}$$

$$\Delta a_\mu \equiv a_\mu^{\rm exp} - a_\mu^{\rm SM} = (2.74 \pm 0.73) \times 10^{-9}$$

$$a_\ell = \frac{g-2}{2}$$

- **2.4-σ anomaly in electron g-2**

$$\mathcal{L}_{\rm eff} = i \frac{a_\ell}{m_\ell} \cdot \bar{\psi} \sigma^{\mu\nu} \psi F_{\mu\nu}$$

$$\Delta a_e \equiv a_e^{\rm exp} - a_e^{\rm SM} = -(8.8 \pm 3.6) \times 10^{-13}$$

Observation tells: $$\frac{m_\mu^2}{m_e^2} \frac{\Delta a_e}{\Delta a_\mu} \sim -14$$

- **magnitude**
- **sign**

Any flavour blind new physics predict: $$\frac{m_\mu^2}{m_e^2} \frac{a_e^{\rm NP}}{a_\mu^{\rm NP}} \sim 1$$

flavour violating NP is necessary

- Smuon-Selectron mass splitting is difficult

$$\mathbf{Y} \longrightarrow \mathbf{Y}^{\mathrm{diag}} = V_L^\dagger \mathbf{Y} V_R$$

$$\begin{pmatrix} m_1^2 & \\ & m_2^2 \end{pmatrix} \xrightarrow{V^\dagger \mathbf{m}^2 V} \begin{pmatrix} m_1'^2 & \Delta \\ \Delta & m_2'^2 \end{pmatrix}$$

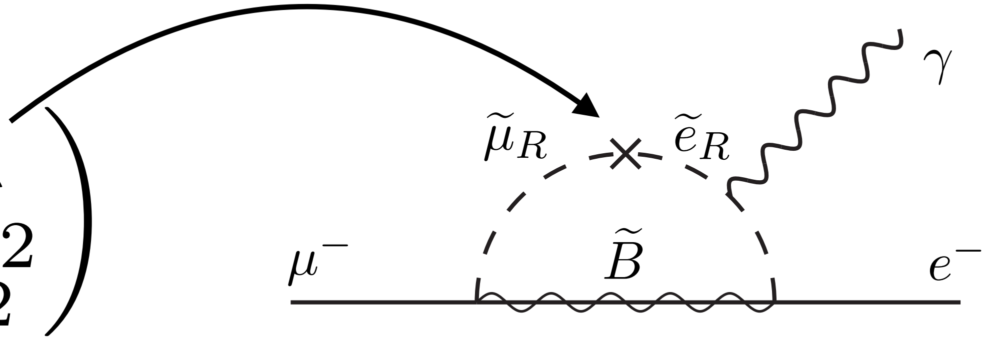

too large contribution to μ→eγ

Higgs mediation

SUSY breaking

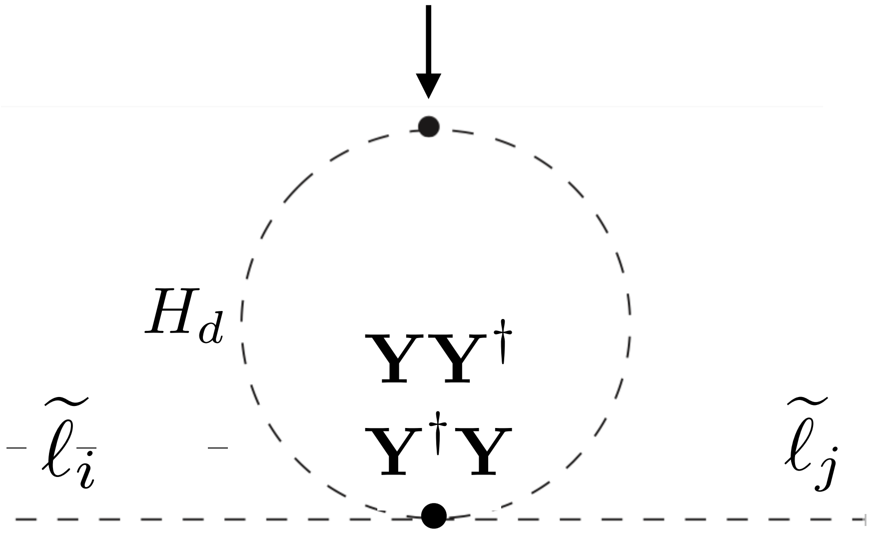

usual diagonal contribution (gravity, GMSB, AMSB, ..)

Higgs mediation contribution

$$\widetilde{\mathbf{m}}^2_L = m^2_L \cdot \mathbf{1} + m^2_H \cdot Y_\mu^{-2} \cdot \mathbf{Y}\mathbf{Y}^\dagger$$

$$\widetilde{\mathbf{m}}^2_R = m^2_R \cdot \mathbf{1} + m^2_H \cdot Y_\mu^{-2} \cdot \mathbf{Y}^\dagger\mathbf{Y}$$

$$\mathbf{Y} \longrightarrow \mathbf{Y}^{\text{diag}} = V_L^\dagger \mathbf{Y} V_R$$

$$\widetilde{\mathbf{m}}_L \longrightarrow (\widetilde{\mathbf{m}}^2_L)^{\text{diag}} = V_L^\dagger \widetilde{\mathbf{m}}^2_L V_L$$

$$\widetilde{\mathbf{m}}^2_R \longrightarrow (\widetilde{\mathbf{m}}^2_R)^{\text{diag}} = V_R^\dagger \widetilde{\mathbf{m}}^2_R V_R$$

soft mass matrices can be diagonalised together with Yukawa

Bino contribution

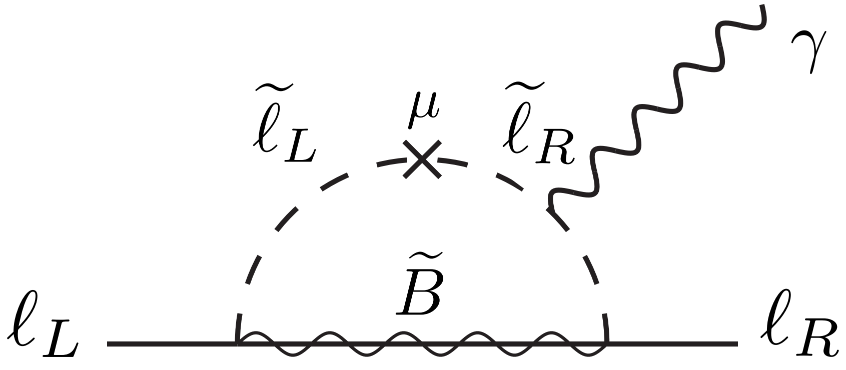

$\gg$

(for light sleptons)

Chargino cotr.

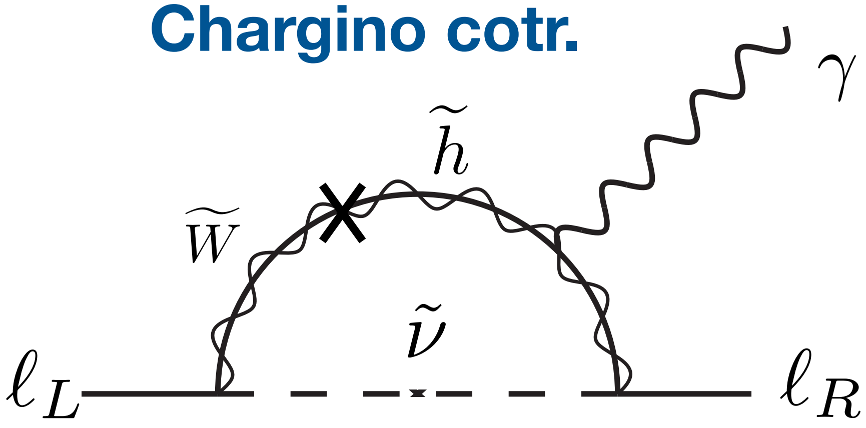

$$a_\ell^0 \propto \frac{\mu M_1}{m^2_{\tilde\ell_L} m^2_{\tilde\ell_R}}$$

$$a_\ell^\pm \propto \frac{\mu M_2}{m^2_{\tilde\chi_1^\pm} m^2_{\tilde\ell_L}}$$

take M1 < 0, M2 >0 $\longrightarrow$ $a_\ell^0 < 0$ $a_\ell^\pm > 0$

take small selectron mass $\longrightarrow$ $|a_e^0| \gg |a_e^\pm|$ $\longrightarrow$ $a_e^{\rm SUSY} < 0$

take large smuon mass $\longrightarrow$ $|a_\mu^0| \ll |a_\mu^\pm|$ $\longrightarrow$ $a_\mu^{\rm SUSY} > 0$

M. Badziak, KS, 1908.03607

$$R_l^{\chi^\pm/\chi^0} = \frac{2a_l^{\chi^\pm/\chi^0} - \Delta a_l}{2\sigma_l}$$

$$m^2_{\tilde{E}_1} = m^2_R\,, \qquad m^2_{\tilde{L}_1} = m^2_L\,,$$

$$m^2_{\tilde{E}_2} = m^2_R + m^2_H \qquad m^2_{\tilde{L}_2} = m^2_L + m^2_H$$

$$R_l^{\mathrm{SUSY}} = \frac{a_l^{\mathrm{SUSY}} - \Delta a_l}{\sigma_l} = R_l^{\chi^\pm} + R_l^{\chi^0}$$

$\tan\beta = 60,\ M_1 = -130\,\mathrm{GeV},\ M_2 = 130\,\mathrm{GeV},\ \mu = 800\,\mathrm{GeV},\ m_L = 130\,\mathrm{GeV},\ m_R = 130\,\mathrm{GeV},$

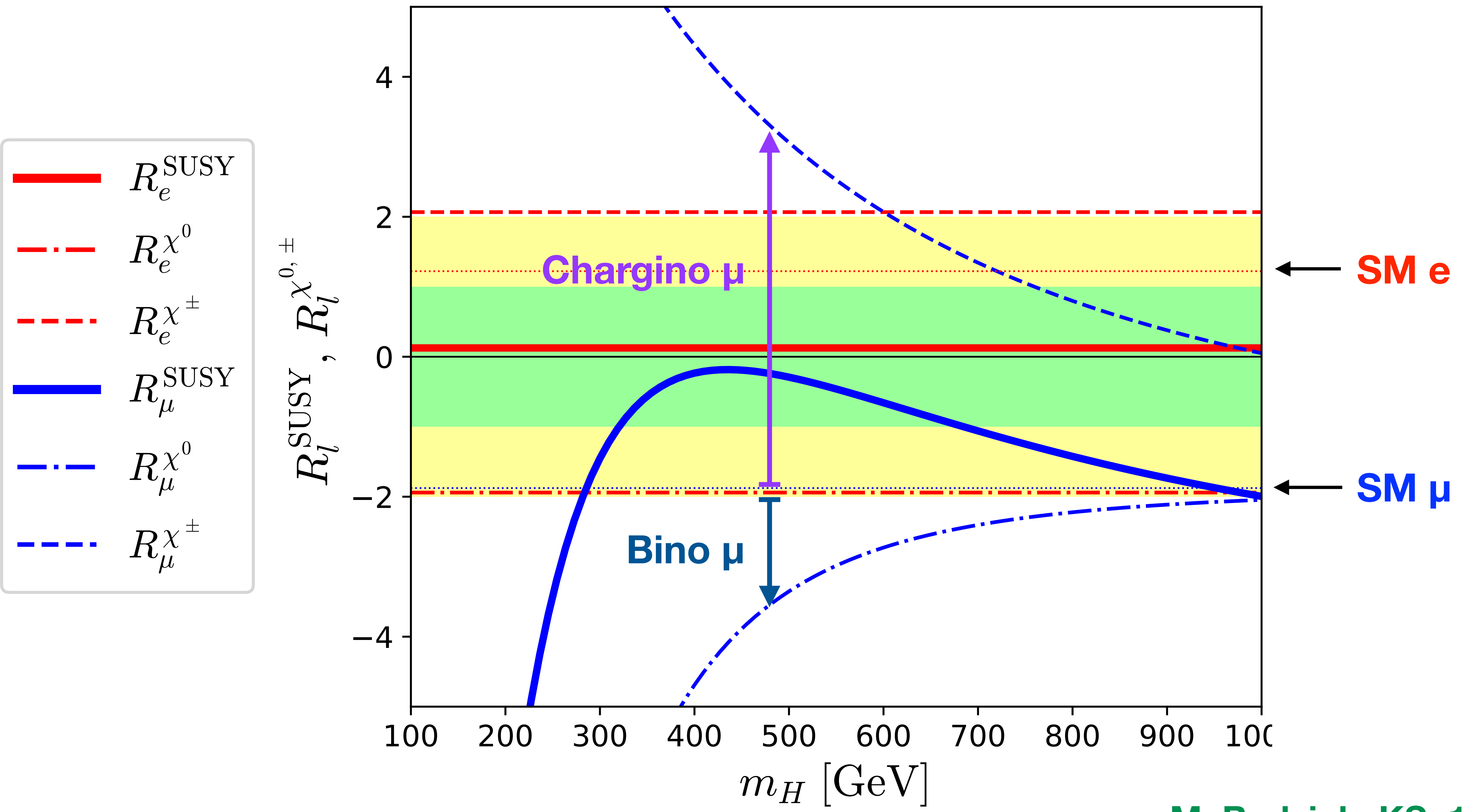

M. Badziak, KS, 1908.03607

Favoured Regions

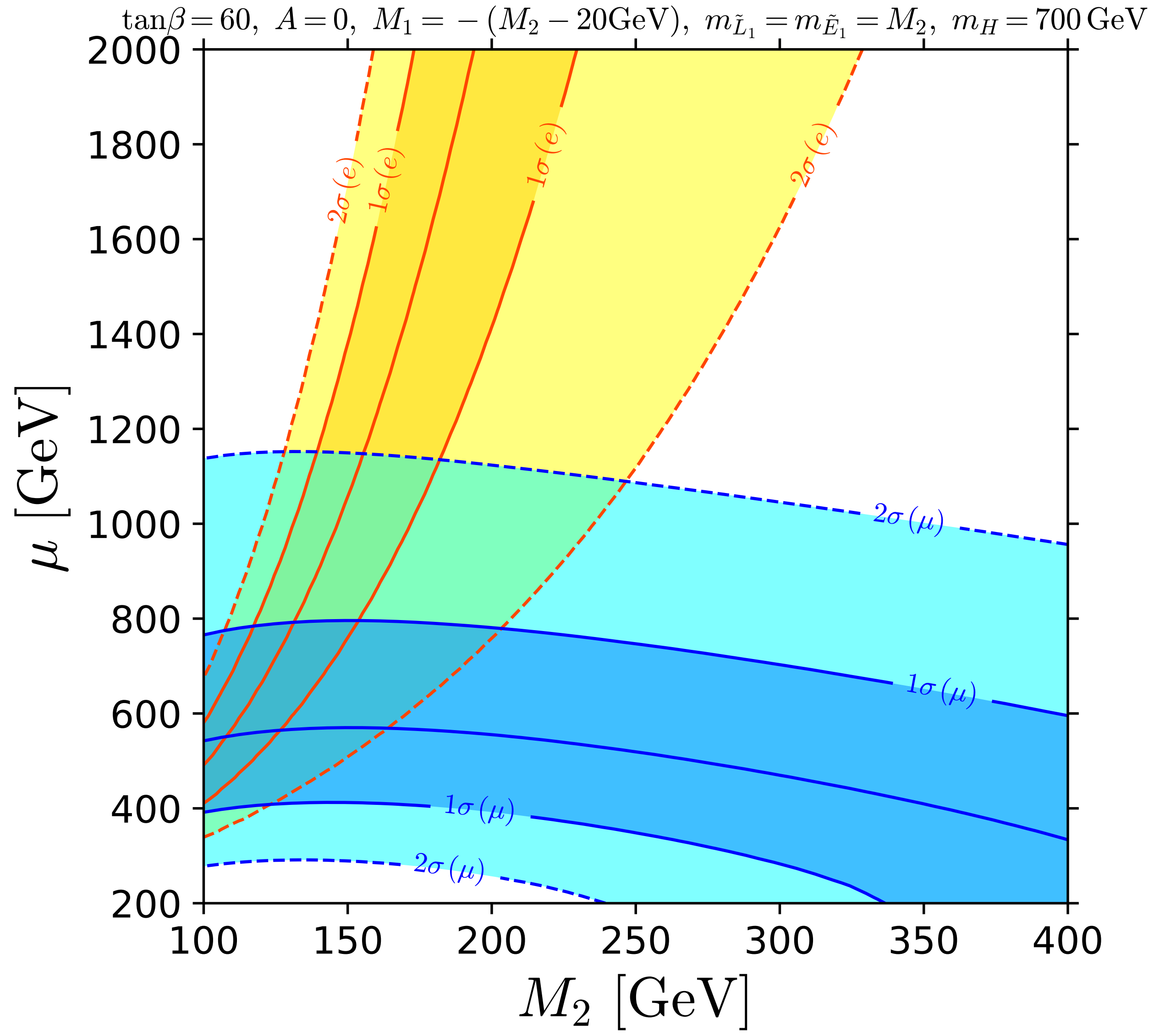

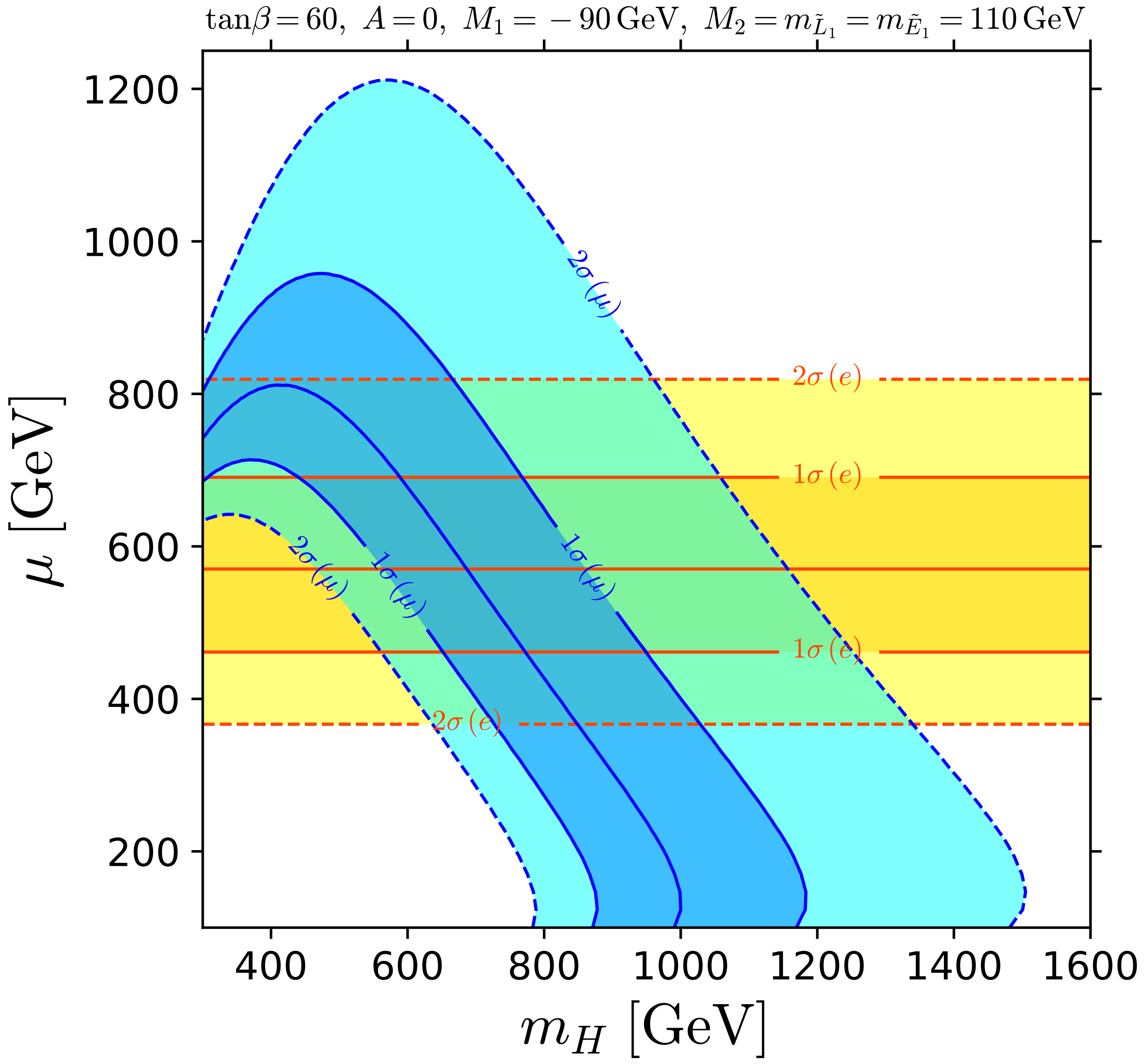

M. Badziak, KS, 1908.03607

LHC constraint

- physical masses

$\tilde{\chi}_1^0$	121.2	$\tilde{\nu}_e$	124.7	$\tilde{\nu}_\mu$	711	$\tilde{\chi}_3^0$	711.9
$\tilde{\chi}_2^0$	123.5	$\tilde{e}_L$	147.3	$\tilde{\mu}_L$	715.3	$\tilde{\chi}_4^0$	713.3
$\tilde{\chi}_1^\pm$	123.5	$\tilde{e}_R$	127.9	$\tilde{\mu}_R$	711.6	$\tilde{\chi}_2^\pm$	715.7

- Benchmark point

$$M_1 = -125\,\mathrm{GeV}, \quad M_2 = 118\,\mathrm{GeV}, \quad m_R = 120\,\mathrm{GeV}, \quad m_L = 140\,\mathrm{GeV},$$

$$m_H = 700\,\mathrm{GeV}, \quad \mu = 700\,\mathrm{GeV}, \quad A = 0, \quad \tan\beta = 60,$$

- g-2 prediction

$$a_e^{\mathrm{SUSY}} = -6.71 \cdot 10^{-13}, \quad R_e^{\mathrm{SUSY}} = 0.58, \quad (a_e^{\tilde{\chi}_1^0}, a_e^{\tilde{\chi}_1^\pm}) = (-10.170,\ 3.459) \cdot 10^{-13},$$

$$a_\mu^{\mathrm{SUSY}} = 2.21 \cdot 10^{-9}, \quad R_\mu^{\mathrm{SUSY}} = -0.73, \quad (a_\mu^{\tilde{\chi}_1^0}, a_\mu^{\tilde{\chi}_1^\pm}) = (-0.336,\ 2.544) \cdot 10^{-9},$$

M. Badziak, KS, 1908.03607

LHC constraint

- **physical masses**

$\tilde{\chi}_1^0$	121.2	$\tilde{\nu}_e$	124.7	$\tilde{\nu}_\mu$	711	$\tilde{\chi}_3^0$	711.9
$\tilde{\chi}_2^0$	123.5	$\tilde{e}_L$	147.3	$\tilde{\mu}_L$	715.3	$\tilde{\chi}_4^0$	713.3
$\tilde{\chi}_1^\pm$	123.5	$\tilde{e}_R$	127.9	$\tilde{\mu}_R$	711.6	$\tilde{\chi}_2^\pm$	715.7

mode		BR [%]
$\tilde{\chi}_1^\pm$	$\to \tilde{\chi}_1^0 \nu_e e^\pm$	100
$\tilde{\chi}_2^0$	$\to \tilde{\chi}_1^0 \gamma$	12
	$\to \tilde{\chi}_1^0 \nu_e \bar{\nu}_e$	88

invisible

ATLAS-CONF-2019-014

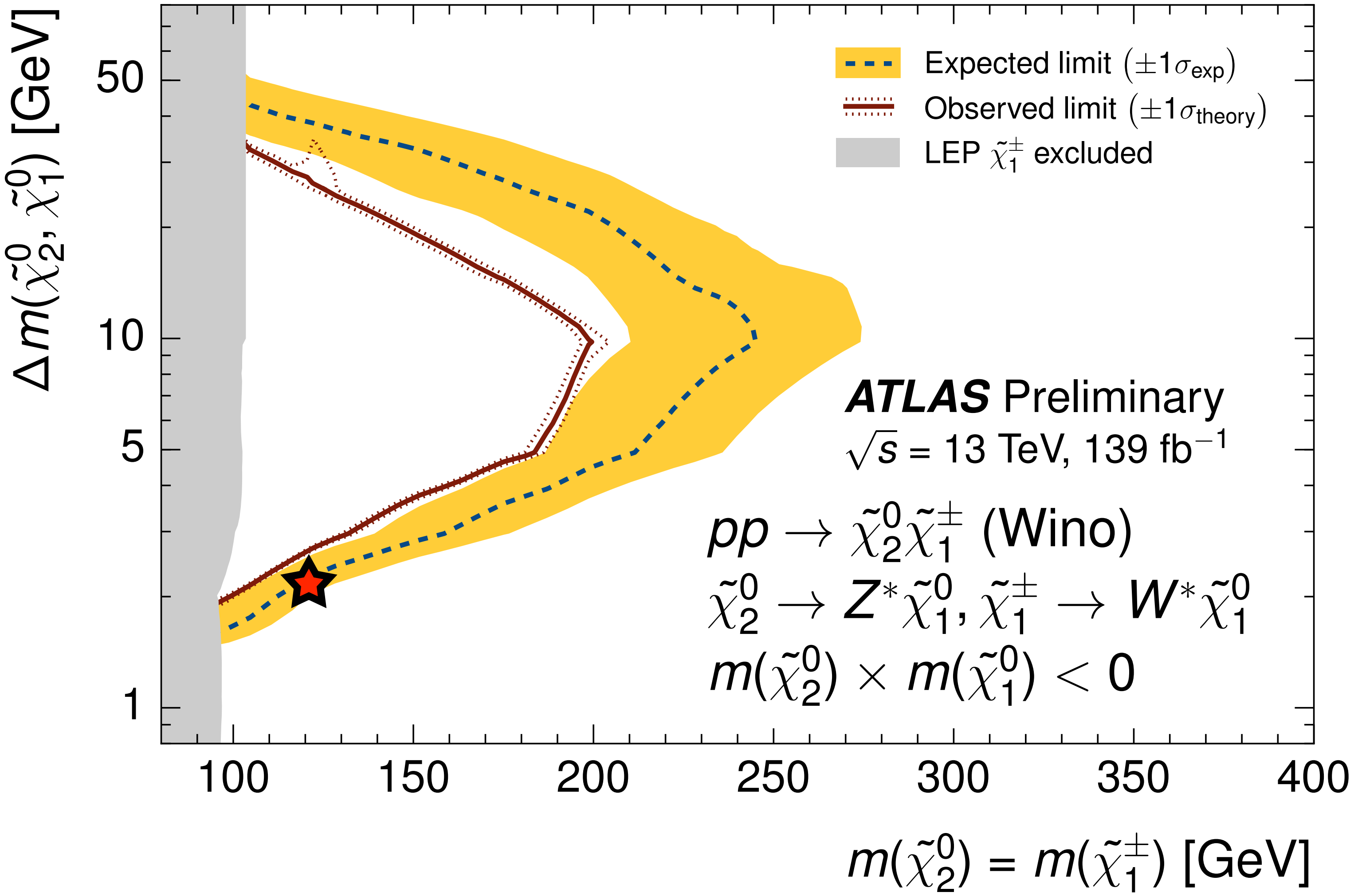

LHC constraint

- **physical masses**

$\tilde{\chi}_1^0$	121.2	$\tilde{\nu}_e$	124.7	$\tilde{\nu}_\mu$	711	$\tilde{\chi}_3^0$	711.9
$\tilde{\chi}_2^0$	123.5	$\tilde{e}_L$	147.3	$\tilde{\mu}_L$	715.3	$\tilde{\chi}_4^0$	713.3
$\tilde{\chi}_1^\pm$	123.5	$\tilde{e}_R$	127.9	$\tilde{\mu}_R$	711.6	$\tilde{\chi}_2^\pm$	715.7

$\tilde{e}_R^\pm$	$\rightarrow \tilde{\chi}_1^0 e^\pm$	100
$\tilde{e}_L^\pm$	$\rightarrow \tilde{\chi}_1^\pm \nu_e$	59
	$\rightarrow \tilde{\chi}_2^0 e^\pm$	30
	$\rightarrow \tilde{\chi}_1^0 e^\pm$	11
$\tilde{\nu}_e$	$\rightarrow \tilde{\chi}_1^\pm e^\mp$	36
	$\rightarrow \tilde{\chi}_2^0 \nu_e$	18
	$\rightarrow \tilde{\chi}_1^0 \nu_e$	47

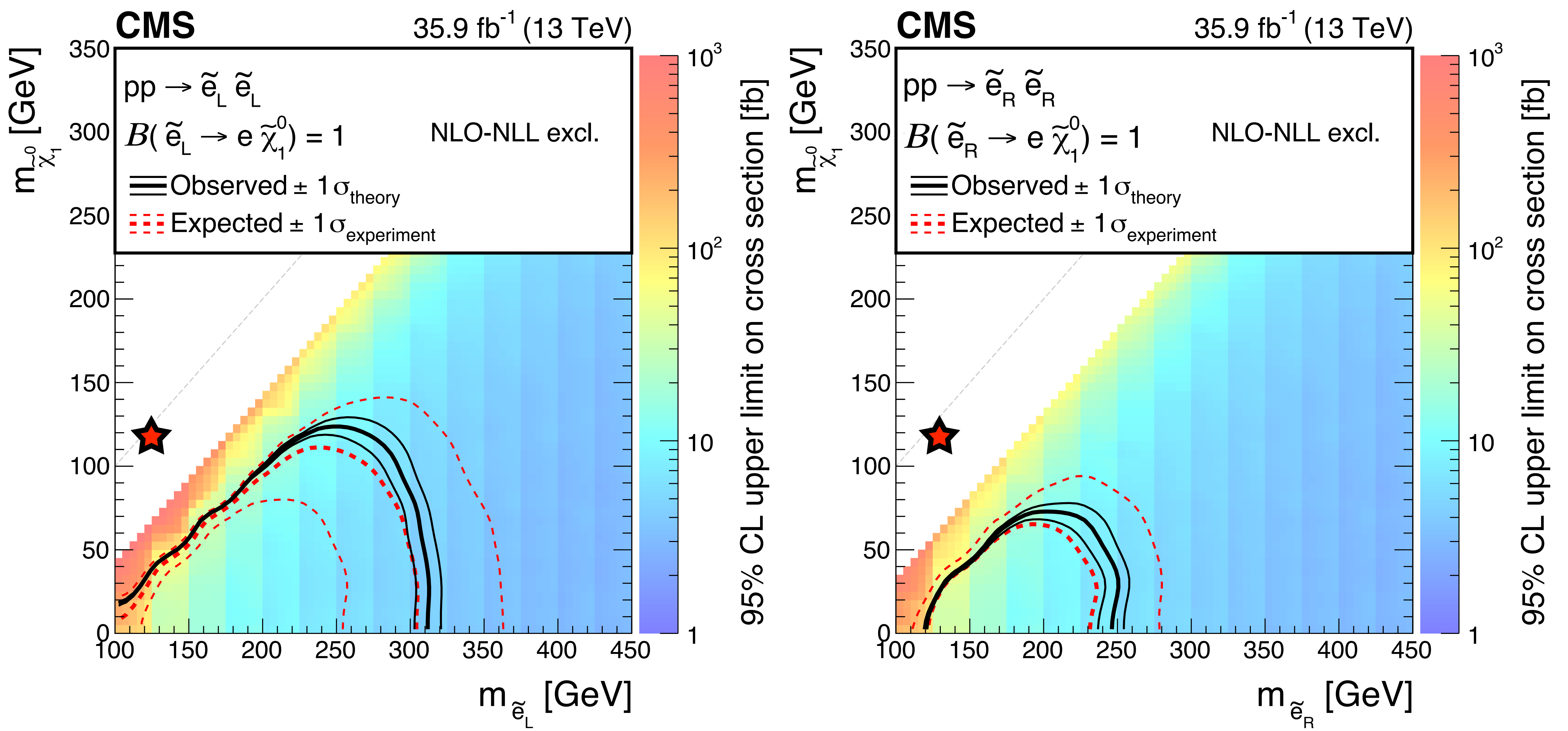

LHC constraint

$\tilde{\chi}_1^0$	121.2	$\tilde{\nu}_e$	124.7	$\tilde{\nu}_\mu$	711	$\tilde{\chi}_3^0$	711.9
$\tilde{\chi}_2^0$	123.5	$\tilde{e}_L$	147.3	$\tilde{\mu}_L$	715.3	$\tilde{\chi}_4^0$	713.3
$\tilde{\chi}_1^\pm$	123.5	$\tilde{e}_R$	127.9	$\tilde{\mu}_R$	711.6	$\tilde{\chi}_2^\pm$	715.7

- physical masses

$\tilde{\mu}_R^\pm$	$\to \tilde{\chi}_1^0 \mu^\pm$	100
$\tilde{\mu}_L^\pm$	$\to \tilde{\chi}_1^\pm \nu_\mu$	60
	$\to \tilde{\chi}_2^0 \mu^\pm$	30
	$\to \tilde{\chi}_1^0 \mu^\pm$	10
$\tilde{\nu}_\mu$	$\to \tilde{\chi}_1^\pm \mu^\mp$	61
	$\to \tilde{\chi}_2^0 \nu_\mu$	30
	$\to \tilde{\chi}_1^0 \nu_\mu$	10

ATLAS-CONF-2019-008

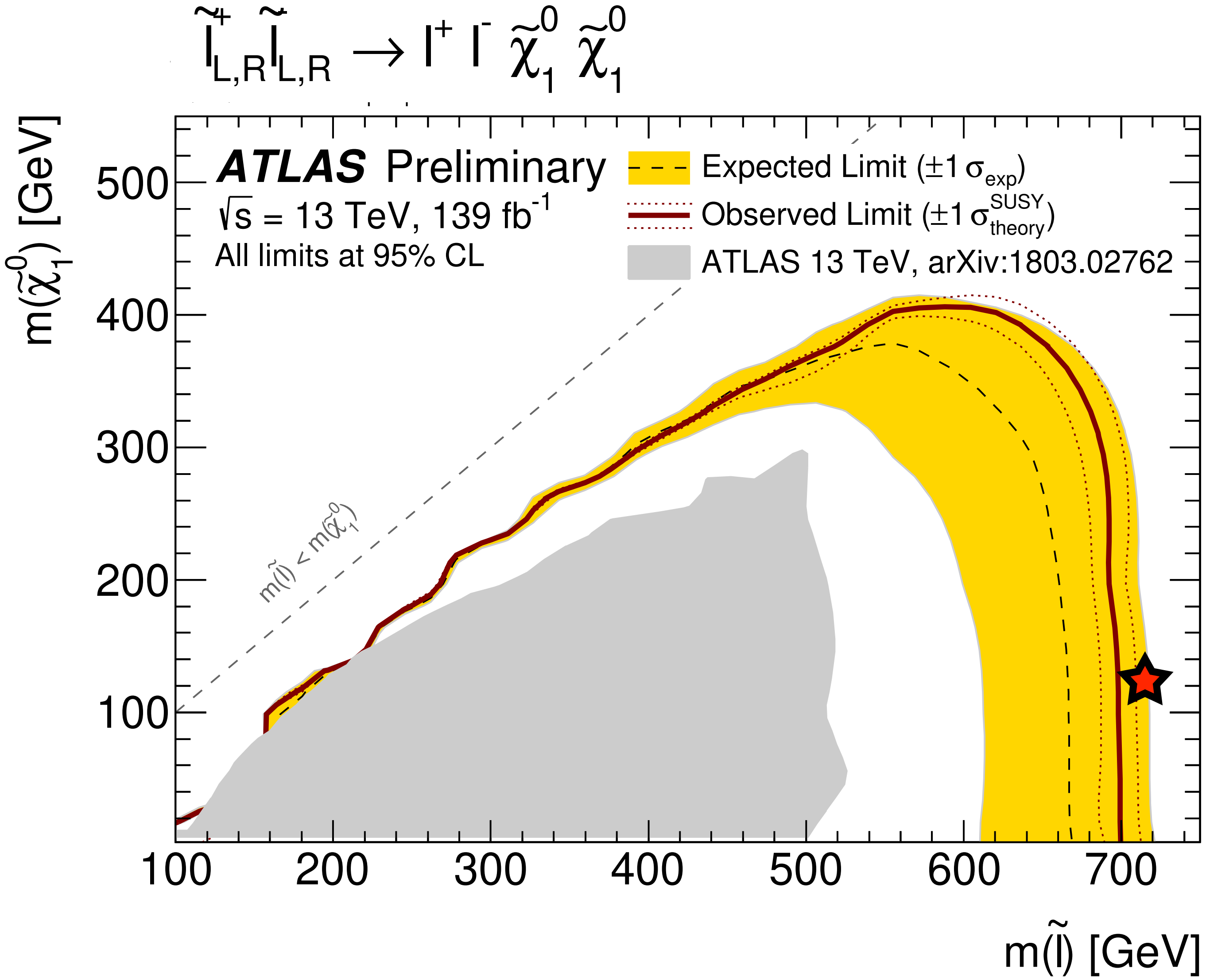

LHC constraint

- **physical masses**

$\tilde{\chi}_1^0$	121.2	$\tilde{\nu}_e$	124.7	$\tilde{\nu}_\mu$	711	$\tilde{\chi}_3^0$	711.9
$\tilde{\chi}_2^0$	123.5	$\tilde{e}_L$	147.3	$\tilde{\mu}_L$	715.3	$\tilde{\chi}_4^0$	713.3
$\tilde{\chi}_1^\pm$	123.5	$\tilde{e}_R$	127.9	$\tilde{\mu}_R$	711.6	$\tilde{\chi}_2^\pm$	715.7

mode		BR [%]
$\tilde{\chi}_3^0$	$\to \tilde{\chi}_1^\pm W^\mp$	59
	$\to \tilde{\chi}_2^0 Z$	20
	$\to \tilde{\chi}_1^0 Z$	3
	$\to \tilde{\chi}_2^0 h$	9
	$\to \tilde{\chi}_1^0 h$	6
$\tilde{\chi}_4^0$	$\to \tilde{\chi}_1^\pm W^\mp$	59
	$\to \tilde{\chi}_2^0 h$	20
	$\to \tilde{\chi}_1^0 h$	3
	$\to \tilde{\chi}_2^0 Z$	10
	$\to \tilde{\chi}_1^0 Z$	6
$\tilde{\chi}_2^\pm$	$\to \tilde{\chi}_1^\pm Z$	30
	$\to \tilde{\chi}_1^\pm h$	29
	$\to \tilde{\chi}_2^0 W^\pm$	29
	$\to \tilde{\chi}_1^0 W^\pm$	9
	$\to \tilde{e}^\pm \nu_e$	1.5

ATLAS-CONF-2019-031

$\tilde{\chi}_1^\pm \tilde{\chi}_2^0 \to Wh\, \tilde{\chi}_1^0 \tilde{\chi}_1^0,\ W \to l\nu,\ h \to b\bar{b}$

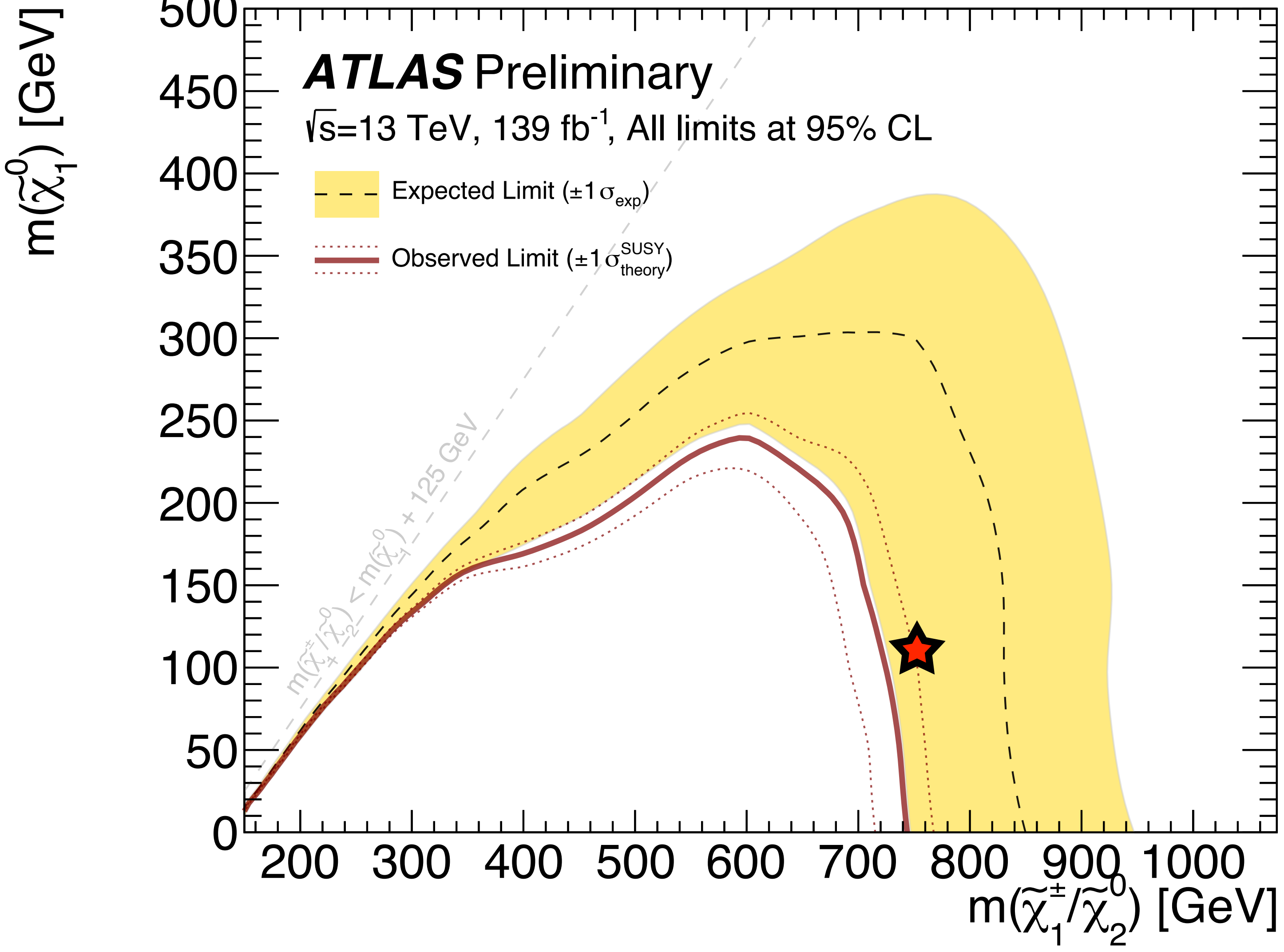

LHC constraint

- physical masses

$\tilde{\chi}_1^0$	121.2	$\tilde{\nu}_e$	124.7	$\tilde{\nu}_\mu$	711	$\tilde{\chi}_3^0$	711.9
$\tilde{\chi}_2^0$	123.5	$\tilde{e}_L$	147.3	$\tilde{\mu}_L$	715.3	$\tilde{\chi}_4^0$	713.3
$\tilde{\chi}_1^\pm$	123.5	$\tilde{e}_R$	127.9	$\tilde{\mu}_R$	711.6	$\tilde{\chi}_2^\pm$	715.7

mode		BR [%]
$\tilde{\chi}_3^0$	$\to \tilde{\chi}_1^\pm W^\mp$	59
	$\to \tilde{\chi}_2^0 Z$	20
	$\to \tilde{\chi}_1^0 Z$	3
	$\to \tilde{\chi}_2^0 h$	9
	$\to \tilde{\chi}_1^0 h$	6
$\tilde{\chi}_4^0$	$\to \tilde{\chi}_1^\pm W^\mp$	59
	$\to \tilde{\chi}_2^0 h$	20
	$\to \tilde{\chi}_1^0 h$	3
	$\to \tilde{\chi}_2^0 Z$	10
	$\to \tilde{\chi}_1^0 Z$	6
$\tilde{\chi}_2^\pm$	$\to \tilde{\chi}_1^\pm Z$	30
	$\to \tilde{\chi}_1^\pm h$	29
	$\to \tilde{\chi}_2^0 W^\pm$	29
	$\to \tilde{\chi}_1^0 W^\pm$	9
	$\to \tilde{e}^\pm \nu_e$	1.5

1801.03957

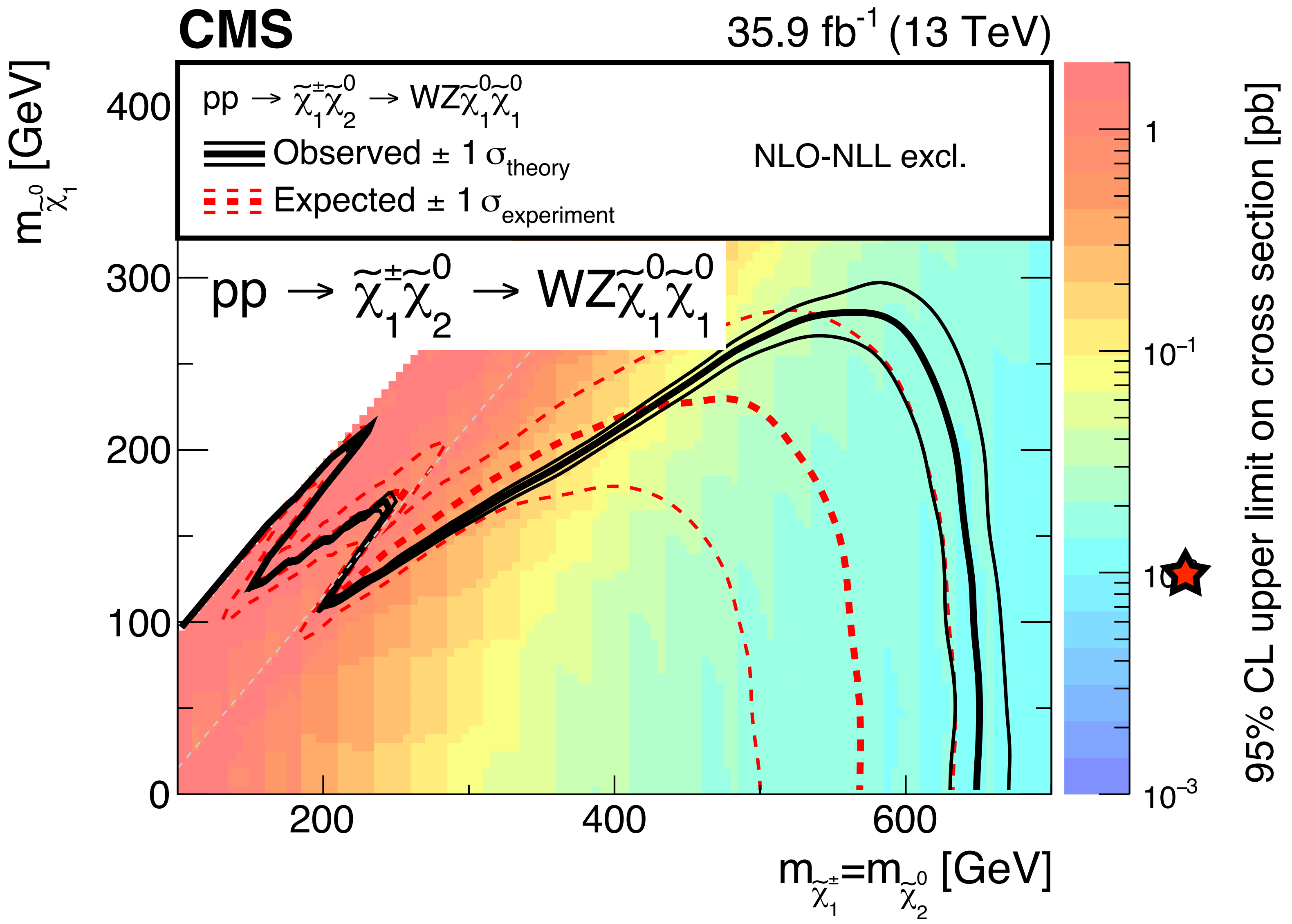

Summary 1

- Simultaneous explanations for Electron and Muon g-2 anomalies ask for flavour violating new physics.

$$\frac{m_\mu^2}{m_e^2}\frac{\Delta a_e}{\Delta a_\mu} \sim -14$$

- The Higgs mediation contribution provides a source of mass splitting without introducing dangerous μ→eγ.

- By exploiting different decoupling nature and the possibly opposite signs of Bino and Wino contributions, both electron and muon g-2 anomalies can be explained.

- This explanation requires very light EWKinos and sleptons, but the current LHC constraints can be avoided by very small mass splitting.

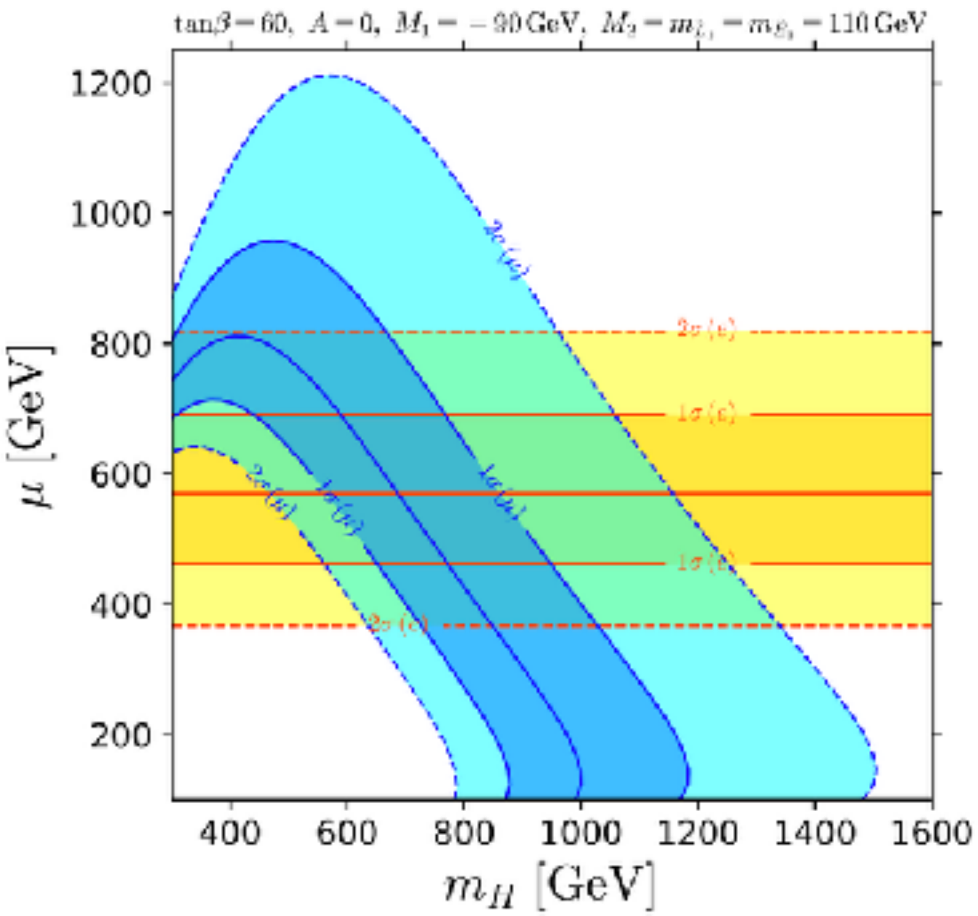

Long-lived sparticle search at MoEDAL

Long-lived (charged) particles in SUSY models:

- Split SUSY

$(m_{\tilde q} \gg m_{\tilde g})$

long-lived $\tilde g$

$$c\tau_{\tilde g} = \mathcal{O}(1-10)\ \mathrm{cm} \times \left(\frac{\Delta m}{10\ \mathrm{GeV}}\right)^{-5} \left(\frac{\widetilde m}{10\ \mathrm{TeV}}\right)^{4}$$

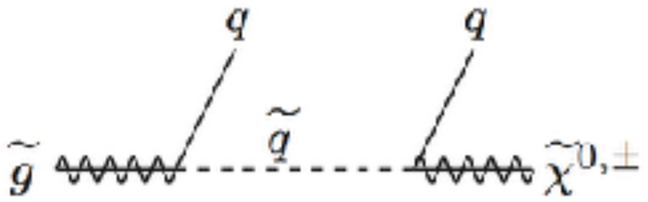

- Gravitino LSP

LL NLSP: e.g. $\tilde\tau$

$$\tau_{\tilde f} = 6 \times 10^{-12}\mathrm{sec} \cdot \left(\frac{m_{3/2}}{10\mathrm{eV}}\right)^{2} \left(\frac{m_{\tilde f}}{100\mathrm{GeV}}\right)^{-5}$$

- RPV

LL LSP: e.g. $\tilde t$

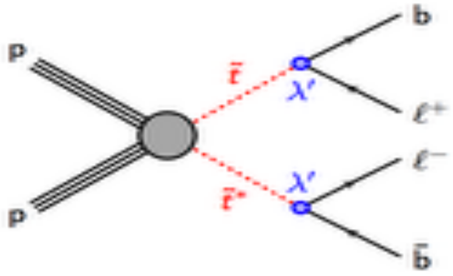

- Stau-Coannihilaiton

long-lived $\tilde\tau$

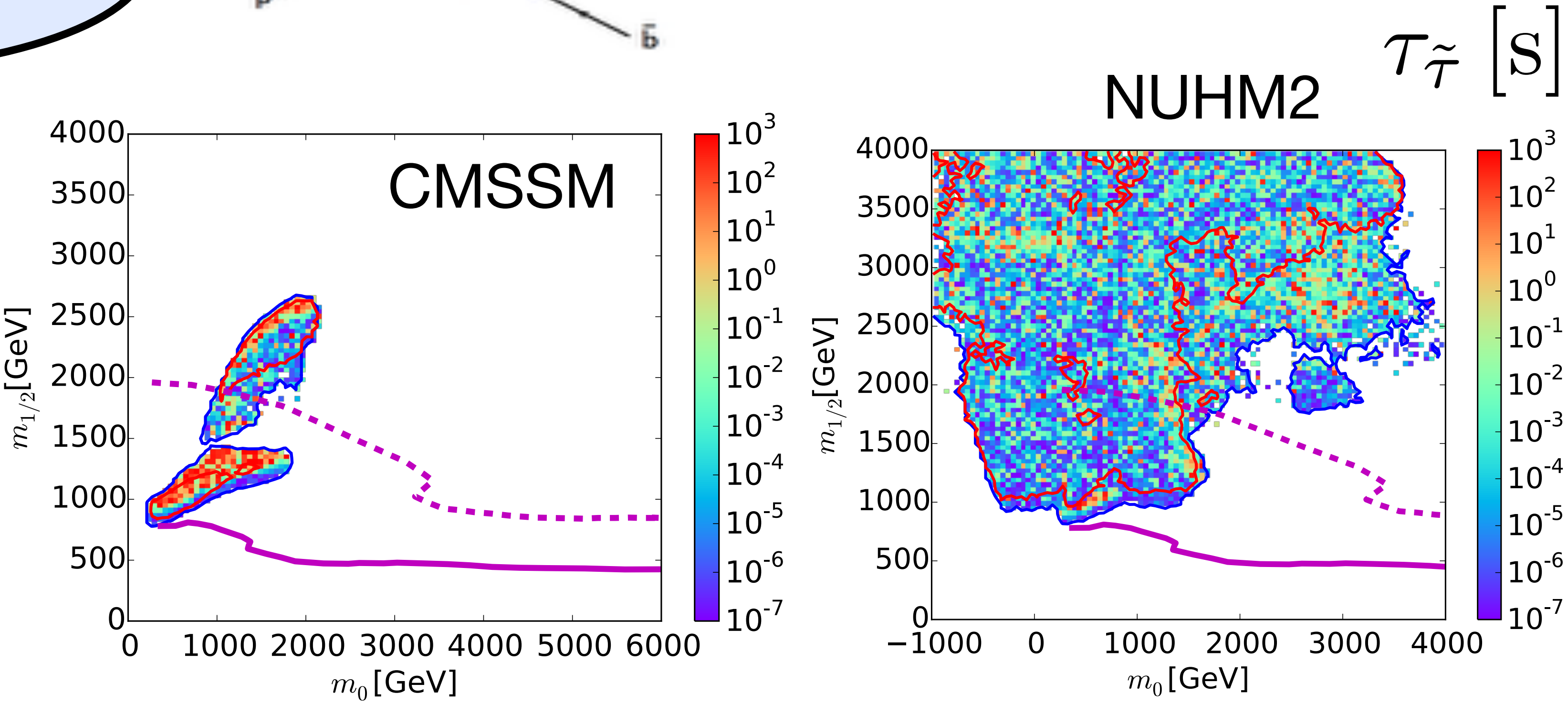

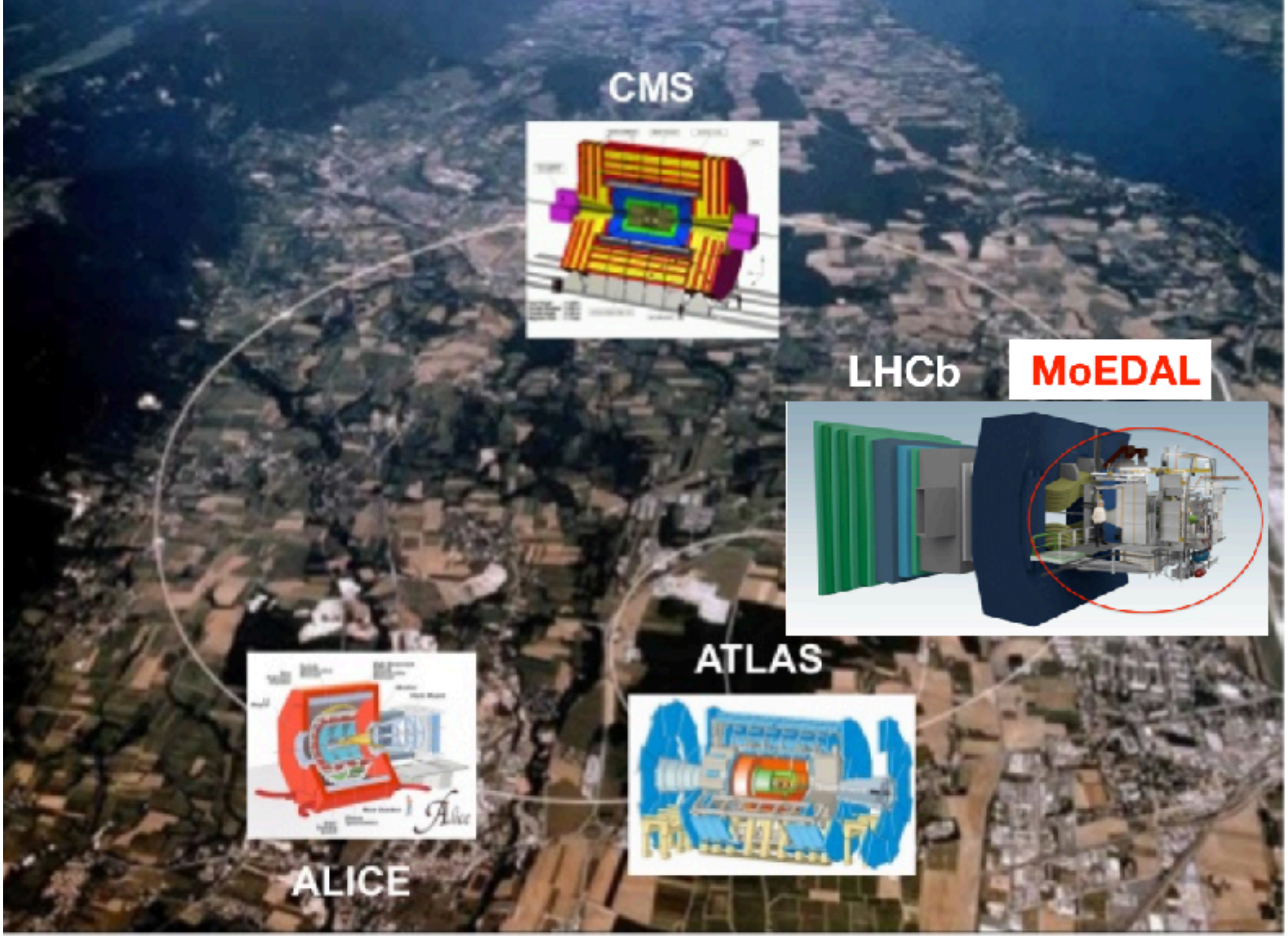

- Independent searches (with very different systematics, environment, assumptions, ..) are important for robust science.
- There could be a model which is sensitive for MoEDAL but not much for ATLAS/CMS.

Signatures at MoEDAL

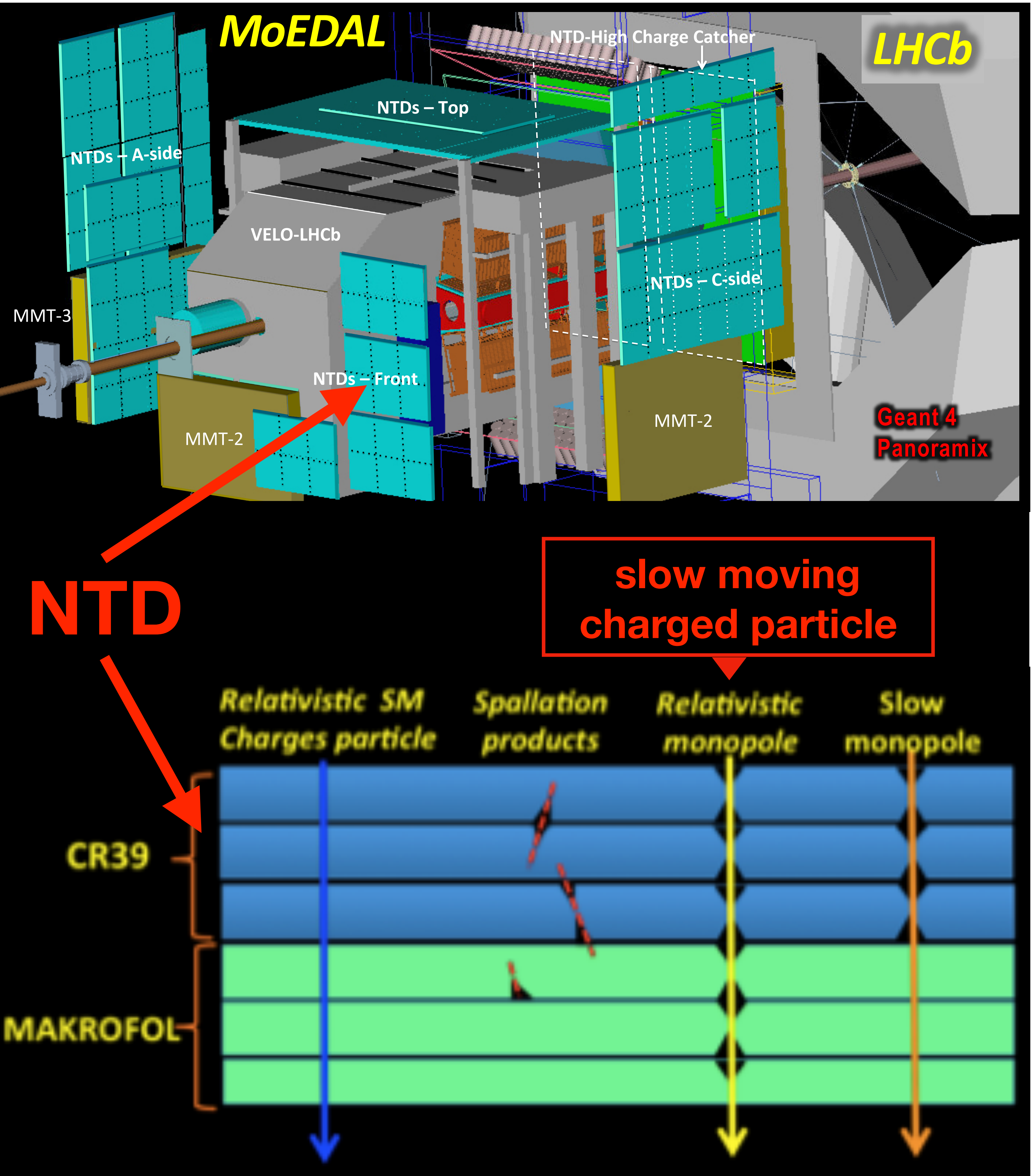

- MoEDAL is primarily designed to look for Magnetic Monopoles (MMs)
- MoEDAL deploys Nuclear Track Detectors (NTD) ~2*m* away from the interaction point, and only MMs or slow moving charged particles can punch through the detector, leaving the etching signature
- Essentially no SM background.

MoEDAL can detect a charged particle if it is moving sufficiently slowly:

$\beta < 0.2|Q| = 0.2$ (Q=1).

The particle must pass the detector shell located ~**2m** away from the interaction point.

$$\boxed{\text{probability of traveling more than 2m}} = \exp\left[-\left(\frac{2\mathrm{m}}{c\tau}\right)\left(\frac{1}{\gamma\beta}\right)\right]$$

$$= \exp\left[-\left(\frac{0.7\cdot 10^{-8}\,\mathrm{s}}{\tau}\right)\left(\frac{1}{\gamma\beta}\right)\right]$$

$$\Rightarrow \boxed{\tau \gtrsim 10^{-8}\,\mathrm{s}}$$

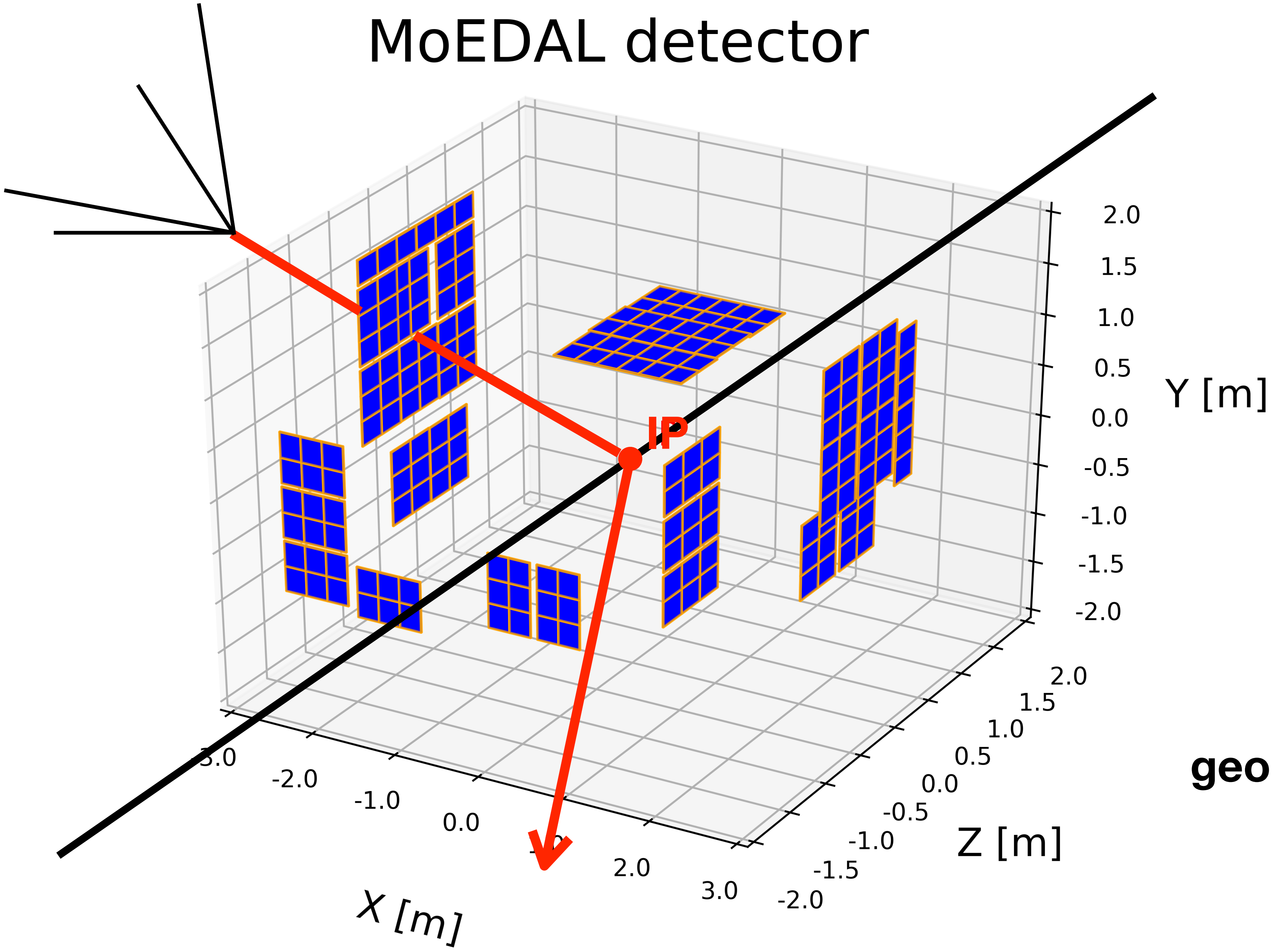

geometrical acceptance ~ 20%

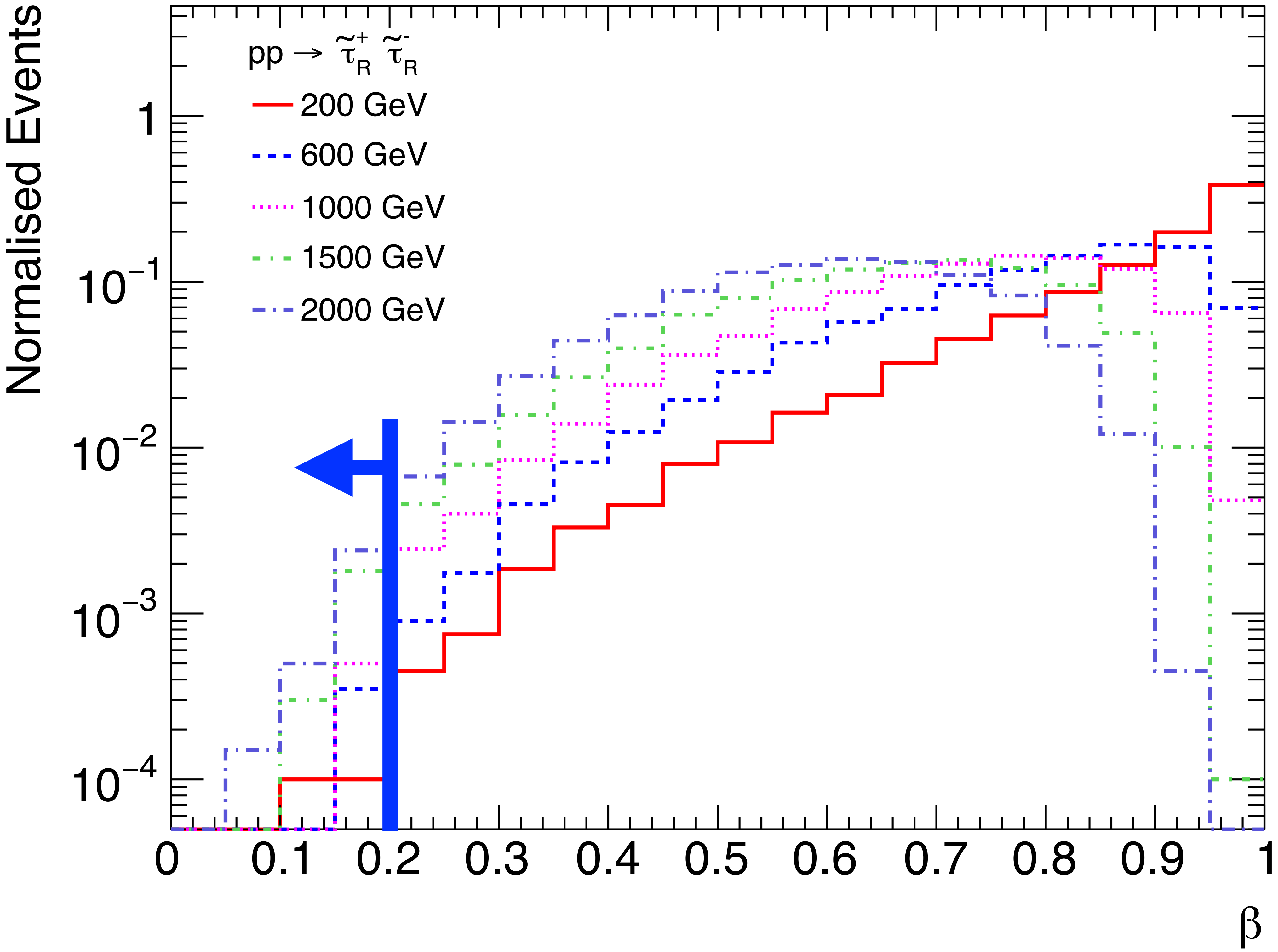

Typically β is not small for light particles…

Signal Efficiency (β < 0.2)

Signal Cross-Section

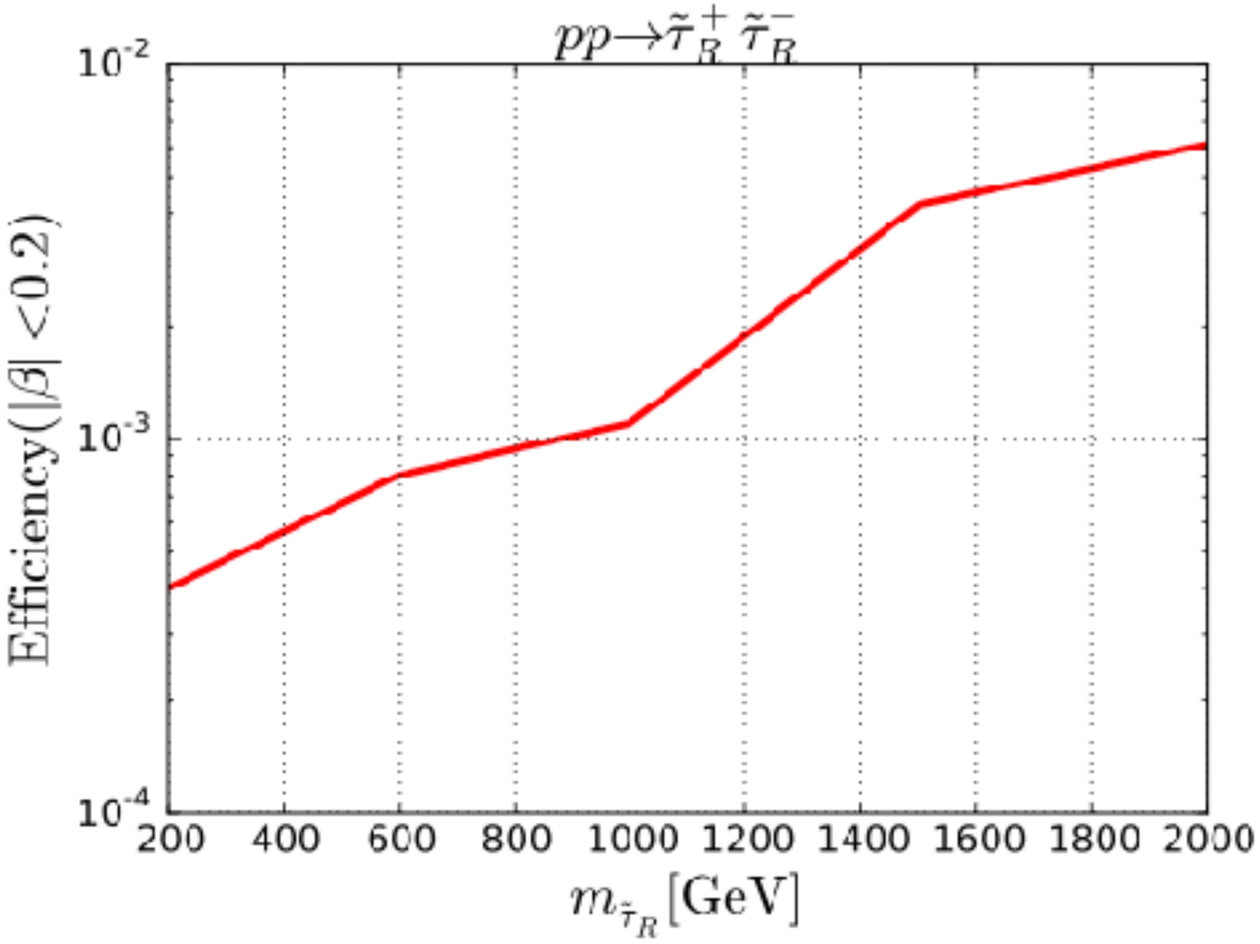

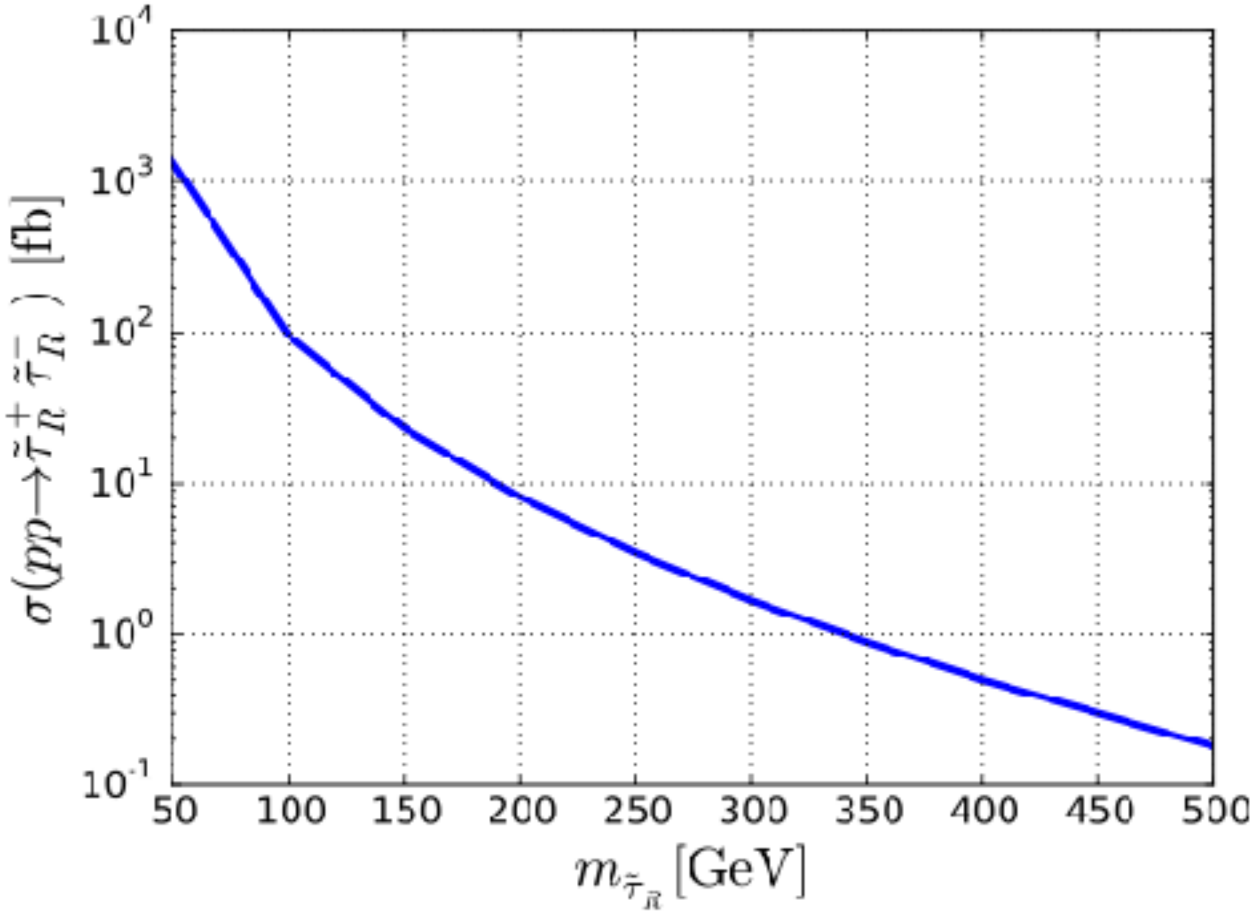

For heavier particles, cross-sections are small…

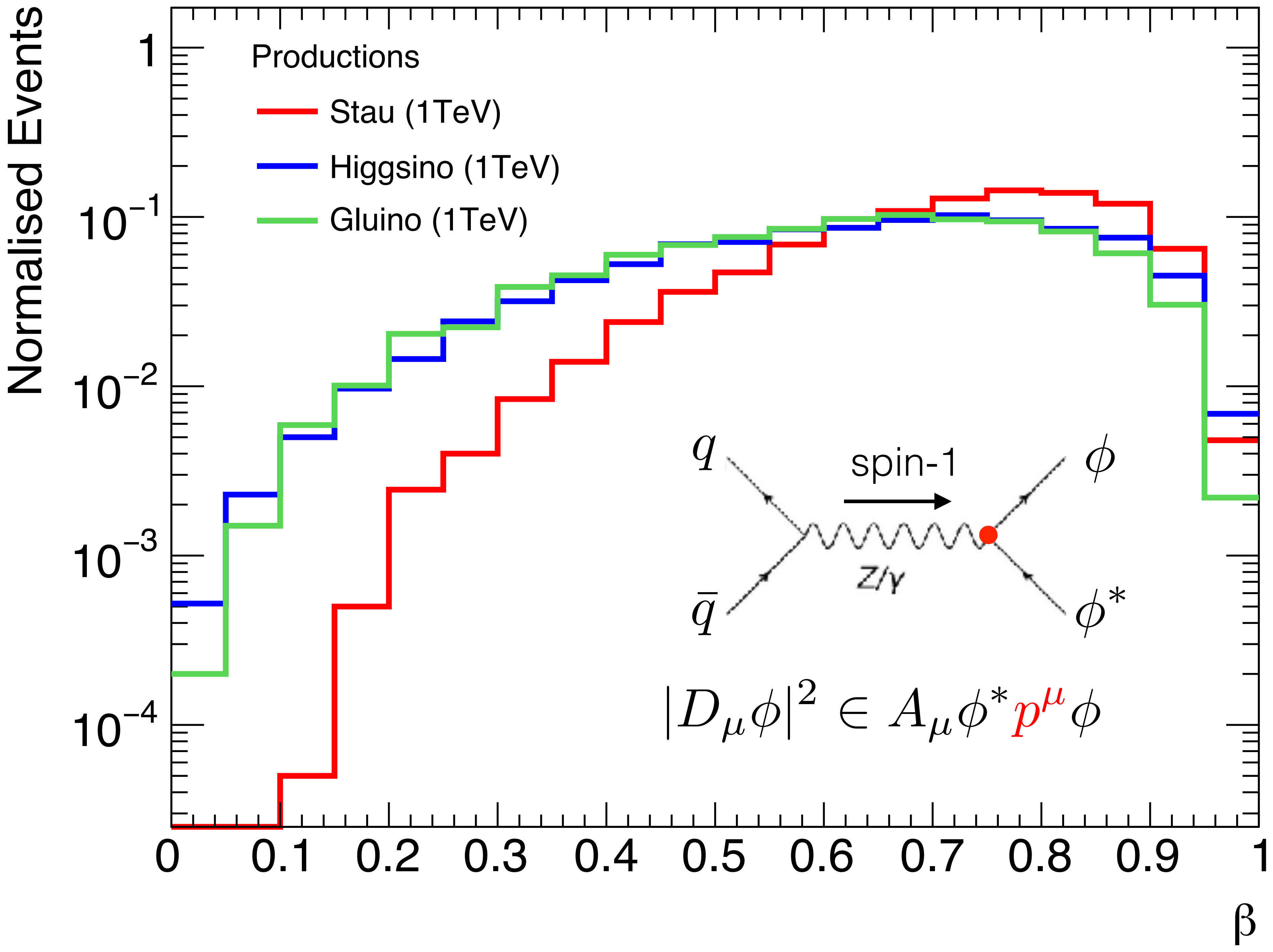

$$|D_\mu \phi|^2 \in A_\mu \phi^* p^\mu \phi$$

The velocity is smaller for **fermion** pair production.

(s-wave)

small β, large σ → gluino pair production

small β, large σ → **gluino** pair production

However, long-lived gluinos are severely constrained by Pixel dE/dx analyses.

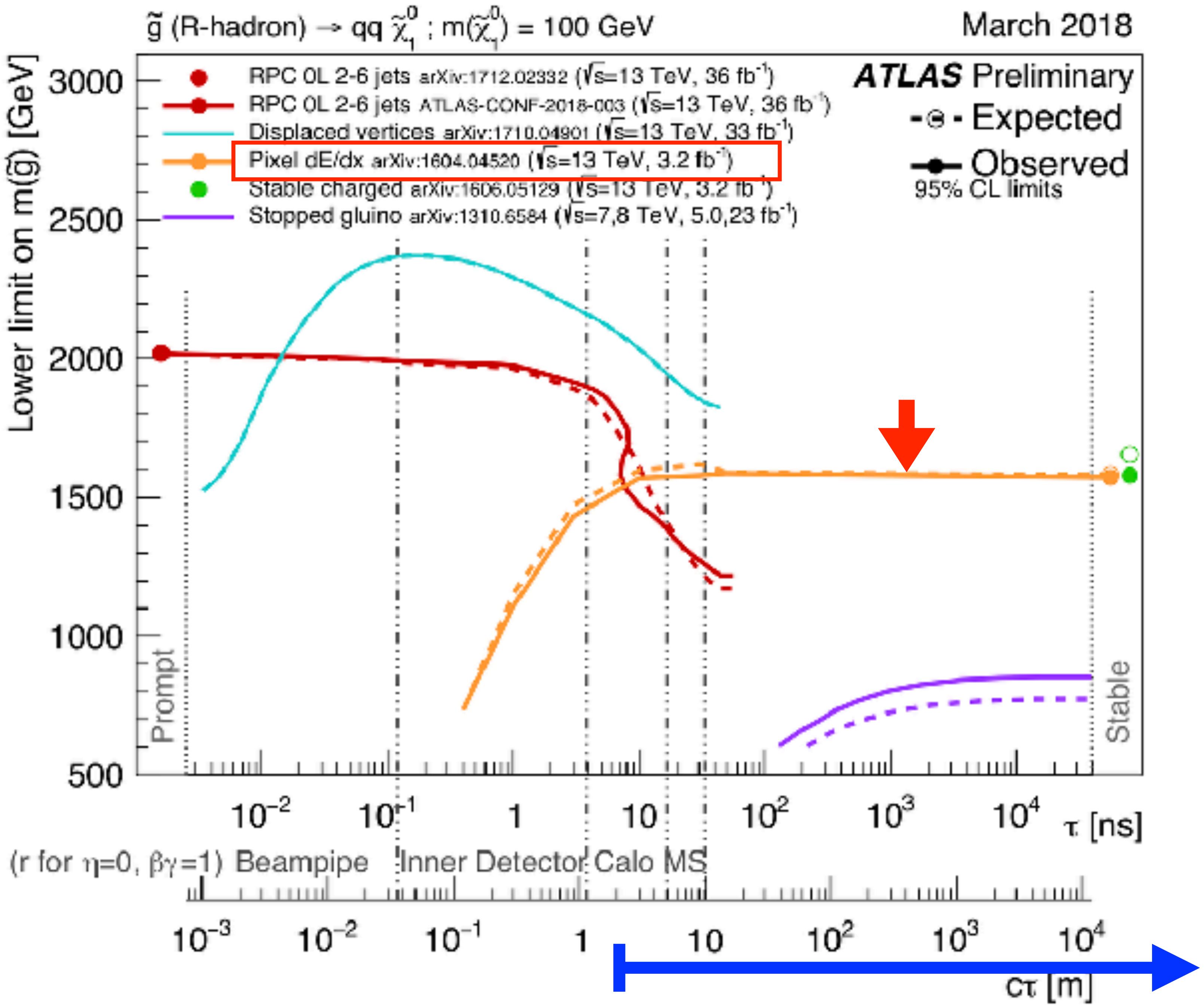

MoEDAL

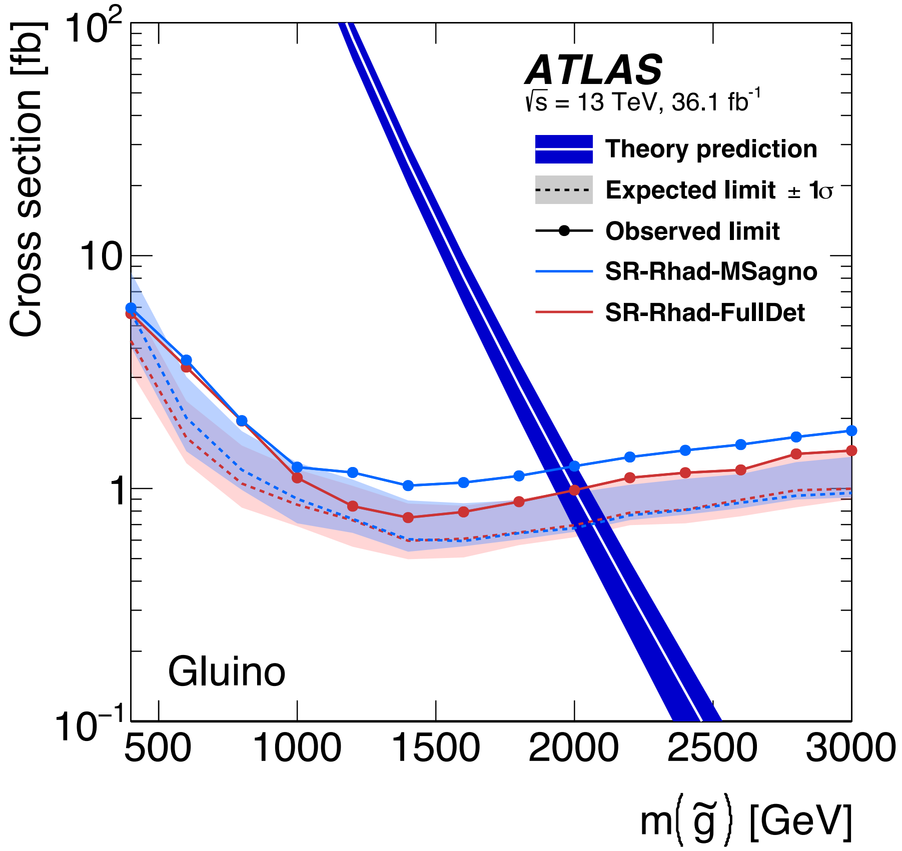

current limit (36/fb)

$$m_{\tilde{g}} > 2000\,\mathrm{GeV}$$

- **How pixel dE/dx limit can be avoided?**

  - Pixel hits are required for the heavy charged tracks.

- **How pixel dE/dx limit can be avoided?**

  - Pixel hits are required for the heavy charged tracks.

$$\tilde{g} \to q\,\bar{q}\,\tilde{\chi}_1^0, \quad \tilde{\chi}_1^0 \to \tau^{(*)}\,\tilde{\tau}_1^{\pm}$$

Compressed

long-lived

collider-stable

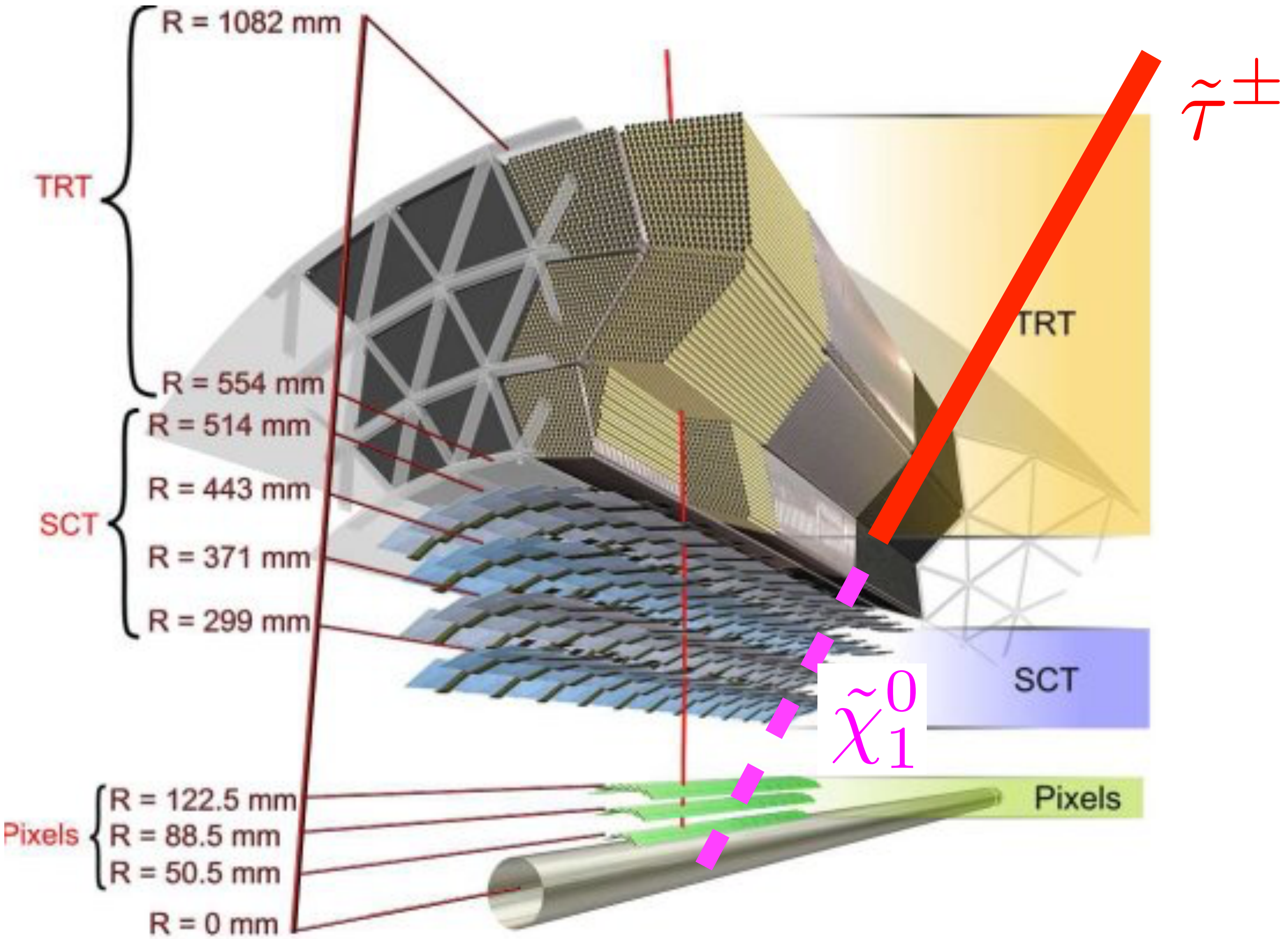

- **How pixel dE/dx limit can be avoided?**

  - Pixel hits are required for the heavy charged tracks.

$$\tilde{g} \to q\,\bar{q}\,\tilde{\chi}_1^0, \quad \tilde{\chi}_1^0 \to \tau^{(*)}\,\tilde{\tau}_1^{\pm}$$

Compressed

long-lived

collider-stable

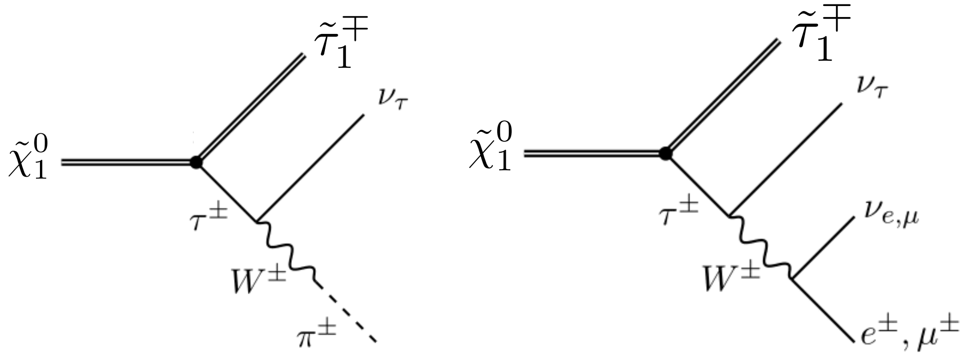

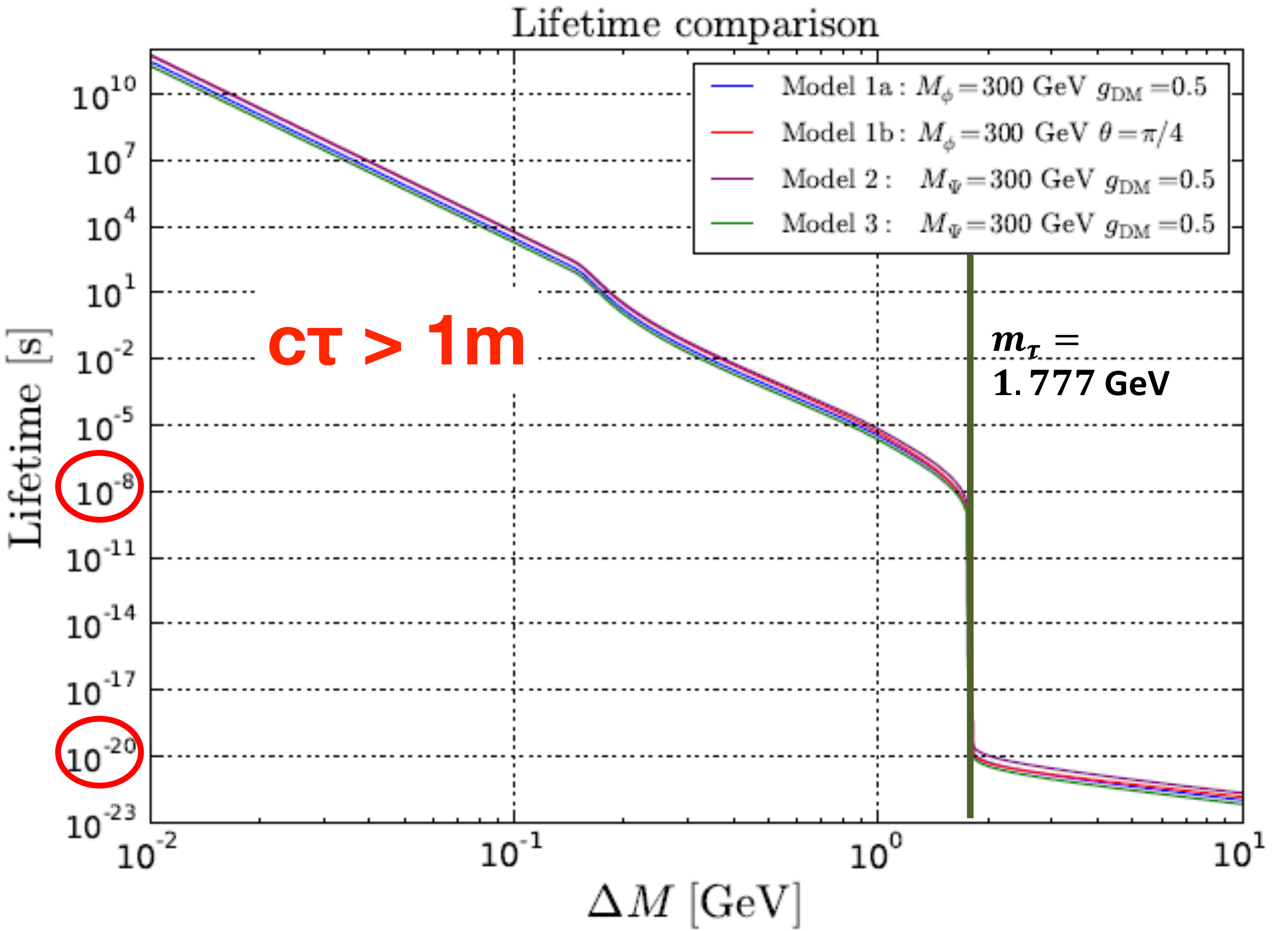

meta-stable staus, in gauge mediation:

$$\Gamma_{\tilde{\tau}}(\tilde{\tau} \to \psi_{3/2}\tau) = \frac{m_{\tilde{\tau}}^5}{48\pi m_{3/2}^2 M_{\rm P}^2}\left(1 - \frac{m_{3/2}^2}{m_{\tilde{\tau}}^2}\right)^4$$

Reinterpretation of pixel dE/dx search

[1902.01636]

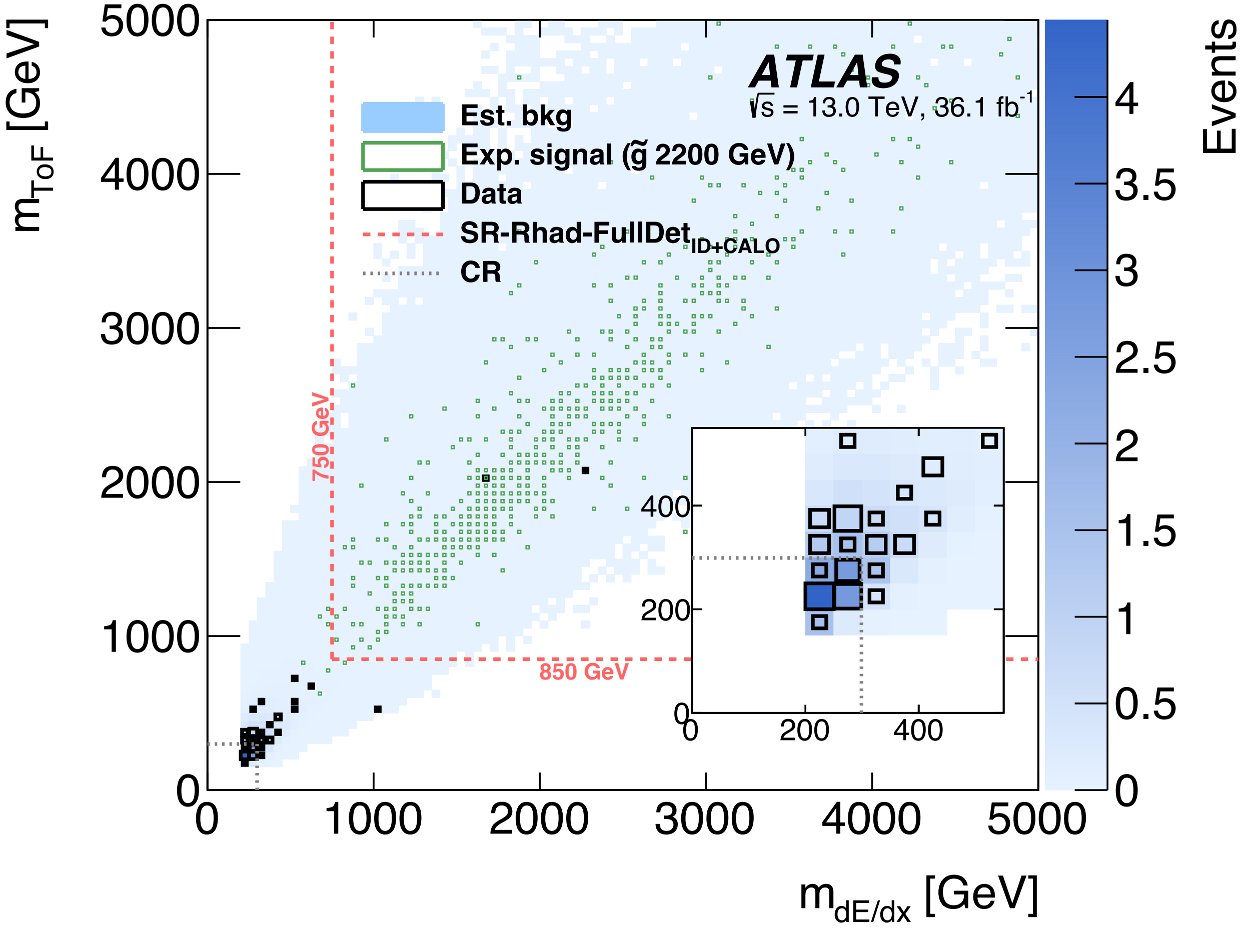

reinterpretation is non-trivial…

Reinterpretation of pixel dE/dx search

[1902.01636]

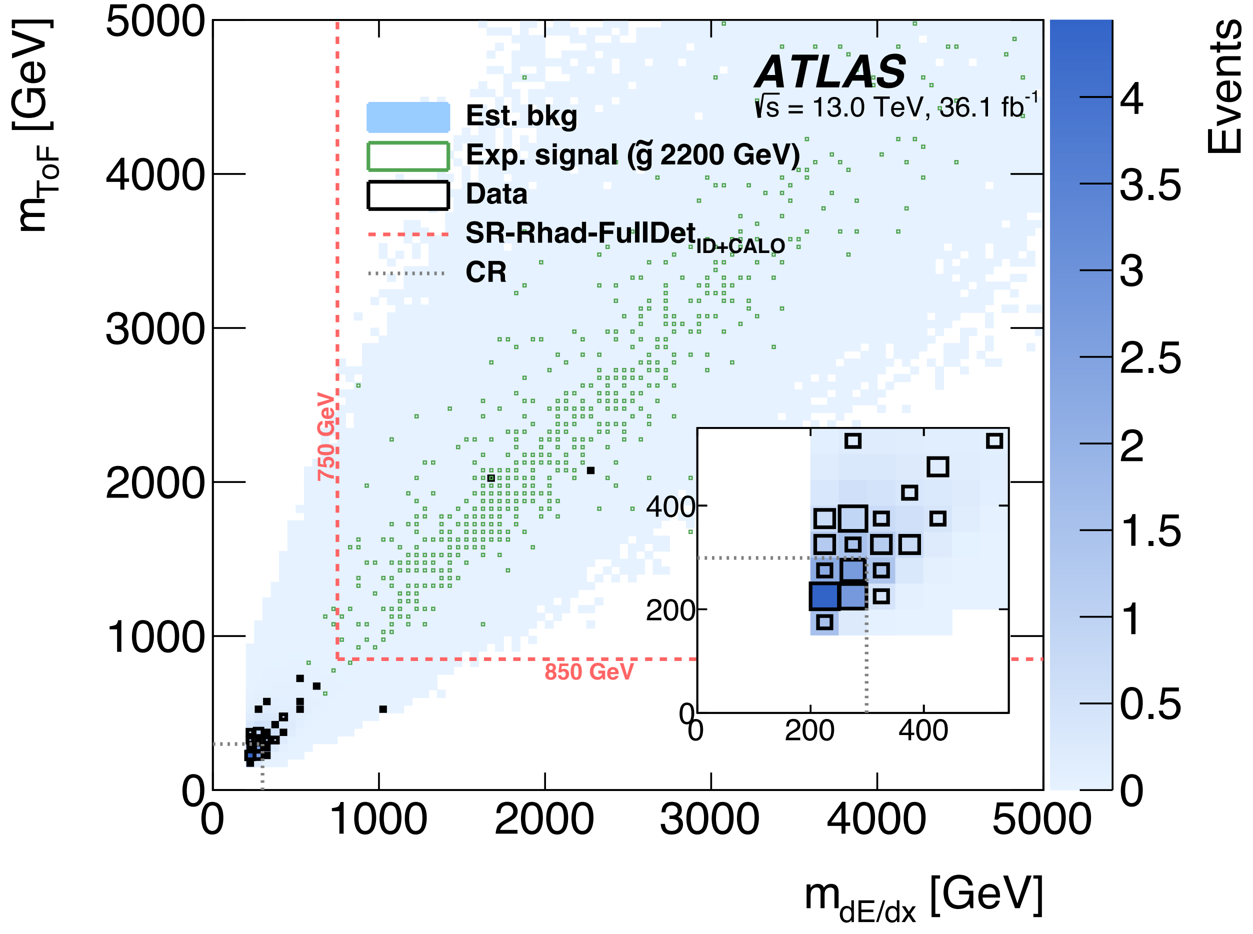

reinterpretation is non-trivial…

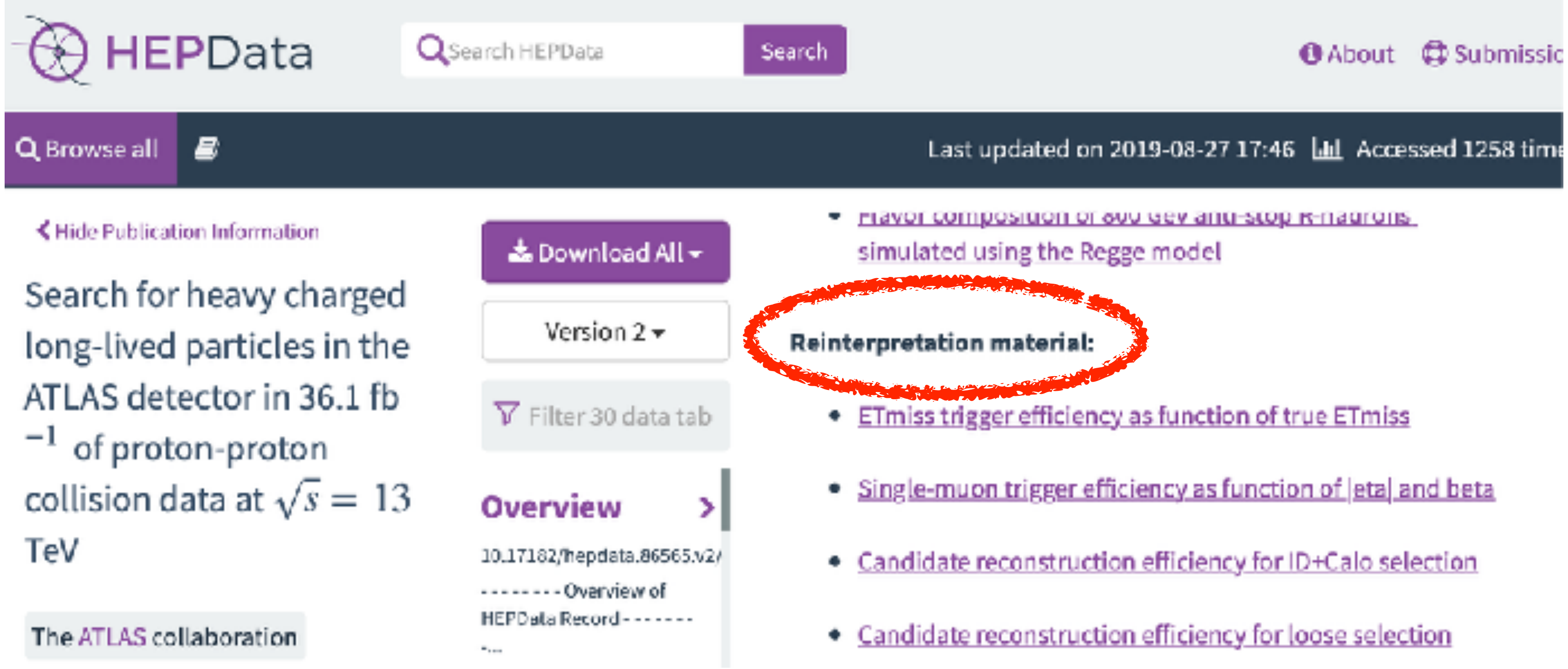

Last updated on 2019-08-27 17:46 Accessed 1258 tim

Search for heavy charged long-lived particles in the ATLAS detector in 36.1 fb^{-1} of proton-proton collision data at $\sqrt{s} = 13$ TeV

The ATLAS collaboration

10.17182/hepdata.86565.v2/

-------- Overview of HEPData Record ------- ...

- Flavor composition of 800 GeV anti-stop R-hadrons simulated using the Regge model

Reinterpretation material:

- ETmiss trigger efficiency as function of true ETmiss
- Single-muon trigger efficiency as function of |eta| and beta
- Candidate reconstruction efficiency for ID+Calo selection
- Candidate reconstruction efficiency for loose selection

Reinterpretation of pixel dE/dx search

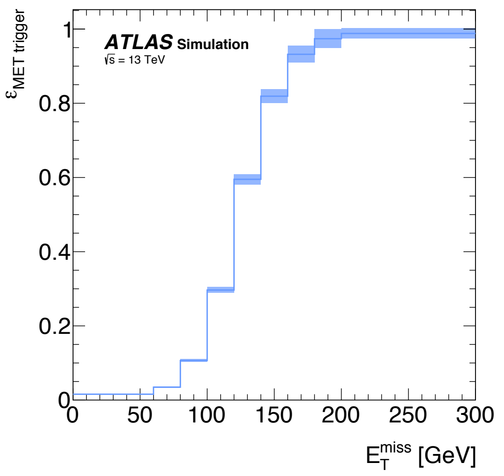

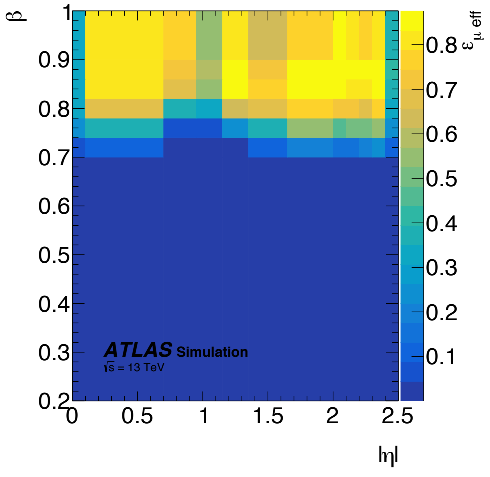

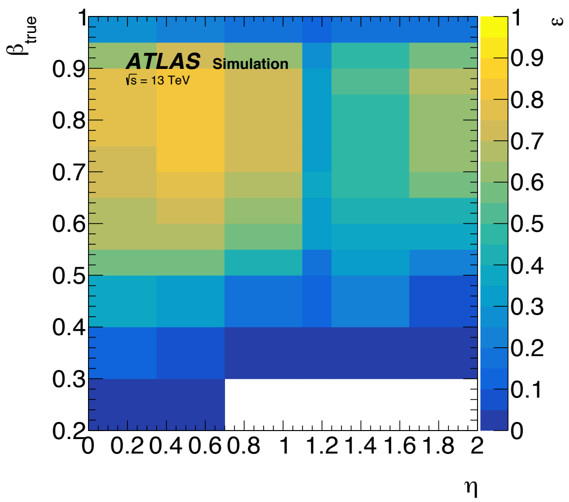

efficiency maps

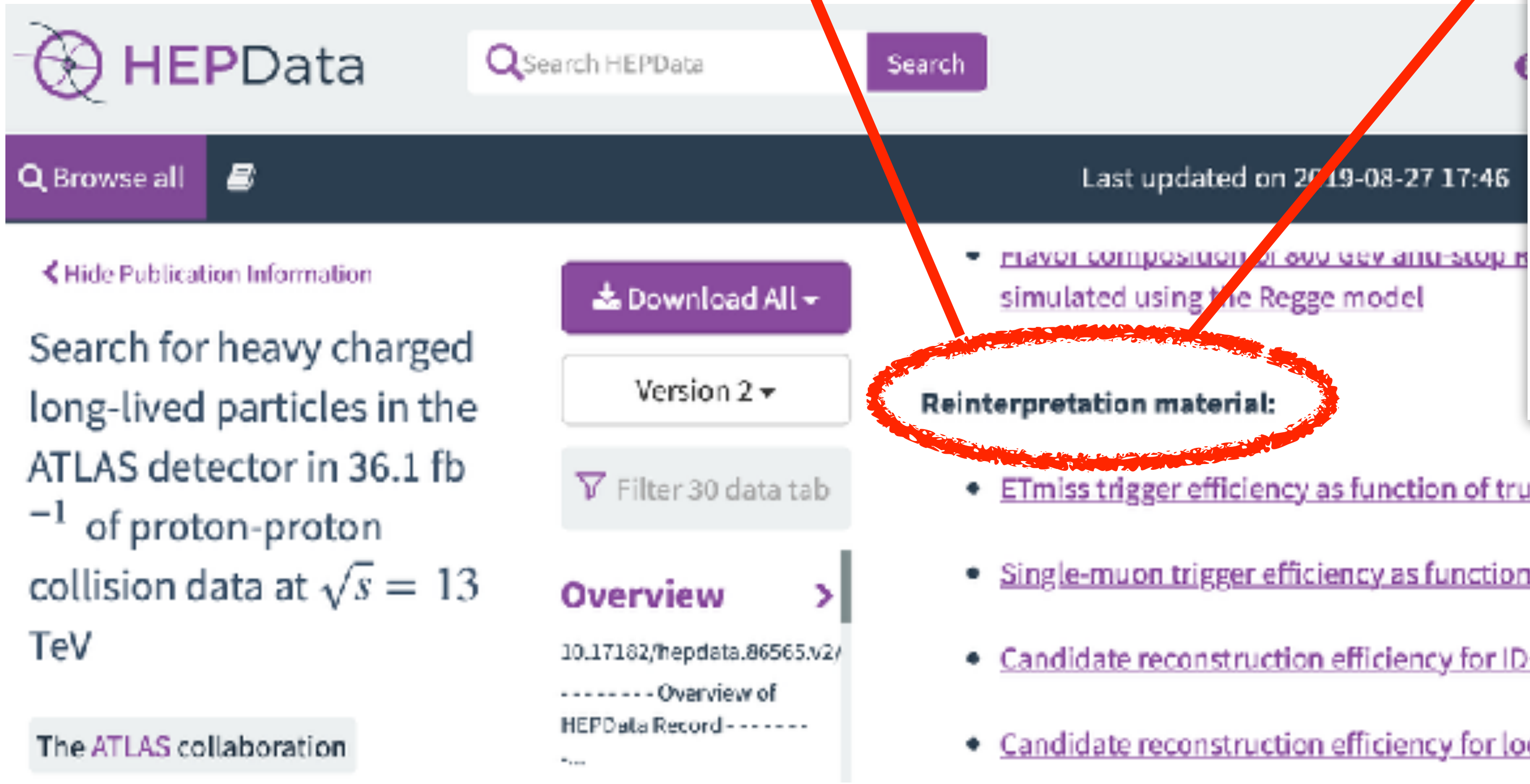

Last updated on 2019-08-27 17:46

Hide Publication Information

Search for heavy charged long-lived particles in the ATLAS detector in 36.1 fb $^{-1}$ of proton-proton collision data at $\sqrt{s} = 13$ TeV

The ATLAS collaboration

10.17182/hepdata.86565.v2/

-------- Overview of HEPData Record -------
-...

- Flavor composition of 800 GeV anti-stop R
simulated using the Regge model

Reinterpretation material:

- ETmiss trigger efficiency as function of true ETmiss
- Single-muon trigger efficiency as function of |eta| and beta
- Candidate reconstruction efficiency for ID+Calo selection
- Candidate reconstruction efficiency for loose selection

code snippet

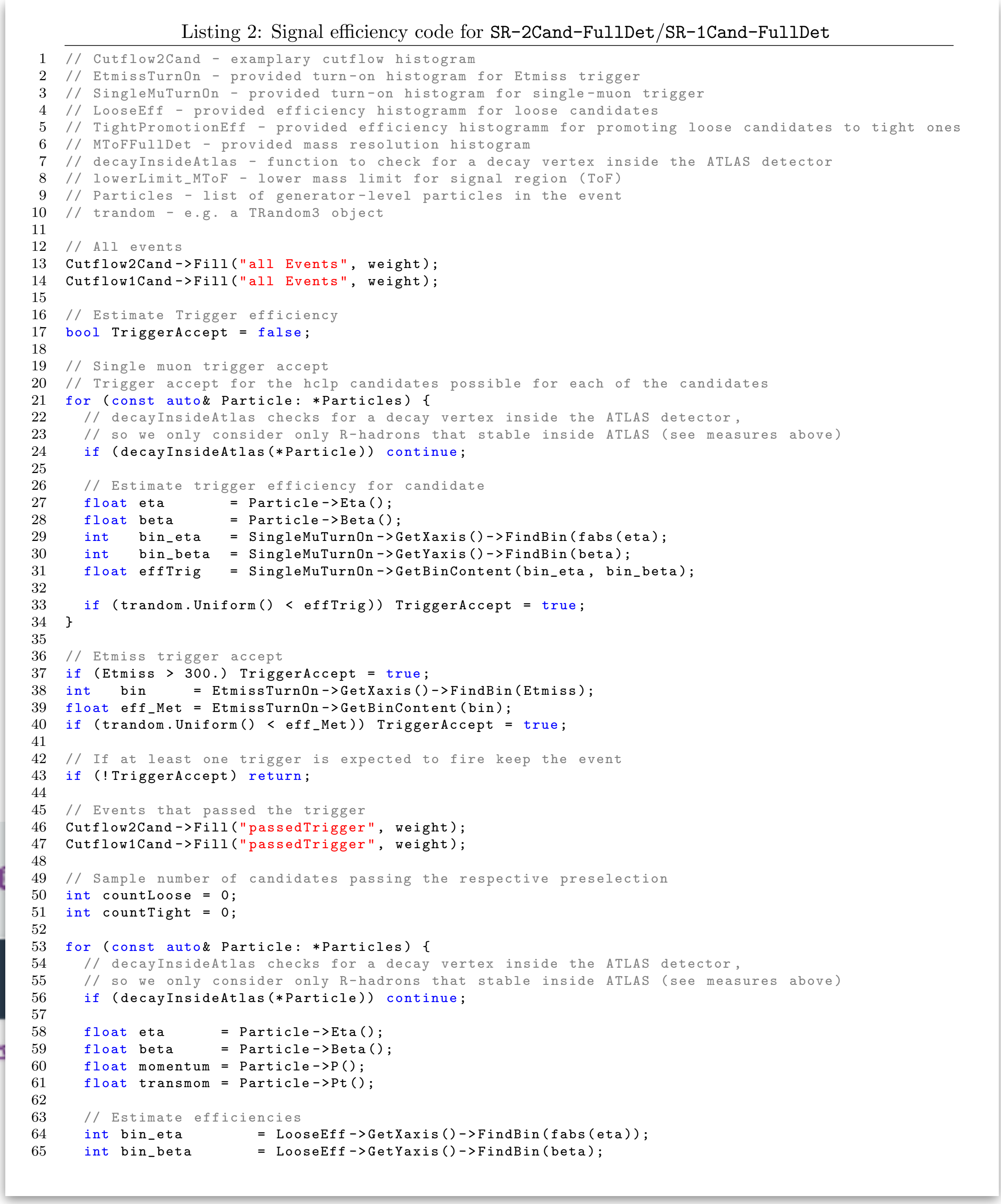

Listing 2: Signal efficiency code for SR-2Cand-FullDet/SR-1Cand-FullDet

```
// Cutflow2Cand - examplary cutflow histogram
// EtmissTurnOn - provided turn-on histogram for Etmiss trigger
// SingleMuTurnOn - provided turn-on histogram for single-muon trigger
// LooseEff - provided efficiency histogramm for loose candidates
// TightPromotionEff - provided efficiency histogramm for promoting loose candidates to tight ones
// MToFFullDet - provided mass resolution histogram
// decayInsideAtlas - function to check for a decay vertex inside the ATLAS detector
// lowerLimit_MToF - lower mass limit for signal region (ToF)
// Particles - list of generator-level particles in the event
// trandom - e.g. a TRandom3 object

// All events
Cutflow2Cand->Fill("all Events", weight);
Cutflow1Cand->Fill("all Events", weight);

// Estimate Trigger efficiency
bool TriggerAccept = false;

// Single muon trigger accept
// Trigger accept for the hclp candidates possible for each of the candidates
for (const auto& Particle: *Particles) {
  // decayInsideAtlas checks for a decay vertex inside the ATLAS detector,
  // so we only consider only R-hadrons that stable inside ATLAS (see measures above)
  if (decayInsideAtlas(*Particle)) continue;

  // Estimate trigger efficiency for candidate
  float eta      = Particle->Eta();
  float beta     = Particle->Beta();
  int   bin_eta  = SingleMuTurnOn->GetXaxis()->FindBin(fabs(eta);
  int   bin_beta = SingleMuTurnOn->GetYaxis()->FindBin(beta);
  float effTrig  = SingleMuTurnOn->GetBinContent(bin_eta, bin_beta);

  if (trandom.Uniform() < effTrig)) TriggerAccept = true;
}

// Etmiss trigger accept
if (Etmiss > 300.) TriggerAccept = true;
int   bin     = EtmissTurnOn->GetXaxis()->FindBin(Etmiss);
float eff_Met = EtmissTurnOn->GetBinContent(bin);
if (trandom.Uniform() < eff_Met)) TriggerAccept = true;

// If at least one trigger is expected to fire keep the event
if (!TriggerAccept) return;

// Events that passed the trigger
Cutflow2Cand->Fill("passedTrigger", weight);
Cutflow1Cand->Fill("passedTrigger", weight);

// Sample number of candidates passing the respective preselection
int countLoose = 0;
int countTight = 0;

for (const auto& Particle: *Particles) {
  // decayInsideAtlas checks for a decay vertex inside the ATLAS detector,
  // so we only consider only R-hadrons that stable inside ATLAS (see measures above)
  if (decayInsideAtlas(*Particle)) continue;

  float eta      = Particle->Eta();
  float beta     = Particle->Beta();
  float momentum = Particle->P();
  float transmom = Particle->Pt();

  // Estimate efficiencies
  int bin_eta        = LooseEff->GetXaxis()->FindBin(fabs(eta));
  int bin_beta       = LooseEff->GetYaxis()->FindBin(beta);
```

Reinterpretation of pixel dE/dx search

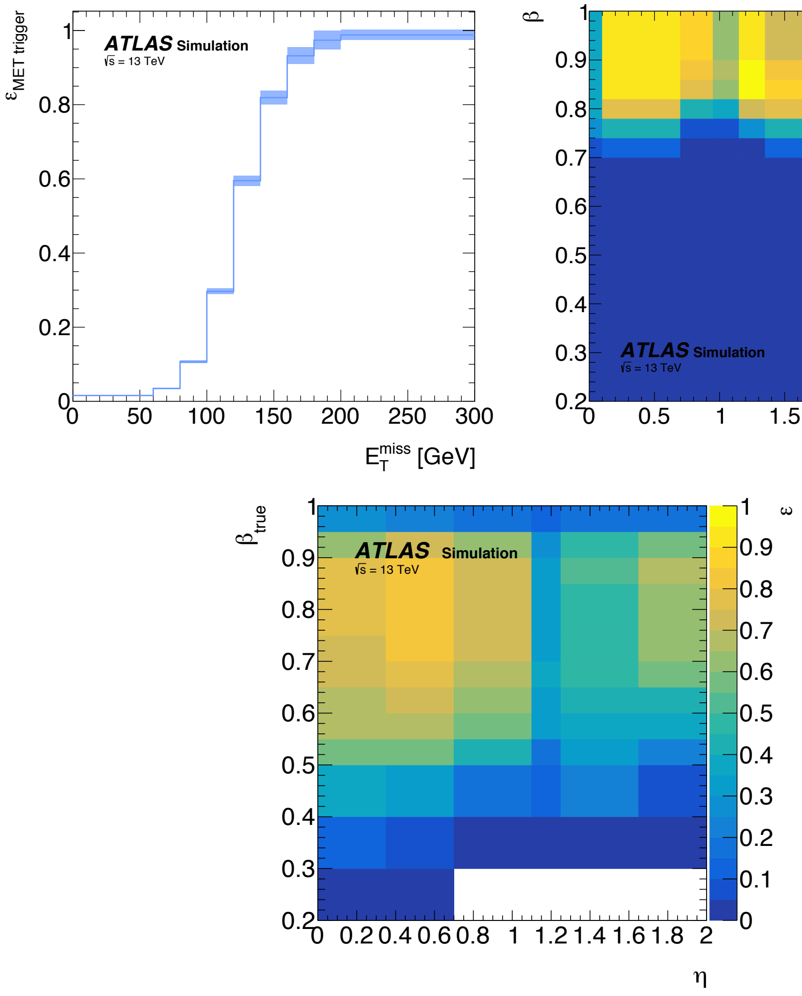

efficiency maps

code snippet

Listing 2: Signal efficiency code for SR-2Cand-FullDet/SR-1Cand-FullDet

```
// Cutflow2Cand - examplary cutflow histogram
// EtmissTurnOn - provided turn-on histogram for Etmiss trigger
// SingleMuTurnOn - provided turn-on histogram for single-muon trigger
// LooseEff - provided efficiency histogramm for loose candidates
// TightPromotionEff - provided efficiency histogramm for promoting loose candidates to tight ones
// MToFFullDet - provided mass resolution histogram
// decayInsideAtlas - function to check for a decay vertex inside the ATLAS detector
// lowerLimit_MToF - lower mass limit for signal region (ToF)
// Particles - list of generator-level particles in the event
// trandom - e.g. a TRandom3 object

// All events
Cutflow2Cand->Fill("all Events", weight);
Cutflow1Cand->Fill("all Events", weight);

// Estimate Trigger efficiency
bool TriggerAccept = false;

// Single muon trigger accept
// Trigger accept for the hclp candidates possible for each of the candidates
for (const auto& Particle: *Particles) {
  // decayInsideAtlas checks for a decay vertex inside the ATLAS detector,
  // so we only consider only R-hadrons that stable inside ATLAS (see measures above)
  if (decayInsideAtlas(*Particle)) continue;

  // Estimate trigger efficiency for candidate
  float eta      = Particle->Eta();
  float beta     = Particle->Beta();
  int   bin_eta  = SingleMuTurnOn->GetXaxis()->FindBin(fabs(eta);
  int   bin_beta = SingleMuTurnOn->GetYaxis()->FindBin(beta);
  float effTrig  = SingleMuTurnOn->GetBinContent(bin_eta, bin_beta);

  if (trandom.Uniform() < effTrig)) TriggerAccept = true;
}

// Etmiss trigger accept
if (Etmiss > 300.) TriggerAccept = true;
int   bin     = EtmissTurnOn->GetXaxis()->FindBin(Etmiss);
float eff_Met = EtmissTurnOn->GetBinContent(bin);
if (trandom.Uniform() < eff_Met)) TriggerAccept = true;

// If at least one trigger is expected to fire keep the event
if (!TriggerAccept) return;

// Events that passed the trigger
Cutflow2Cand->Fill("passedTrigger", weight);
Cutflow1Cand->Fill("passedTrigger", weight);

// Sample number of candidates passing the respective preselection
int countLoose = 0;
int countTight = 0;

for (const auto& Particle: *Particles) {
```

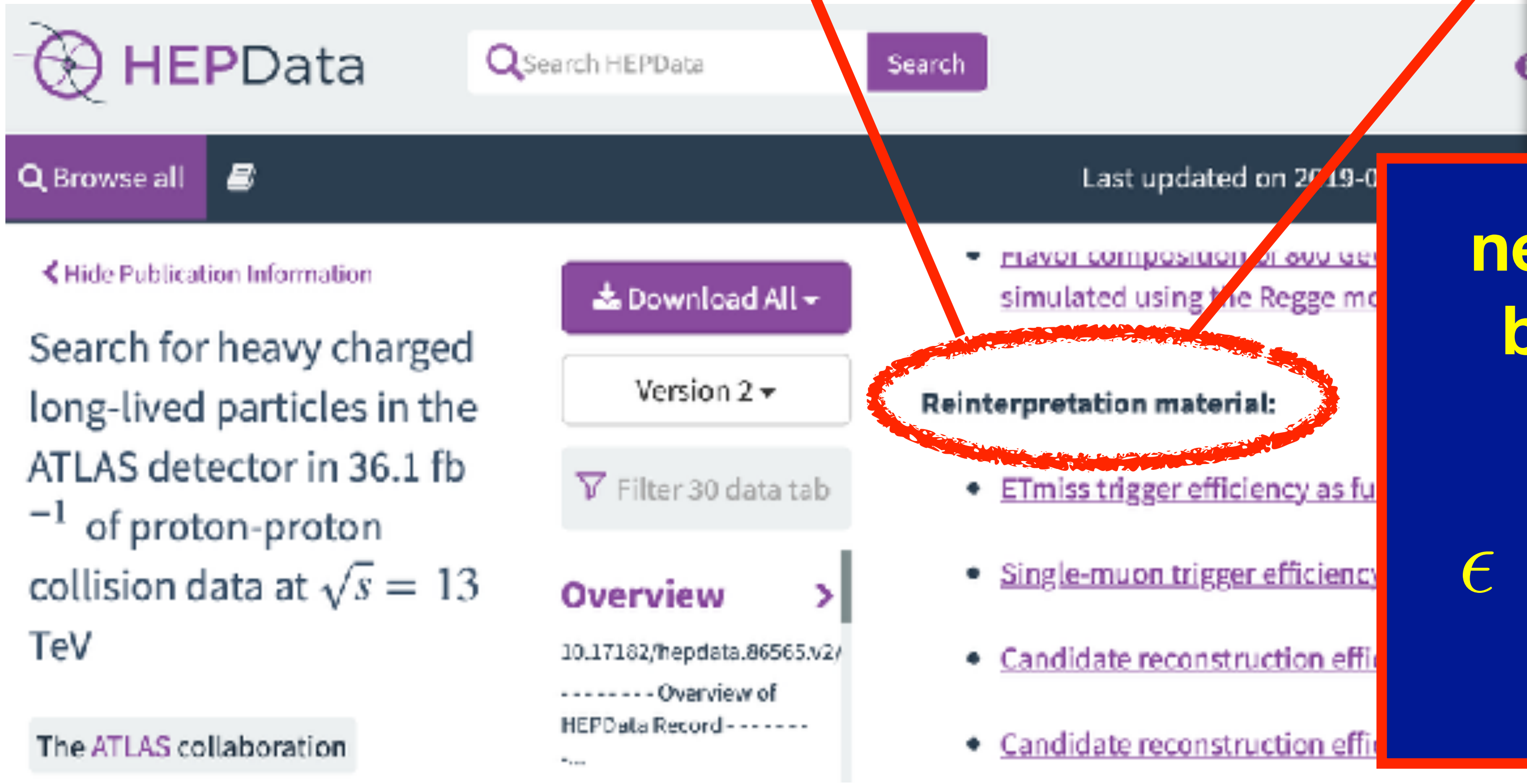

Search for heavy charged long-lived particles in the ATLAS detector in 36.1 fb $^{-1}$ of proton-proton collision data at $\sqrt{s} = 13$ TeV

The ATLAS collaboration

10.17182/hepdata.86565.v2/

-------- Overview of HEPData Record -------
...

- Flavor composition of 800 Ge
simulated using the Regge mo

Reinterpretation material:

- ETmiss trigger efficiency as fu
- Single-muon trigger efficienc
- Candidate reconstruction effi
- Candidate reconstruction effi

neutralinos must decay into stau before reaching pixel detector:

$$\epsilon \longrightarrow \epsilon \cdot \left(1 - \exp\left(-\frac{L_{\mathrm{pixel}}}{c\beta\gamma\tau}\right)\right)$$

Simulation for MoEDAL

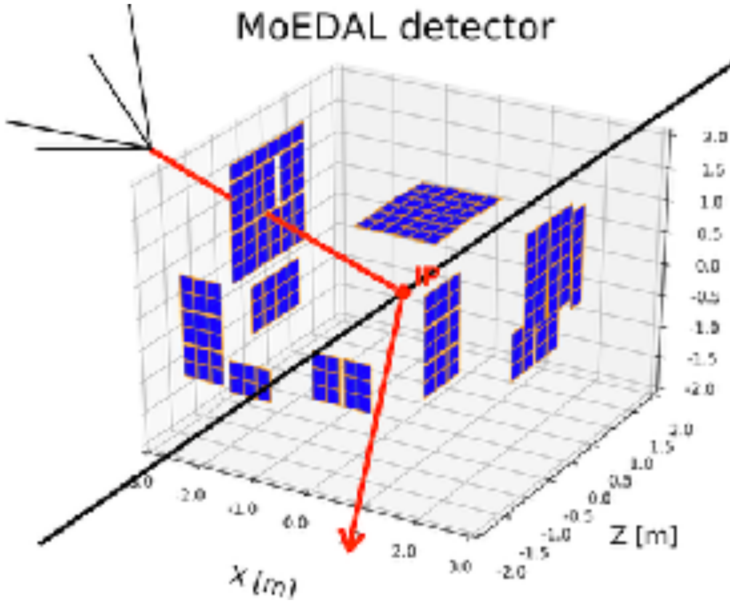

cross-section lumi efficiency

# of detected events

$$N_{\rm sig} = \sigma \cdot L \cdot \epsilon$$

incident angle

$$\boxed{\epsilon = \left\langle \sum_{i=1,2} P_{\rm NTD}(\mathbf{p}_i) \cdot \Theta\left(\delta_{\rm max}(\beta_i) - \delta_i\right) \right\rangle_{\rm MC}}$$

$$P_{\rm NTD}(\mathbf{p}_{\tilde\chi_1^0}) = \omega(\mathbf{p}_{\tilde\chi_1^0}) \left[\underbrace{1 - \exp\left(\frac{L_{\rm NTD}(\mathbf{p}_{\tilde\chi_1^0})}{\beta\gamma c\tau_{\tilde\chi_1^0}} \right)}_{\text{neutralino must decay and produce stau before reaching a NTD panel}} \right]$$

$$\text{geometrical acceptance} \begin{cases} \text{no NTD panel} \rightarrow w=0 \\ \text{is a NTD panel} \rightarrow w=1 \end{cases}$$

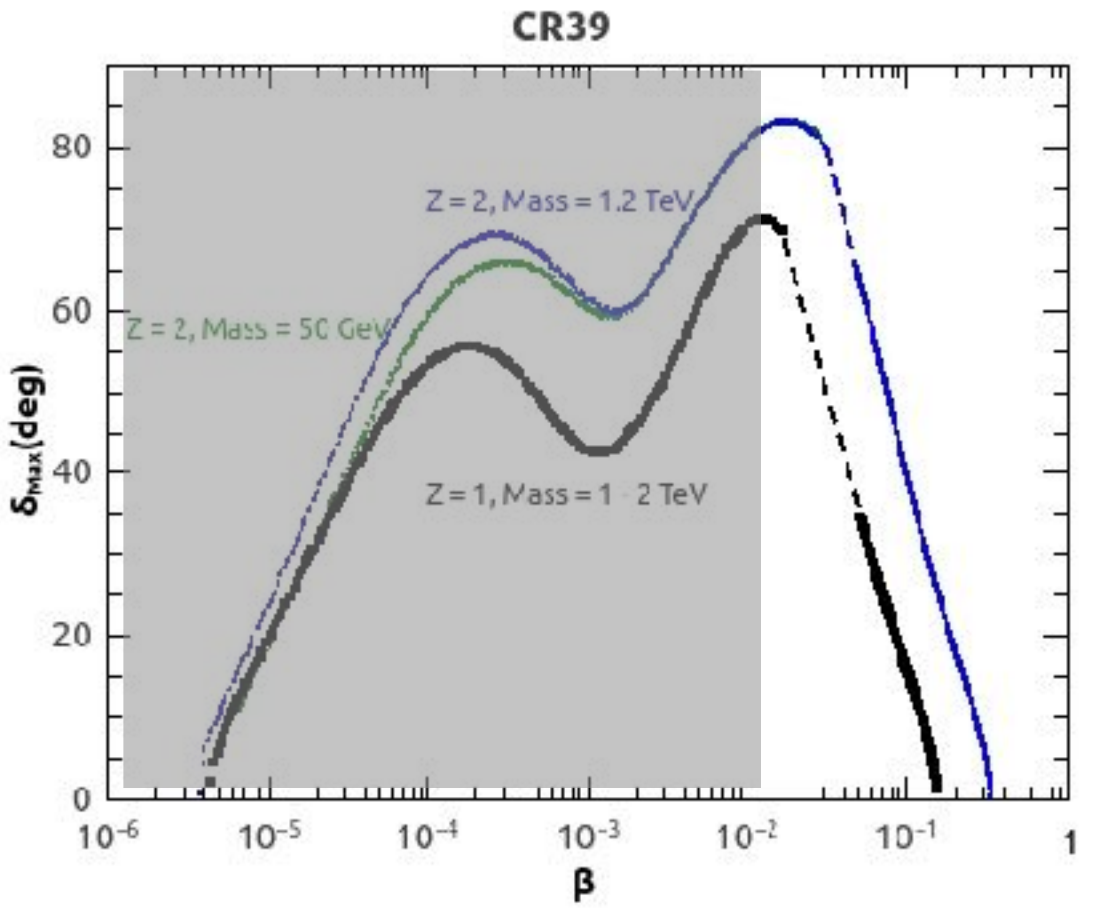

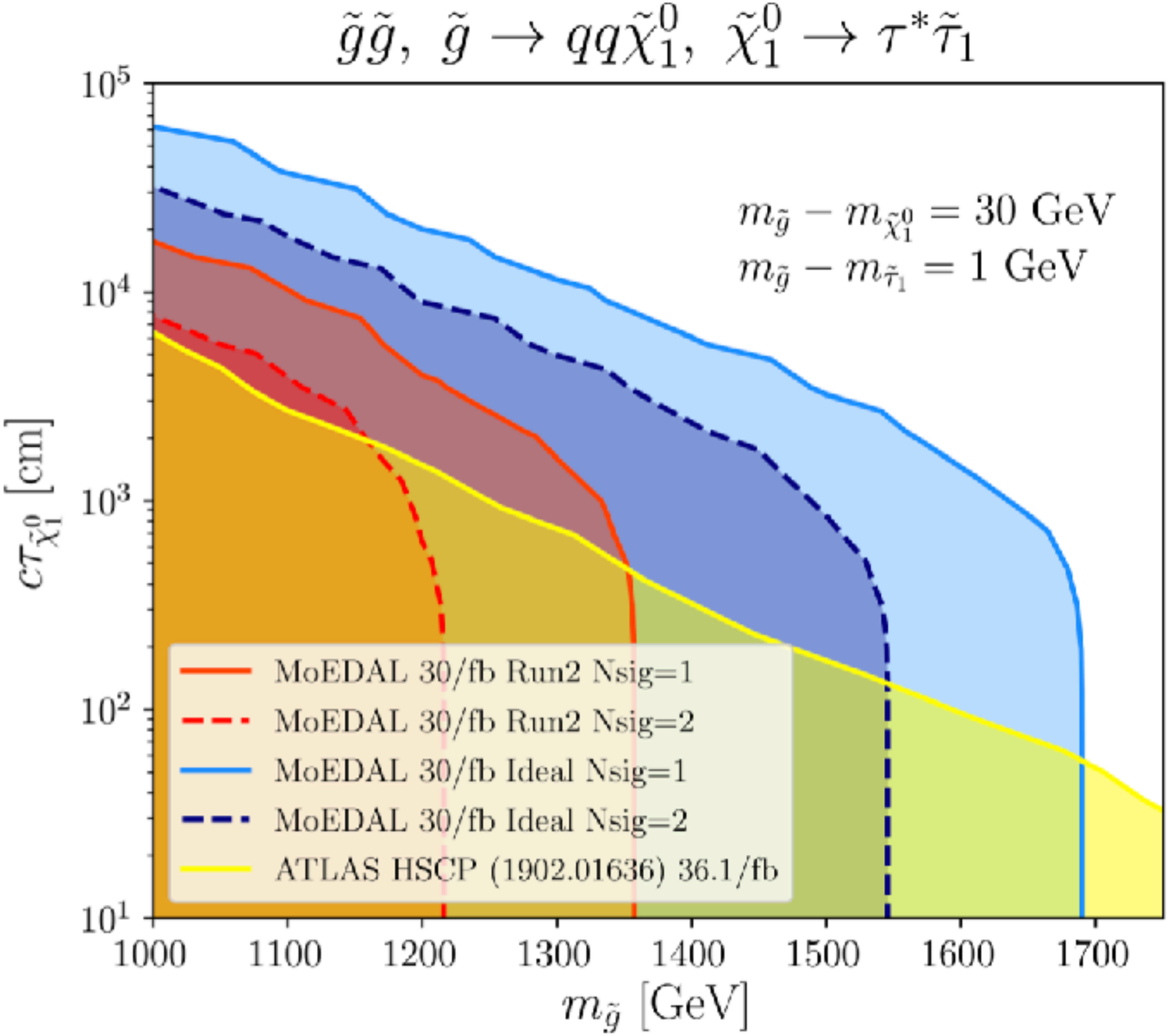
$\tilde{g}\tilde{g},\ \tilde{g} \to qq\tilde{\chi}_1^0,\ \tilde{\chi}_1^0 \to \tau^*\tilde{\tau}_1$
$m_{\tilde{g}} - m_{\tilde{\chi}_1^0} = 30$ GeV
$m_{\tilde{g}} - m_{\tilde{\tau}_1} = 1$ GeV
$c\tau_{\tilde{\chi}_1^0}$ [cm]
10^5
10^4
10^3
10^2
10^1
1000
1100
1200
1300
1400
1500
1600
1700
$m_{\tilde{g}}$ [GeV]
MoEDAL 30/fb Run2 Nsig=1
MoEDAL 30/fb Run2 Nsig=2
MoEDAL 30/fb Ideal Nsig=1
MoEDAL 30/fb Ideal Nsig=2
ATLAS HSCP (1902.01636) 36.1/fb

Summary 2

- MoEDAK

Search for (SM) EW sphaleron/instanton at hadron colliders

Perturbative sector of EW theory is very well understood!

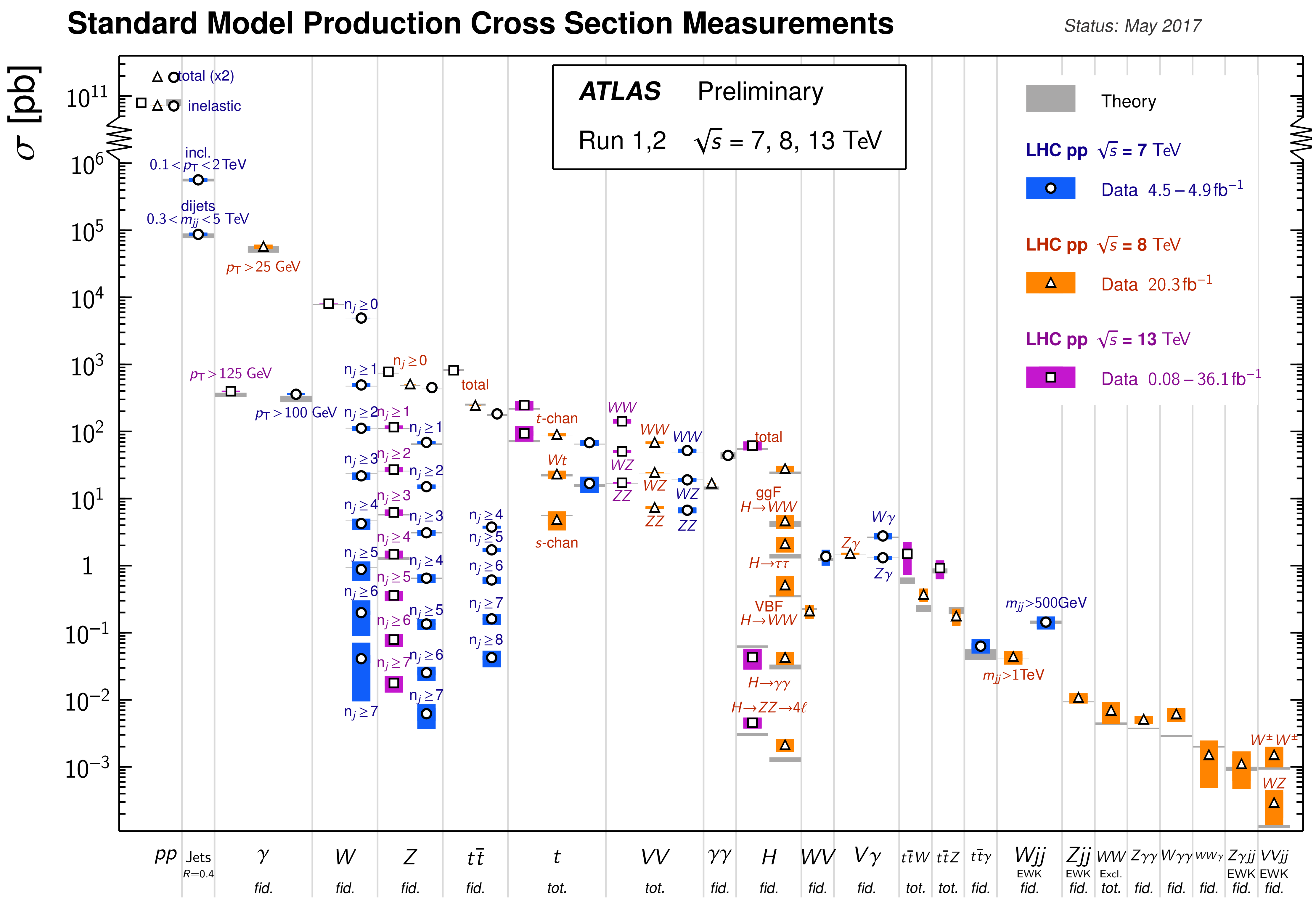

Perturbative sector of EW theory is very well understood!

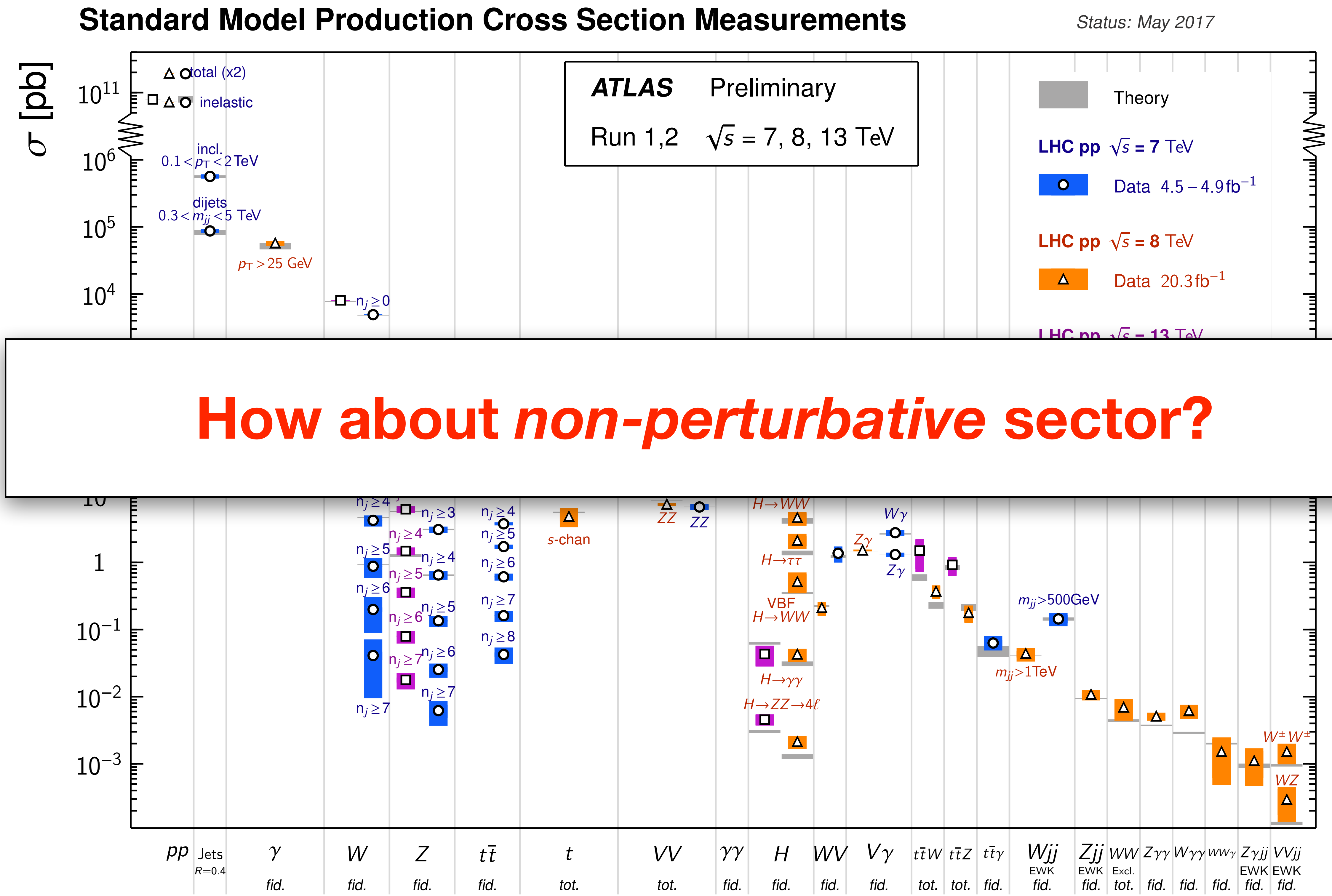

How about *non-perturbative* sector?

- In pure SU(2) YM theory, there are infinitely many gauge equivalent vacua.

$$A_\mu^a T^a = 0 \xrightarrow{\text{gauge trans.}} \frac{i}{g} U \partial_\mu U^\dagger$$

Vacua are as many as $U_{ij}(\mathbf{x})$

- In pure SU(2) YM theory, there are infinitely many gauge equivalent vacua.

$$A^a_\mu T^a = 0 \xrightarrow{\text{gauge trans.}} \frac{i}{g} U \partial_\mu U^\dagger$$

- Some of those vacuum configurations are not continuously connected.

$$U_{ij}(\mathbf{x})$$

$$\mathrm{SU}(2) \simeq S^3 \xleftarrow{\text{map}} S^3 \simeq R^3$$

topological gauge

$$U(\infty) \to \mathbf{1}$$

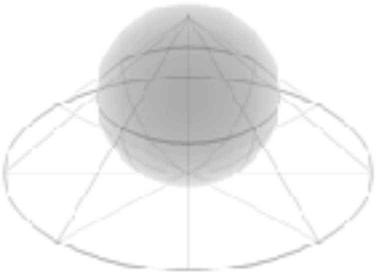

- In pure SU(2) YM theory, there are infinitely many gauge equivalent vacua.

$$A_\mu^a T^a = 0 \xrightarrow{\text{gauge trans.}} \frac{i}{g} U \partial_\mu U^\dagger$$

- Some of those vacuum configurations are not continuously connected.

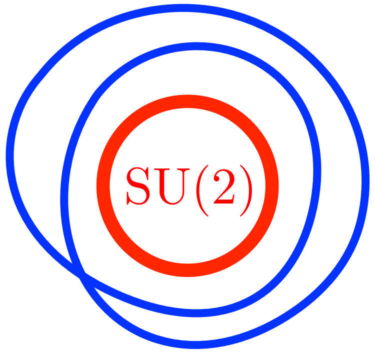

$$\pi_3(S^3) = \mathbb{Z}$$

$$\underbrace{U}_{\mathrm{SU}(2) \simeq S^3}{}_{ij}(\underbrace{\mathbf{x}}_{S^3 \simeq R^3})$$

$$\mathrm{SU}(2) \simeq S^3 \xleftarrow{\text{map}} S^3 \simeq R^3$$

topological gauge

$U(\infty) \to \mathbf{1}$

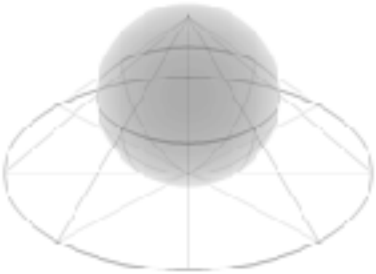

- In pure SU(2) YM theory, there are infinitely many gauge equivalent vacua.

$$A^a_\mu T^a = 0 \xrightarrow{\text{gauge trans.}} \frac{i}{g} U \partial_\mu U^\dagger$$

- Some of those vacuum configurations are not continuously connected.

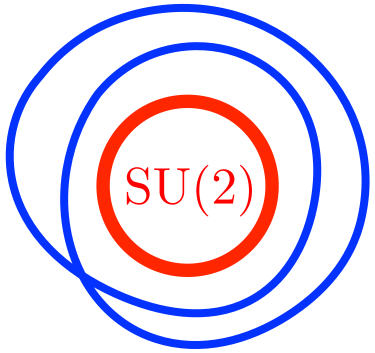

$$\pi_3(S^3) = \mathbb{Z}$$

$$U_{ij}(\mathbf{x})$$

$$\mathrm{SU}(2) \simeq S^3 \xleftarrow{\text{map}} S^3 \simeq R^3$$

topological gauge

$$U(\infty) \to \mathbf{1}$$

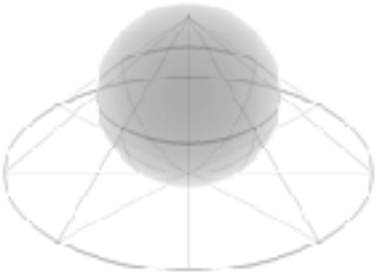

- These disconnected vacua are characterised by the integer *N*CS.

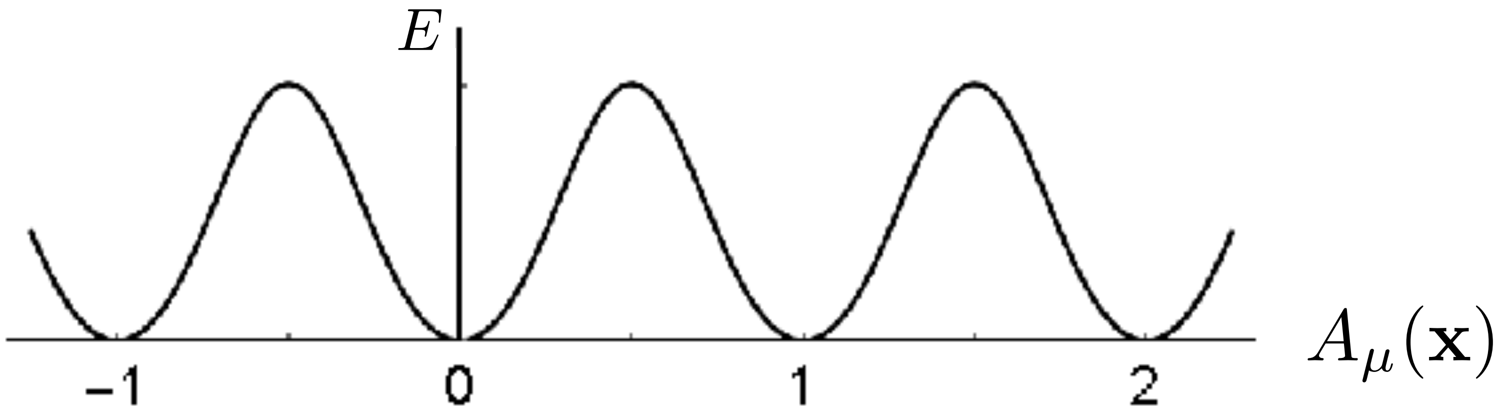

- One can think of transitions between disconnected vacua.

[Klinkhamer, Manton ’84]

$E_{\mathrm{sph}} \simeq 9\,\mathrm{TeV}$

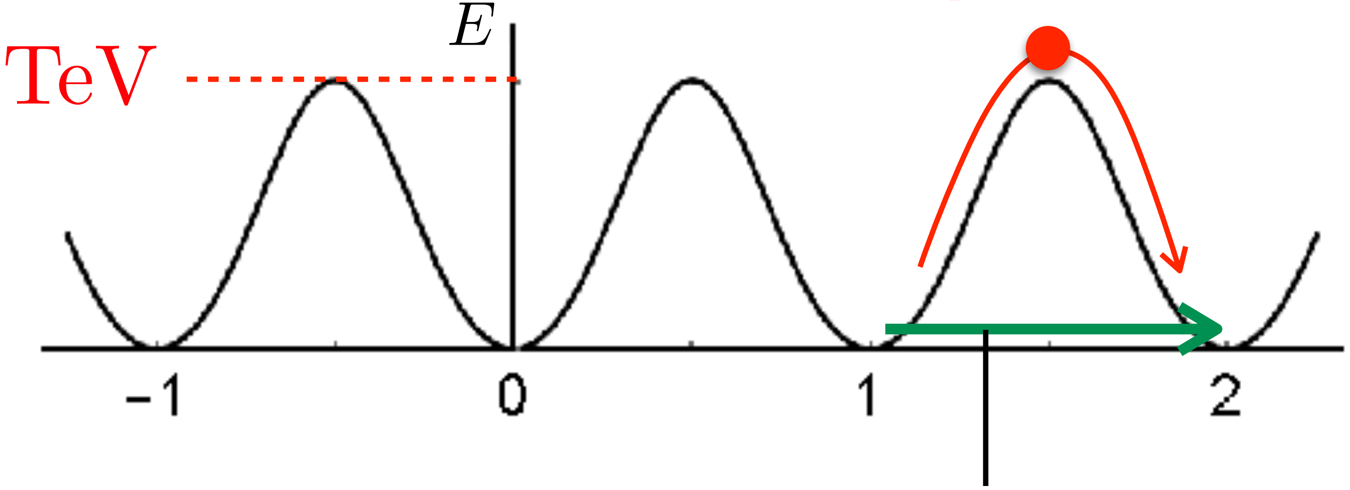

sphaleron — unstable solution sitting on top of the energy barrier

Instanton — quantum tunneling

- One can think of transitions between disconnected vacua.

[Klinkhamer, Manton ’84]

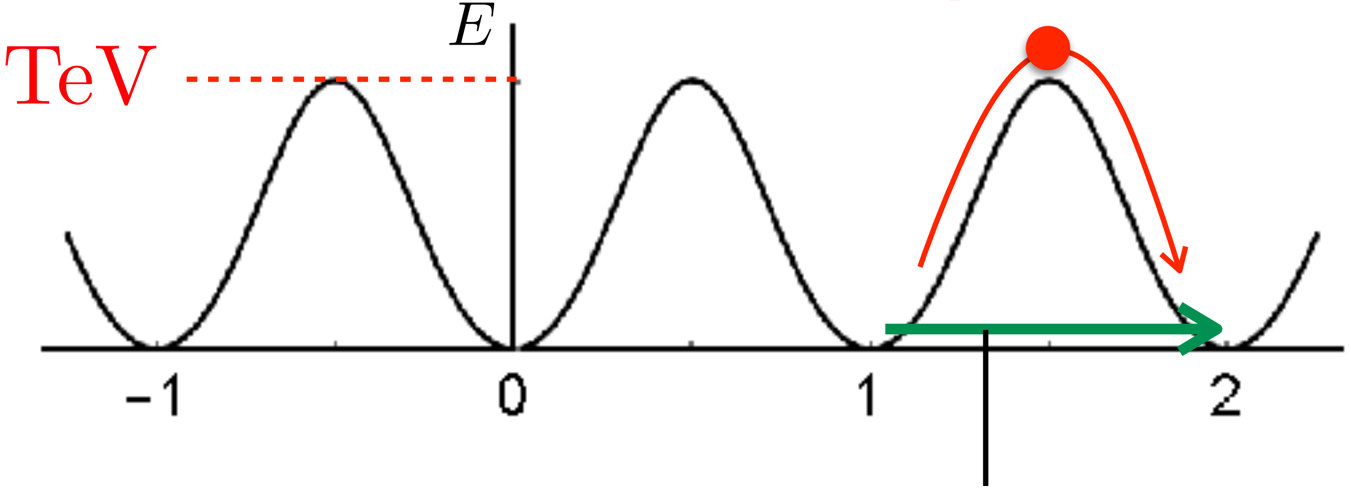

$E_{\rm sph} \simeq 9\,{\rm TeV}$

sphaleron

unstable solution sitting on top of the energy barrier

Instanton

quantum tunneling

- At zero temperature/energy, the instanton rate is exponentially small:

$$\langle N_{CS}|N_{CS}+1\rangle_{\rm instanton} \sim e^{-S[A_{cl}]} = e^{-\frac{2\pi}{\alpha_W}} \sim e^{-180}$$

- One can think of transitions between disconnected vacua.

[Klinkhamer, Manton ’84]

$E_{\rm sph} \simeq 9\,{\rm TeV}$

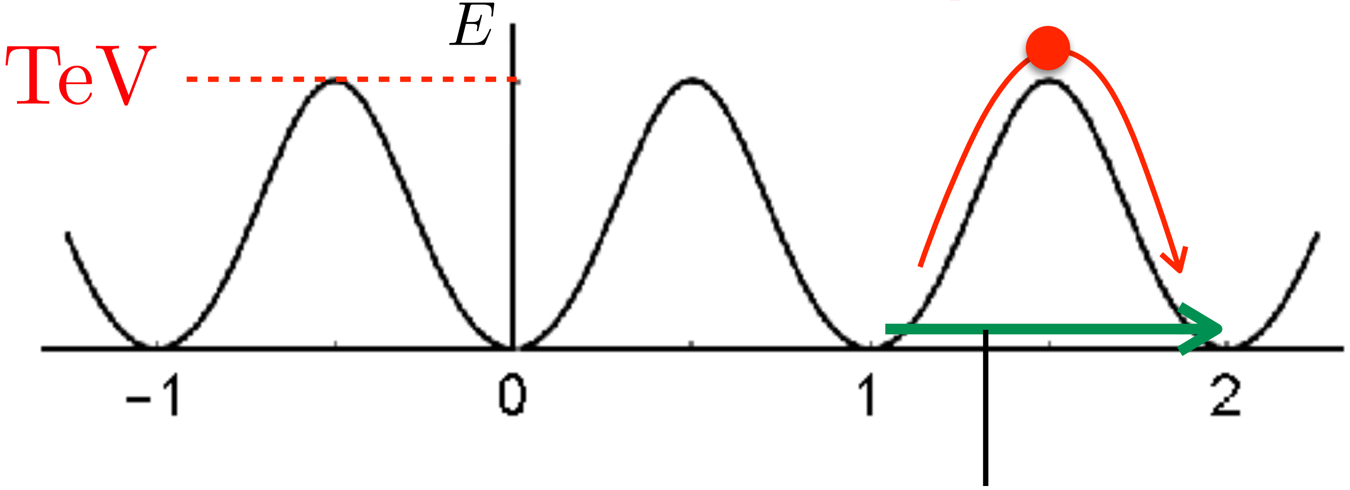

sphaleron — unstable solution sitting on top of the energy barrier

Instanton — quantum tunneling

- At zero temperature/energy, the instanton rate is exponentially small:

$$\langle N_{CS}|N_{CS}+1\rangle_{\rm instanton} \sim e^{-S[A_{cl}]} = e^{-\frac{2\pi}{\alpha_W}} \sim e^{-180}$$

- At temperature around TeV, the sphaleron rate is unsuppressed.

- One can think of transitions between disconnected vacua.

[Klinkhamer, Manton ’84]

$E_{\rm sph} \simeq 9\,{\rm TeV}$

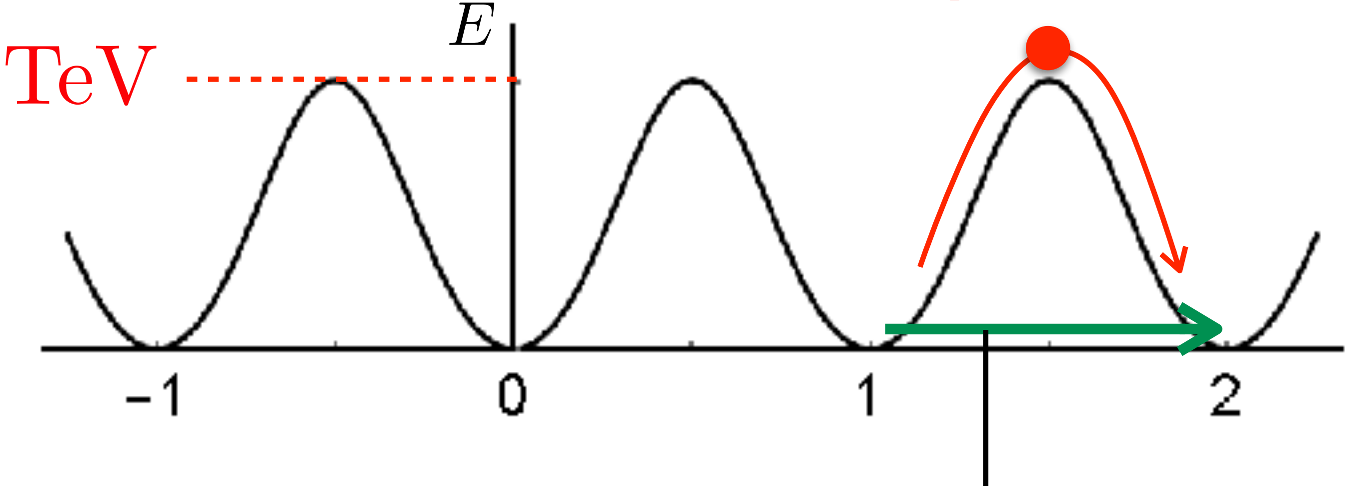

sphaleron — unstable solution sitting on top of the energy barrier

Instanton — quantum tunneling

- At zero temperature/energy, the instanton rate is exponentially small:

$$\langle N_{CS}|N_{CS}+1\rangle_{\rm instanton} \sim e^{-S[A_{cl}]} = e^{-\frac{2\pi}{\alpha_W}} \sim e^{-180}$$

- At temperature around TeV, the sphaleron rate is unsuppressed.

- What about the zero-temperature but high energy?

- The change of N_{CS} is related to the following quantity:

$$\Delta N_{CS} = \frac{g^2}{16\pi^2} \int \mathrm{Tr}\left[F_{\mu\nu}\tilde{F}^{\mu\nu}\right] d^4x$$

- The change of N_{CS} is related to the following quantity:

$$\Delta N_{CS} = \frac{g^2}{16\pi^2}\int \mathrm{Tr}\left[F_{\mu\nu}\tilde{F}^{\mu\nu}\right] d^4x \underset{\text{anomaly}}{=} \Delta N_F$$

SU(2) charged fermion

- The change of N

$$\Delta N_{CS} = \frac{g^2}{16\pi^2}\int \mathrm{Tr}\left[F_{\mu\nu}\tilde{F}^{\mu\nu}\right] d^4x \underset{\text{anomaly}}{=} \left\{ \begin{array}{l} \Delta N_{q_1^r} \\ \Delta N_{q_1^g} \\ \Delta N_{q_1^b} \\ \Delta N_{\ell_1} \end{array} \right. \times 3 \text{ flavour}$$

- The change of N$_{CS}$ is related to the following quantity:

$$\Delta N_{CS} = \frac{g^2}{16\pi^2}\int \mathrm{Tr}\left[F_{\mu\nu}\tilde{F}^{\mu\nu}\right] d^4x \underset{\text{anomaly}}{=} \left\{ \begin{array}{l} \Delta N_{q_1^r} \\ \Delta N_{q_1^g} \\ \Delta N_{q_1^b} \\ \Delta N_{\ell_1} \end{array} \right. \times 3\,\text{flavour}$$

- ΔN$_{CS}$ is related to the change of SU(2) charged fermion numbers.

$$\Delta B = \Delta L = 3\Delta N_{CS}$$

$$\Delta(B+L) \neq 0$$

$$\Delta(B-L) = 0$$

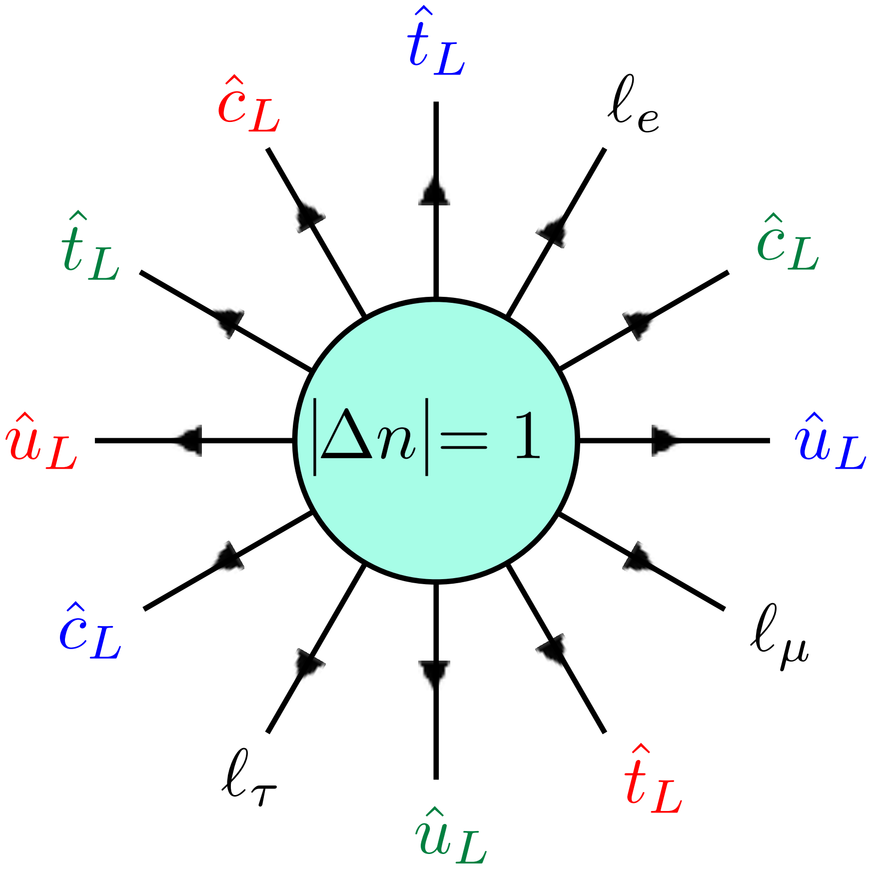

|ΔN$_{CS}$| = 1 transition creates 12 fermions altogether!

Party at collider!

- The LO Matrix Element in the ***instanton* background**

$$i\mathcal{M} \sim \int \mathcal{D}q\mathcal{D}W\mathcal{D}\phi\, q(x_1)\cdots q(x_{12}) W(y_1)\cdots W(y_{n_W}) \phi(z_1)\cdots\phi(z_{n_h})\exp(-S_E)\Big|_{\mathrm{LSZ}}$$

- The LO Matrix Element in the ***instanton* background**

$$i\mathcal{M} \sim \int \mathcal{D}q\mathcal{D}W\mathcal{D}\phi\, q(x_1)\cdots q(x_{12})W(y_1)\cdots W(y_{n_W})\phi(z_1)\cdots\phi(z_{n_h})\exp(-S_E)\Big|_{\mathrm{LSZ}}$$

- Evaluate it at the instanton configuration:

$$W^{\mu a}_{\mathrm{inst}} \simeq \frac{2\rho^2}{g}U_{ab}\frac{\bar{\eta}_{b\mu\nu}(x-x_0)_\nu}{(x-x_0)^2[(x-x_0)^2+\rho^2]} \qquad \phi_{\mathrm{inst}}(x) \simeq v\left[\frac{(x-x_0)^2}{(x-x_0)^2+\rho^2}\right]^{1/2}$$

orientation position size

- The LO Matrix Element in the ***instanton* background**

$$i\mathcal{M} \sim \int \mathcal{D}q\mathcal{D}W\mathcal{D}\phi\, q(x_1)\cdots q(x_{12})W(y_1)\cdots W(y_{n_W})\phi(z_1)\cdots\phi(z_{n_h})\exp(-S_E)\Big|_{\text{LSZ}}$$

- Evaluate it at the instanton configuration:

$$W^{\mu a}_{\text{inst}} \simeq \frac{2\rho^2}{g}U_{ab}\frac{\bar{\eta}_{b\mu\nu}(x-x_0)_\nu}{(x-x_0)^2[(x-x_0)^2+\rho^2]} \qquad \phi_{\text{inst}}(x) \simeq v\left[\frac{(x-x_0)^2}{(x-x_0)^2+\rho^2}\right]^{1/2}$$

orientation position size

- Integration over orientation, position, size and phase-space:

$$\sigma(n_W, n_h) \sim \int |\mathcal{M}|^2 \cdot d\Phi_{\text{PS}}$$

- The LO Matrix Element in the ***instanton* background**

$$i\mathcal{M} \sim \int \mathcal{D}q\mathcal{D}W\mathcal{D}\phi\, q(x_1)\cdots q(x_{12}) W(y_1)\cdots W(y_{n_W}) \phi(z_1)\cdots\phi(z_{n_h}) \exp(-S_E)\Big|_{\text{LSZ}}$$

- Evaluate it at the instanton configuration:

$$W^{\mu a}_{\text{inst}} \simeq \frac{2\rho^2}{g} U_{ab} \frac{\bar{\eta}_{b\mu\nu}(x-x_0)_\nu}{(x-x_0)^2[(x-x_0)^2+\rho^2]} \qquad \phi_{\text{inst}}(x) \simeq v\left[\frac{(x-x_0)^2}{(x-x_0)^2+\rho^2}\right]^{1/2}$$

orientation position size

- Integration over orientation, position, size and phase-space:

$$\sigma(n_W, n_h) \sim \int |\mathcal{M}|^2 \cdot d\Phi_{\text{PS}}$$

- Result

[Ringwald '90, Espinosa '90]

$$\sigma_{\text{LO}}(n_W, n_h) \sim \mathscr{G}^2 2^n v^{-2n} \left[\frac{\Gamma(n+103/12)}{\Gamma(103/12)}\right]^2 \frac{1}{n_B! n_H!} \qquad \mathscr{G} = 1.6\times 10^{-101}\,\text{GeV}^{-14}$$

$$\times \int \prod_{i=1}^{10} \frac{d^3 p_i}{(2\pi)^3 2E_i} E_i \prod_{j=1}^{n_B} \frac{d^3 p_j}{(2\pi)^3 2E_j} \frac{2(4E_j^2 - m_W^2)}{m_W^2} \prod_{k=1}^{n_H} \frac{d^3 p_k}{(2\pi)^3 2E_k} (2\pi)^4 \delta^{(4)}\left(P_{\text{in}} - \sum_{i=1}^{10} p_i - \sum_{j=1}^{n_B} p_j - \sum_{k=1}^{n_H} p_k\right)$$

The cross-section grows exponentially as increasing # of EW and H bosons!

$$i\mathcal{M} \sim \int \mathcal{D}q\mathcal{D}W\mathcal{D}\phi\, q(x_1)\cdots q(x_{12}) W(y_1)\cdots W(y_{n_W})\phi(z_1)\cdots\phi(z_{n_h})\exp(-S_E)\Big|_{\text{LSZ}}$$

$$A^{\text{inst}\,a}_{\ \mu}(x_i) \xrightarrow{\textbf{FT}} \frac{4i\pi^2\rho^2}{g}\frac{\bar\eta^a_{\mu\nu}p_i^\nu}{p_i^2(p_i^2+m_W^2)}\,e^{ip_ix_0} \xrightarrow{\textbf{LSZ}} \boxed{\frac{4i\pi^2\rho^2}{g}\frac{\bar\eta^a_{\mu\nu}p_i^\nu}{p_i^2}\,e^{ip_ix_0}}$$

$$H^{\text{inst}}(x_j) \to -\frac{2\pi^2\rho^2 v}{(p_j^2+m_H^2)}\,e^{ip_jx_0} \to \boxed{-2\pi^2\rho^2 v\, e^{ip_jx_0}}$$

- Multi-particle interaction under the instanton BG is (almost) a point-like vertex

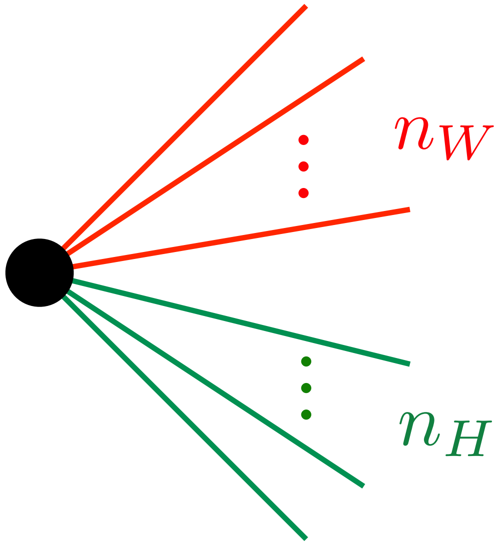

$$i\mathcal{M} \sim \left[\frac{4i\pi^2\rho^2}{g}\frac{\bar\eta^a_{\mu\nu}p_i^\nu}{p_i^2}\,e^{ip_ix_0}\right]^{n_W}\left[-2\pi^2\rho^2 v\, e^{ip_jx_0}\right]^{n_H}$$

$$\Phi_n(Q) \sim (Q^2)^{n-2}$$

Such a vertex is highly unrenormalisable and high energy behaviour is not regulated.

Enhancement at large *n* is understood.

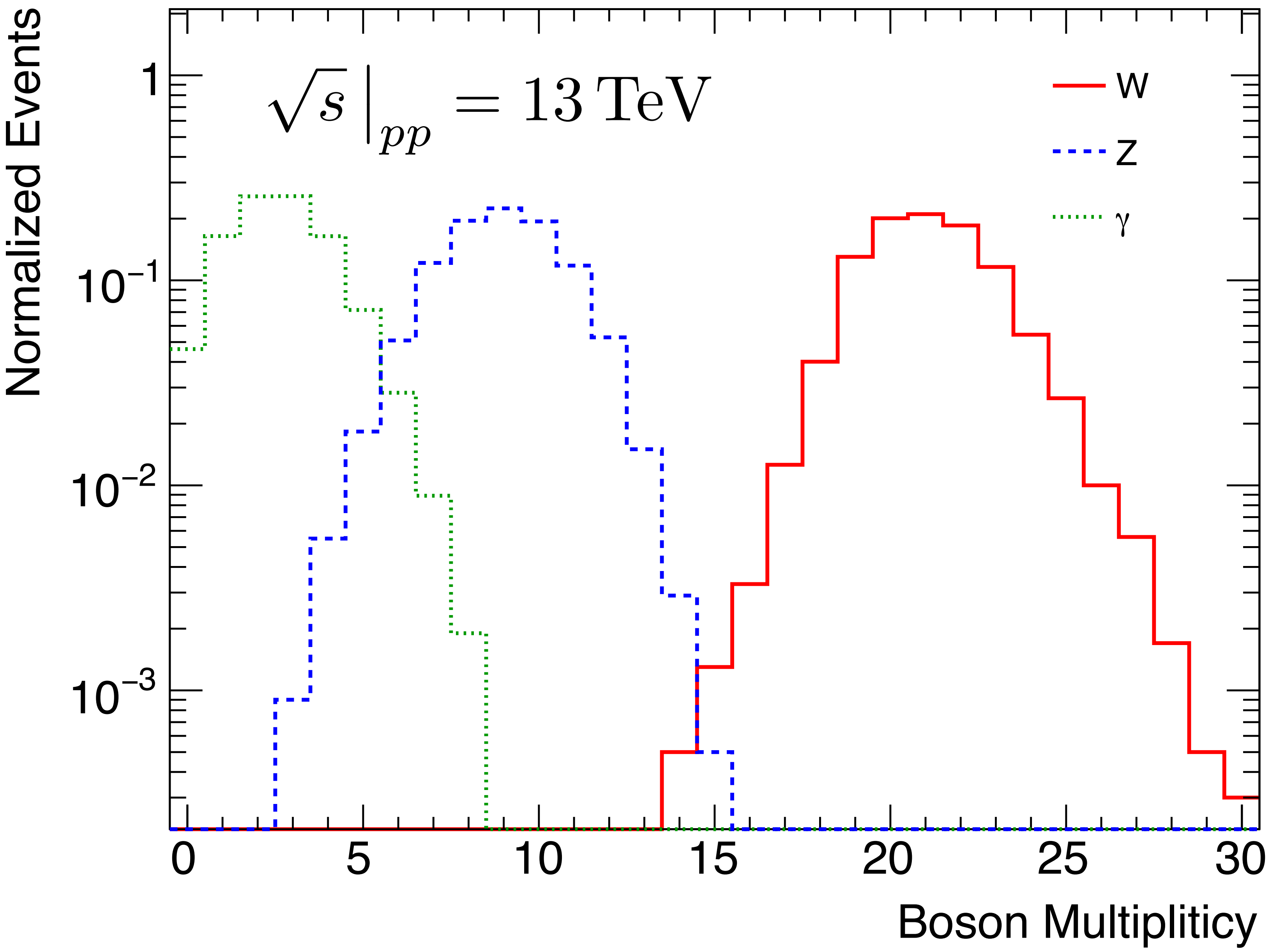

O(30) EW gauge bosons are produced!

Festival at collider!

- The inclusive cross-section can be estimated using the dispersion relations (optical theorem).

[Khoze, Ringwald '91]

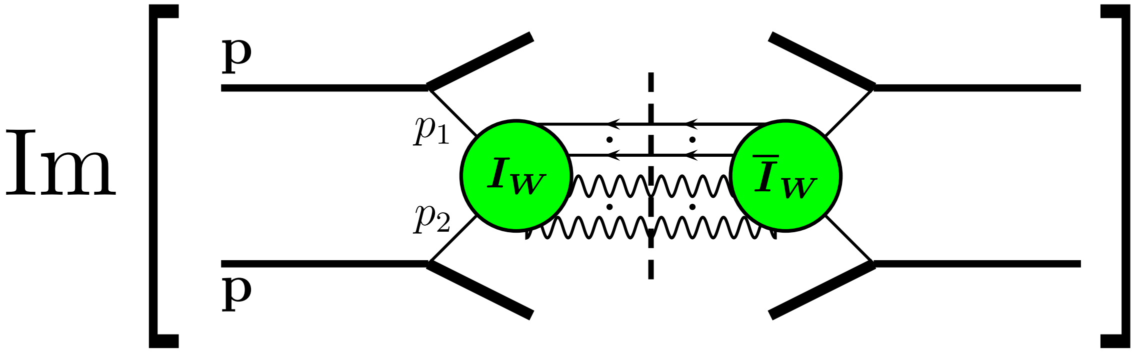

$$\hat{\sigma}^{\rm BV}_{\rm incl} \equiv \sum_{n_W, n_h} \hat{\sigma}^{\rm BV}_{n_W, n_h} = \frac{P(\epsilon)}{m_W^2} \exp\left[-\frac{4\pi}{\alpha_W} F(\epsilon)\right]$$

$$F(\epsilon) = 1 - \frac{9}{8}\epsilon^{4/3} + \frac{9}{16}\epsilon^2 - \frac{3}{32}\left(4 - 3\frac{m_h^2}{m_W^2}\right)\epsilon^{8/3} \ln\frac{1}{\epsilon} + \mathcal{O}(\epsilon^{8/3} \cdot \text{const})$$

$$P(\epsilon) = \frac{\pi^{15/2}}{1024}\left(\frac{3}{2}\right)^{\frac{2}{3}} d^2 \left(\frac{4\pi}{\alpha_W}\right)^{7/2} \epsilon^{\frac{74}{9}} \left[1 + \mathcal{O}\left(\epsilon^{2/3}\right)\right] \qquad d \simeq 0.15$$

$$\epsilon \equiv \frac{\sqrt{\hat{s}}}{M_0} \qquad M_0 \equiv \sqrt{6}\pi \frac{m_W}{\alpha_W} \simeq 18.3\ \text{TeV}$$

- The inclusive cross-section can be estimated using the dispersion relations (optical theorem).

[Khoze, Ringwald '91]

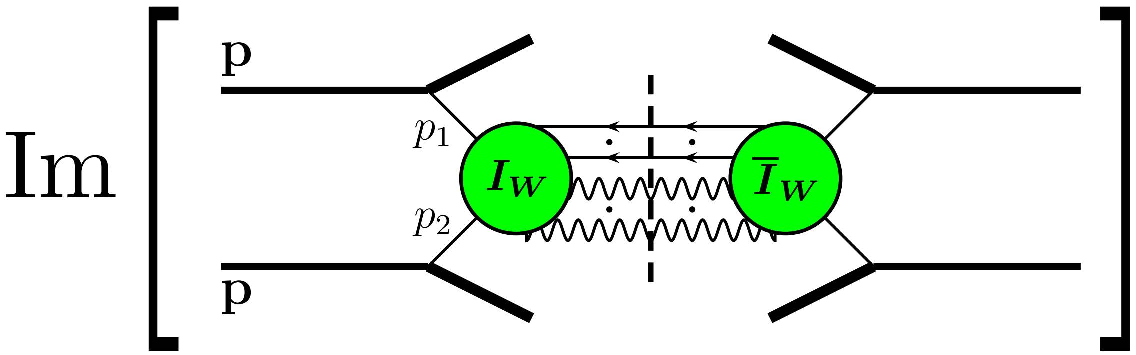

$$\hat{\sigma}^{\mathrm{BV}}_{\mathrm{incl}} \equiv \sum_{n_W,n_h} \hat{\sigma}^{\mathrm{BV}}_{n_W,n_h} = \frac{P(\epsilon)}{m_W^2} \exp\left[-\frac{4\pi}{\alpha_W}\boxed{F(\epsilon)}\right]$$

'holy grail' function

$$\boxed{F(\epsilon)} = 1 - \frac{9}{8}\epsilon^{4/3} + \frac{9}{16}\epsilon^2 - \frac{3}{32}\left(4 - 3\frac{m_h^2}{m_W^2}\right)\epsilon^{8/3}\ln\frac{1}{\epsilon} + \mathcal{O}(\epsilon^{8/3}\cdot\mathrm{const})$$

$$P(\epsilon) = \frac{\pi^{15/2}}{1024}\left(\frac{3}{2}\right)^{\frac{2}{3}} d^2 \left(\frac{4\pi}{\alpha_W}\right)^{7/2} \epsilon^{\frac{74}{9}} \left[1 + \mathcal{O}\left(\epsilon^{2/3}\right)\right] \qquad d \simeq 0.15$$

$$\epsilon \equiv \frac{\sqrt{\hat{s}}}{M_0} \qquad M_0 \equiv \sqrt{6}\pi\frac{m_W}{\alpha_W} \simeq 18.3\ \mathrm{TeV}$$

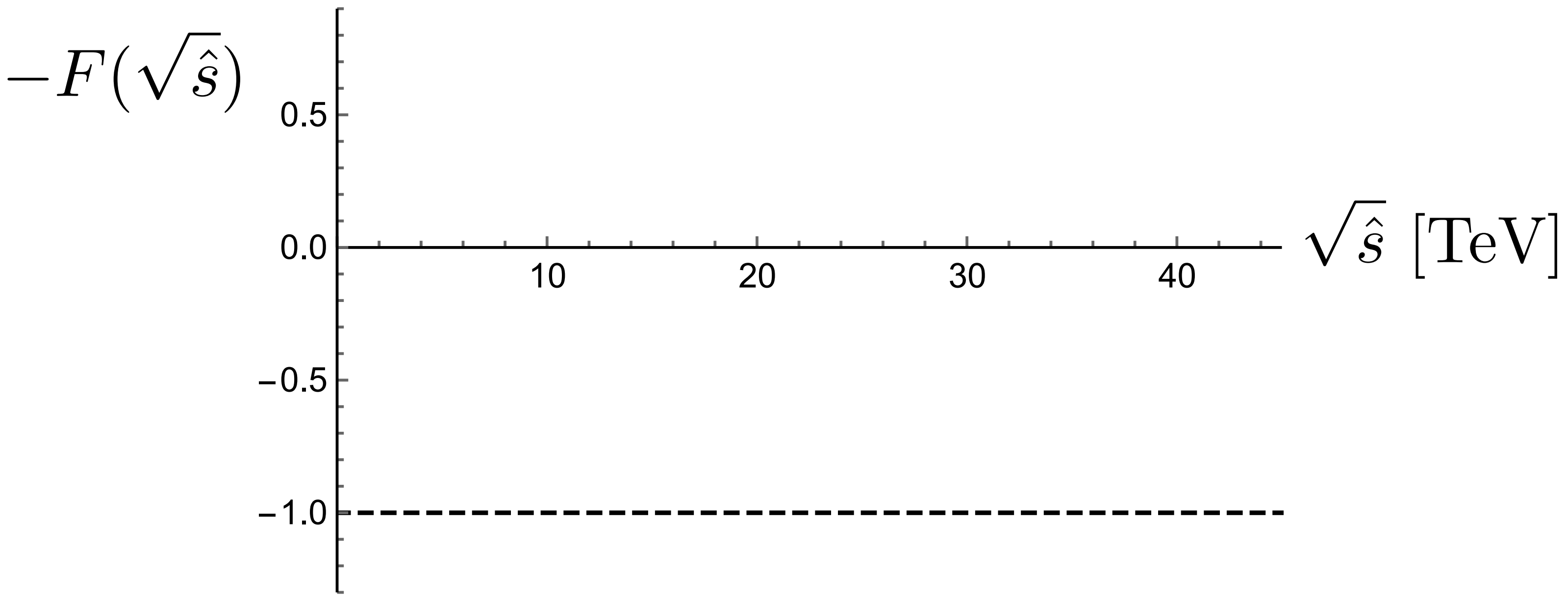

- The inclusive cross-section can be estimated using the dispersion relations (optical theorem).

[Khoze, Ringwald ’91]

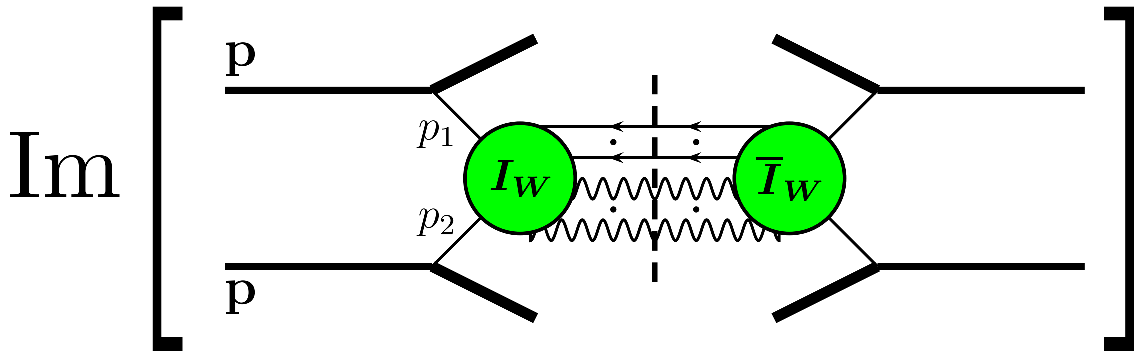

$$\hat{\sigma}^{\mathrm{BV}}_{\mathrm{incl}} \equiv \sum_{n_W,n_h} \hat{\sigma}^{\mathrm{BV}}_{n_W,n_h} = \frac{P(\epsilon)}{m_W^2} \exp\left[-\frac{4\pi}{\alpha_W}\boxed{F\left(\epsilon\right)}\right]$$

‘holy grail’ function

$$\boxed{F(\epsilon)} = 1 - \frac{9}{8}\epsilon^{4/3} + \frac{9}{16}\epsilon^2 - \frac{3}{32}\left(4 - 3\frac{m_h^2}{m_W^2}\right)\epsilon^{8/3}\ln\frac{1}{\epsilon} + \mathcal{O}(\epsilon^{8/3}\cdot\mathrm{const})$$

$$P(\epsilon) = \frac{\pi^{15/2}}{1024}\left(\frac{3}{2}\right)^{\frac{2}{3}} d^2 \left(\frac{4\pi}{\alpha_W}\right)^{7/2} \epsilon^{\frac{74}{9}} \left[1 + \mathcal{O}\left(\epsilon^{2/3}\right)\right] \qquad d \simeq 0.15$$

$$\epsilon \equiv \frac{\sqrt{\hat{s}}}{M_0} \qquad M_0 \equiv \sqrt{6}\pi\frac{m_W}{\alpha_W} \simeq 18.3\ \mathrm{TeV}$$

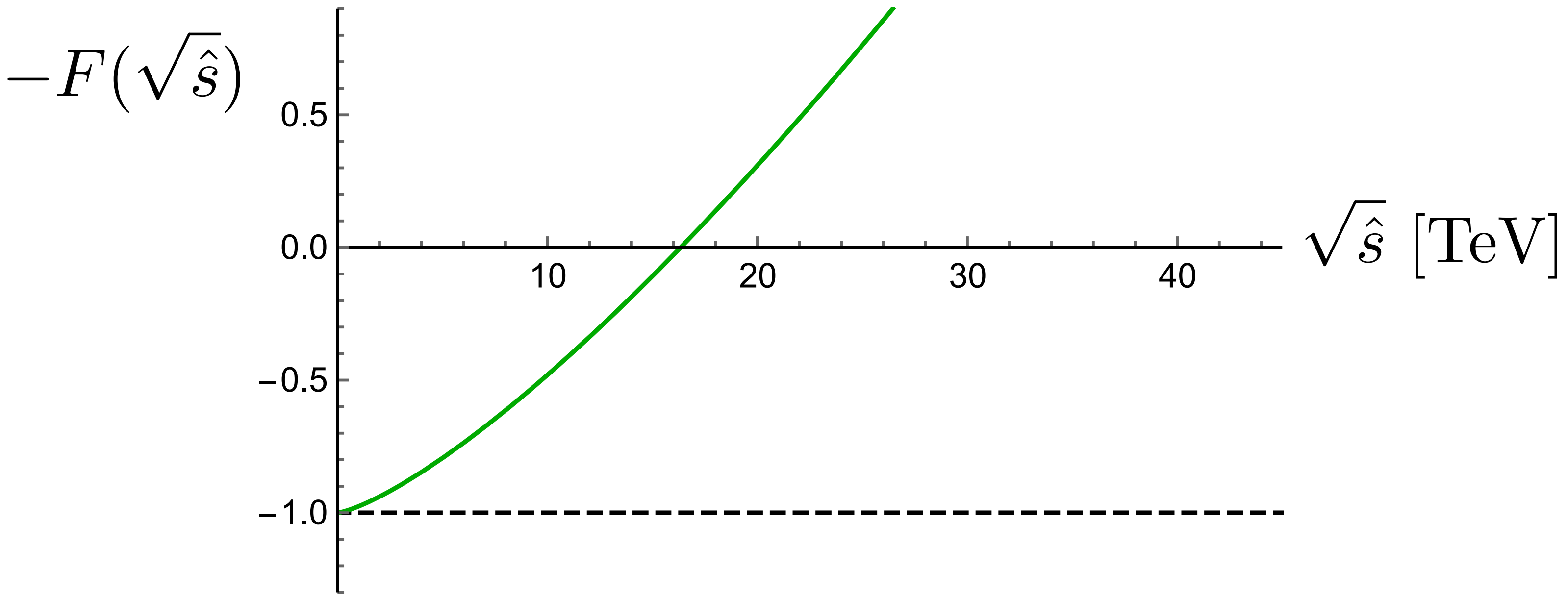

- The inclusive cross-section can be estimated using the dispersion relations (optical theorem).

[Khoze, Ringwald '91]

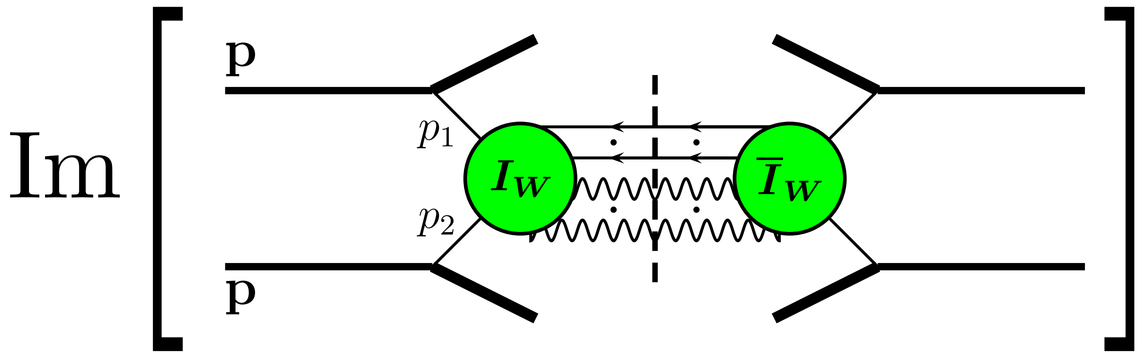

$$\hat{\sigma}^{\mathrm{BV}}_{\mathrm{incl}} \equiv \sum_{n_W,n_h} \hat{\sigma}^{\mathrm{BV}}_{n_W,n_h} = \frac{P(\epsilon)}{m_W^2} \exp\left[-\frac{4\pi}{\alpha_W} \boxed{F(\epsilon)}\right]$$

'holy grail' function $\longrightarrow$

$$\boxed{F(\epsilon)} = 1 - \frac{9}{8}\epsilon^{4/3} + \frac{9}{16}\epsilon^2 - \frac{3}{32}\left(4 - 3\frac{m_h^2}{m_W^2}\right)\epsilon^{8/3}\ln\frac{1}{\epsilon} + \mathcal{O}(\epsilon^{8/3}\cdot\mathrm{const})$$

$$P(\epsilon) = \frac{\pi^{15/2}}{1024}\left(\frac{3}{2}\right)^{\frac{2}{3}} d^2 \left(\frac{4\pi}{\alpha_W}\right)^{7/2} \epsilon^{\frac{74}{9}}\left[1 + \mathcal{O}\left(\epsilon^{2/3}\right)\right] \qquad d \simeq 0.15$$

$$\epsilon \equiv \frac{\sqrt{\hat{s}}}{M_0} \qquad M_0 \equiv \sqrt{6}\pi\frac{m_W}{\alpha_W} \simeq 18.3\ \mathrm{TeV}$$

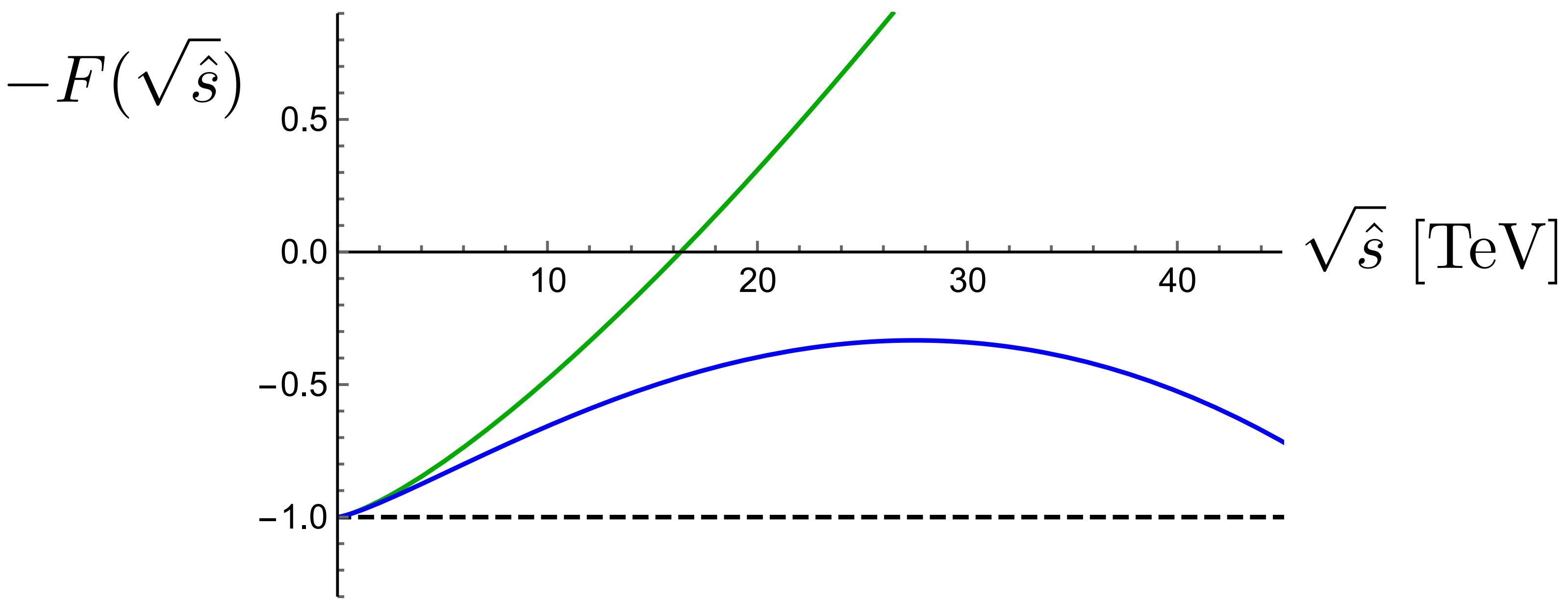

- The inclusive cross-section can be estimated using the dispersion relations (optical theorem).

[Khoze, Ringwald '91]

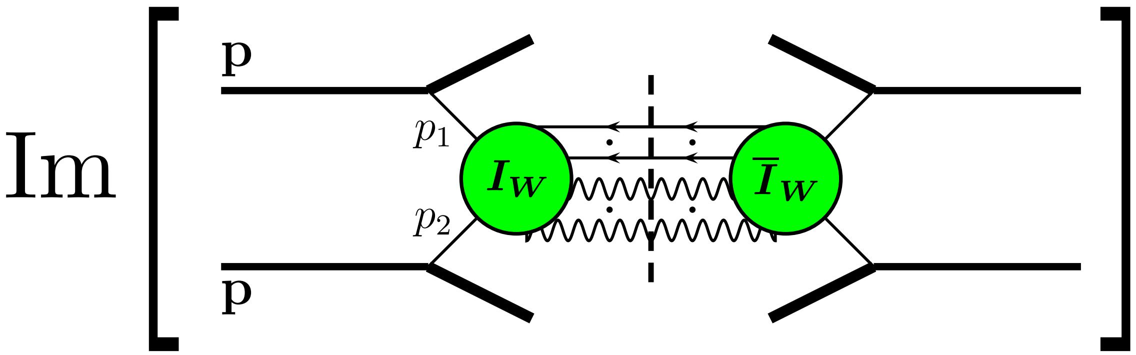

$$\hat{\sigma}^{\rm BV}_{\rm incl} \equiv \sum_{n_W,n_h} \hat{\sigma}^{\rm BV}_{n_W,n_h} = \frac{P(\epsilon)}{m_W^2} \exp\left[-\frac{4\pi}{\alpha_W} \boxed{F(\epsilon)}\right]$$

'holy grail' function

$$\boxed{F(\epsilon)} = 1 - \frac{9}{8}\epsilon^{4/3} + \frac{9}{16}\epsilon^2 - \frac{3}{32}\left(4 - 3\frac{m_h^2}{m_W^2}\right)\epsilon^{8/3}\ln\frac{1}{\epsilon} + \mathcal{O}(\epsilon^{8/3}\cdot{\rm const})$$

$$P(\epsilon) = \frac{\pi^{15/2}}{1024}\left(\frac{3}{2}\right)^{\frac{2}{3}} d^2 \left(\frac{4\pi}{\alpha_W}\right)^{7/2} \epsilon^{\frac{74}{9}} \left[1 + \mathcal{O}\left(\epsilon^{2/3}\right)\right] \qquad d \simeq 0.15$$

$$\epsilon \equiv \frac{\sqrt{\hat{s}}}{M_0} \qquad M_0 \equiv \sqrt{6}\pi\frac{m_W}{\alpha_W} \simeq 18.3~{\rm TeV}$$

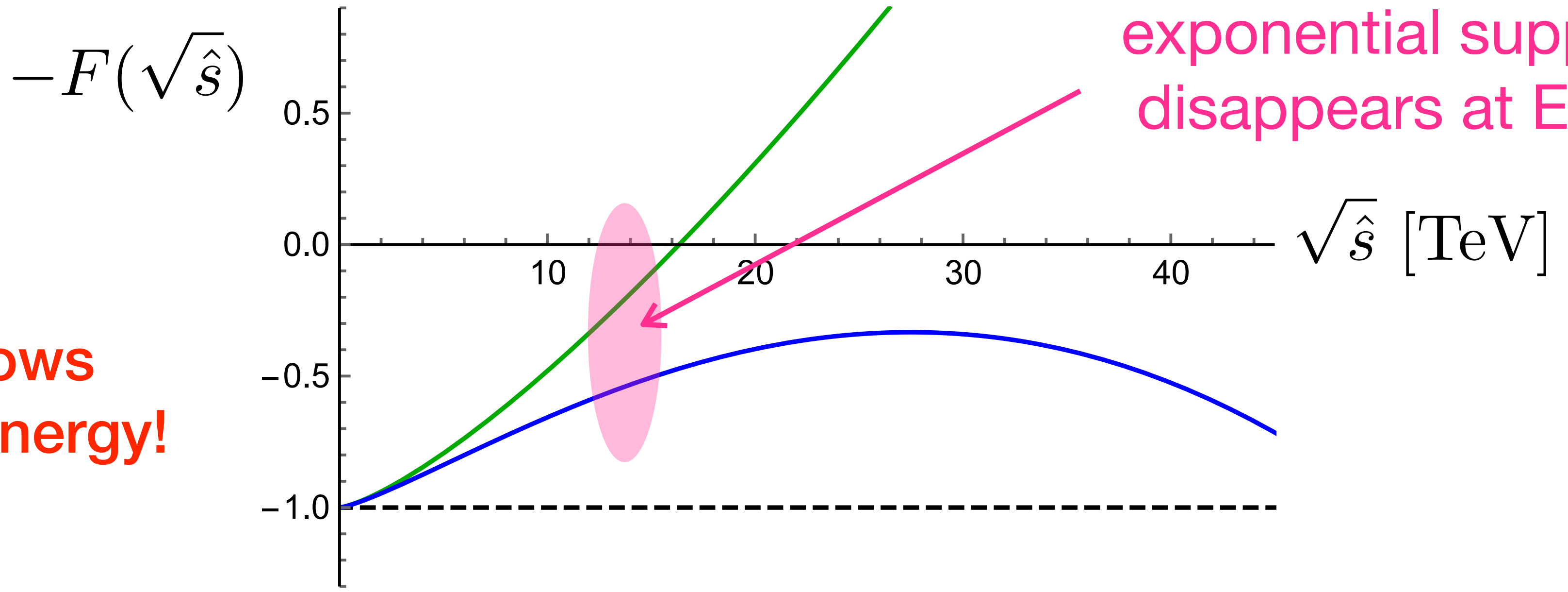

exponential suppression disappears at E ~ $E_{\rm sph}$?

Cross-section grows exponentially with energy!

Phenomenological parametrisation for cross-section:

partonic:

$$\hat{\sigma}_0(\sqrt{\hat{s}}) = \frac{p_{\rm sph}}{m_W^2}\Theta(\sqrt{\hat{s}} - E_{\rm thr}) \qquad \hat{\sigma}^{\rm max}_{\rm unitary}(\sqrt{\hat{s}}) = \frac{16\pi}{\hat{s}}$$

$$\hat{\sigma}(\sqrt{\hat{s}}) = \min(\hat{\sigma}_0, \hat{\sigma}^{\rm max}_{\rm unitary})$$

hadronic:

$$\sigma_{pp}(\sqrt{s}) = \sum_{ab} \int dx_1 dx_2 f_a(x_1) f_a(x_2) \hat{\sigma}(\sqrt{s x_1 s_2})$$

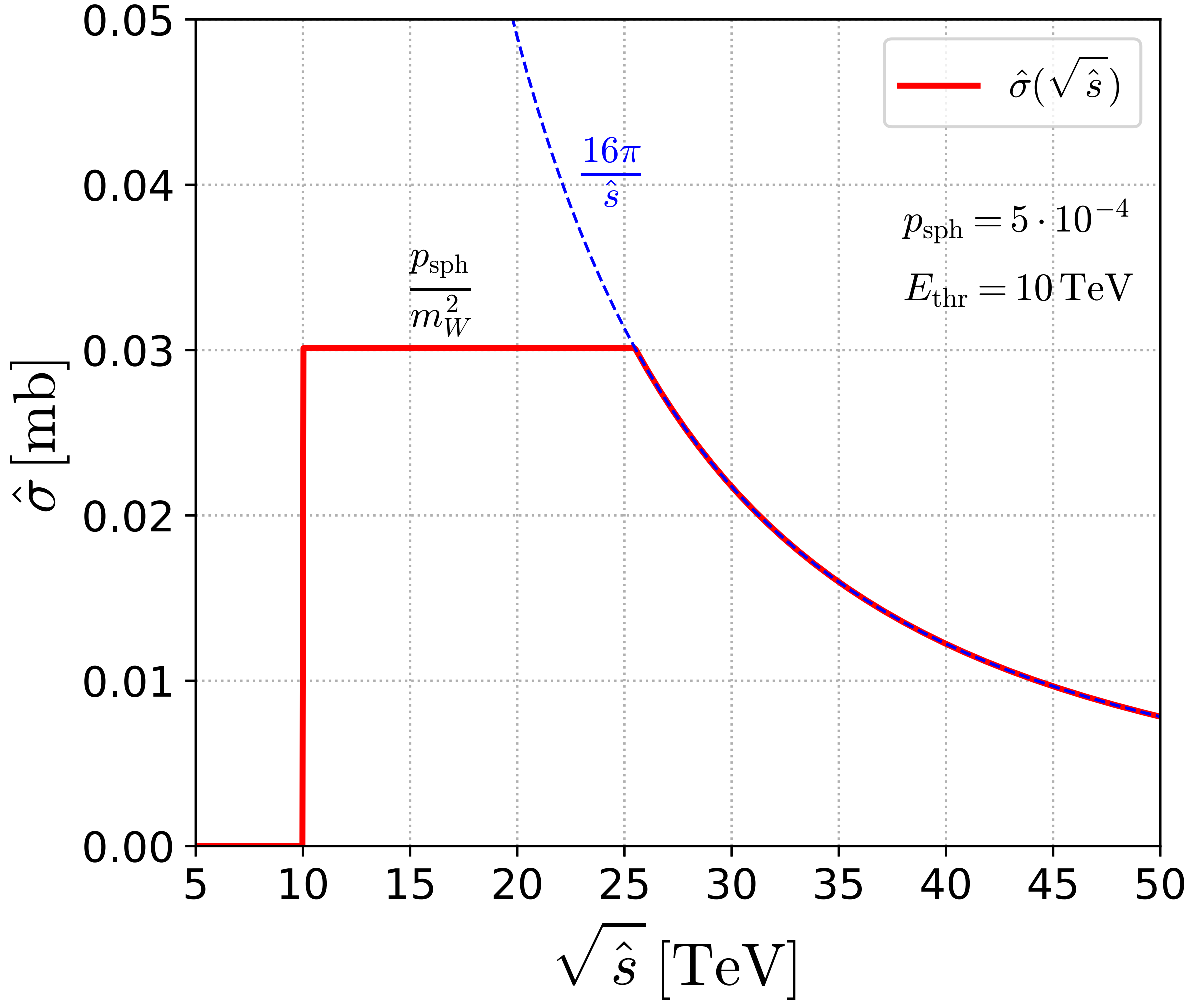

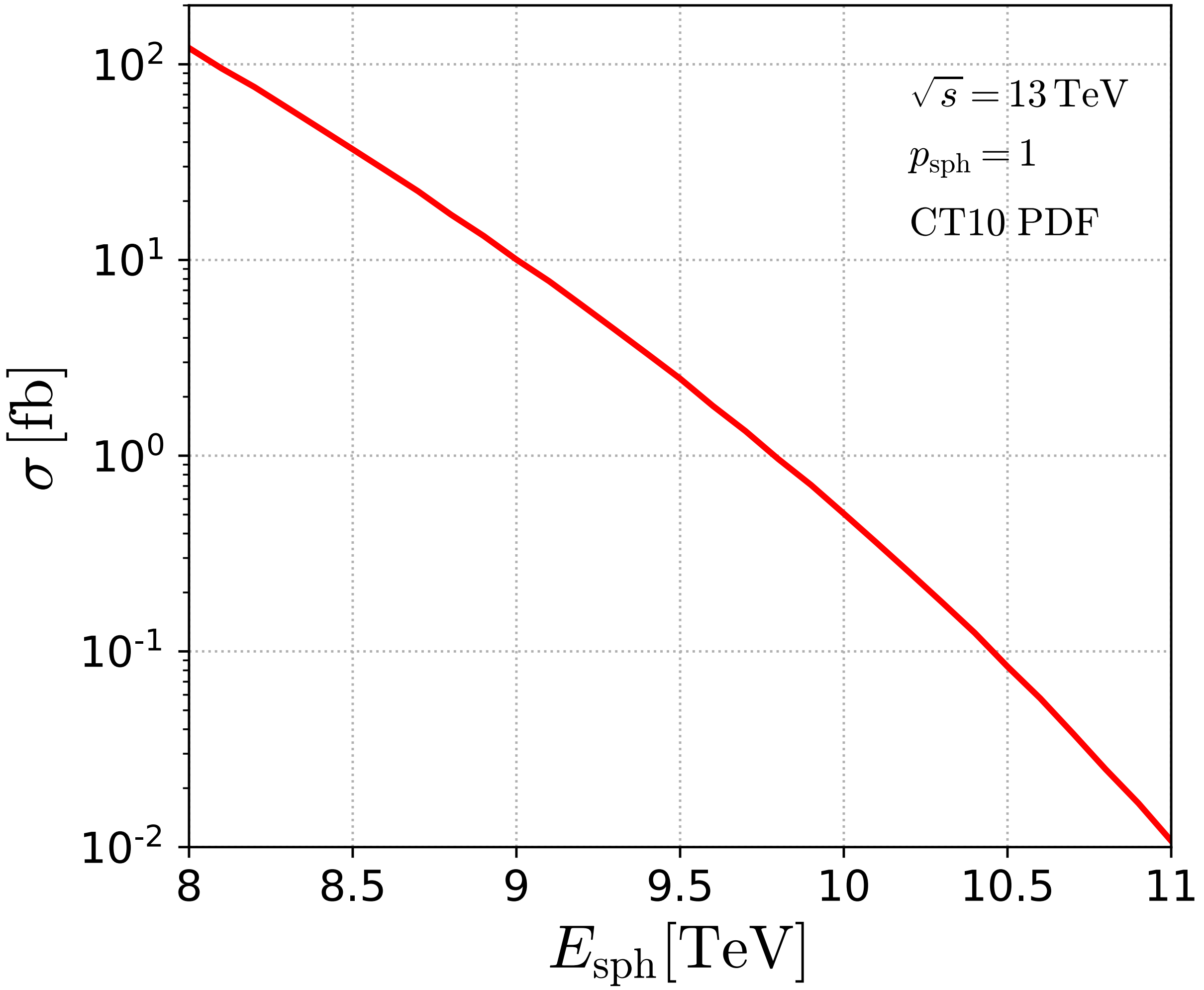

Cross Section

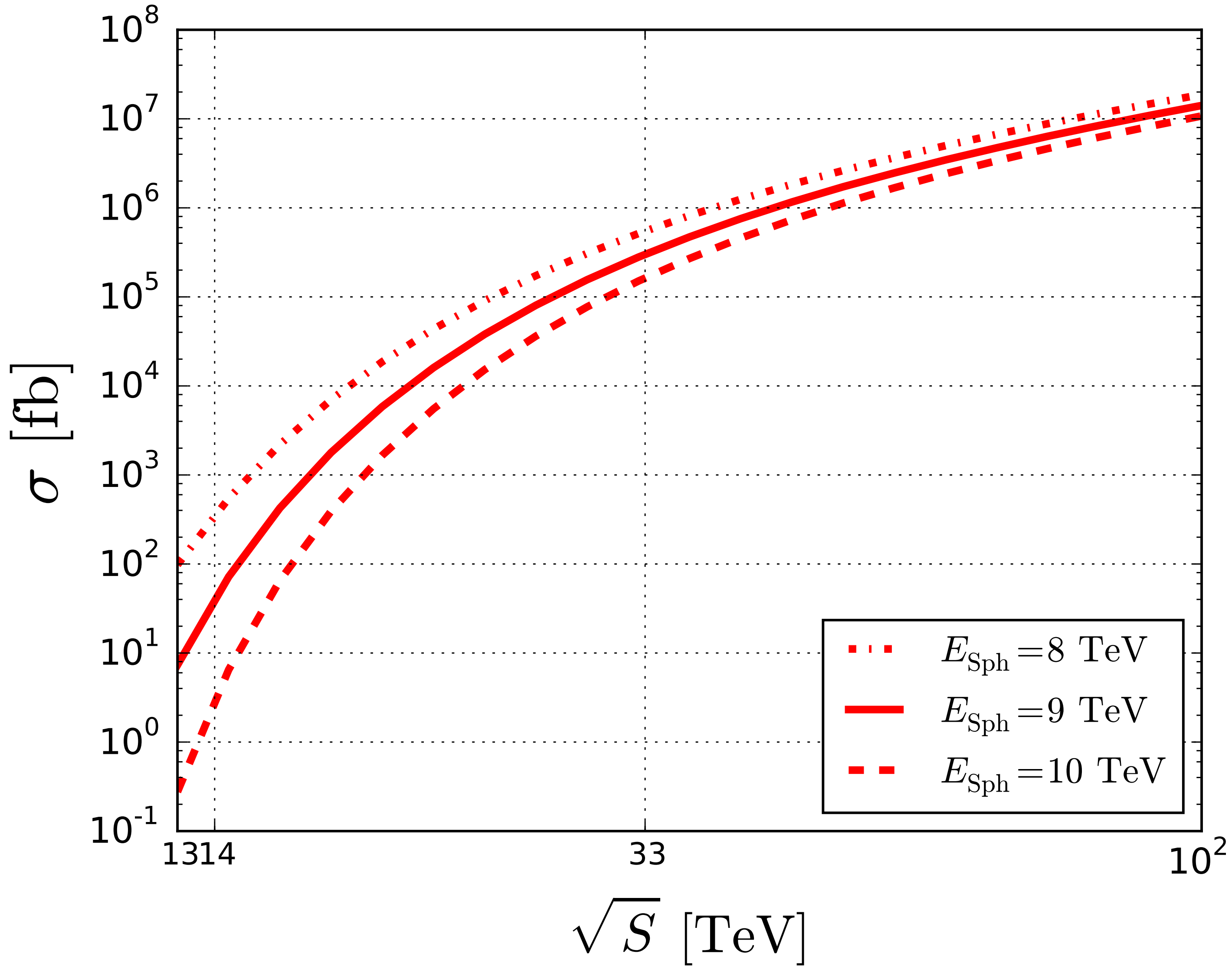

$p = 1$

$E_{\rm Sph} = 9\,{\rm TeV}$

J. Ellis, KS
[1601.03654]

	Sphaleron	gg→H
13 TeV	7.3 fb	44 x 10^3 fb
14 TeV	41 fb	50 x 10^3 fb
33 TeV	0.3 x 10^6 fb	0.2 x 10^6 fb
100 TeV	141 x 10^6 fb	0.7 x 10^6 fb

- We have implemented EW instanton/sphaleron processes at hadron collider in HERWIG7 framework.
- comparison with other generators:

	written in	Multi-Boson	Unitarity
HERBVI	Fortran	**LO**	No
BaryoGEN	**C++**	No	No
HERWIG7	**C++**	**LO + (E_freeze)**	**Yes**

LO prediction cannot be trusted for $\sqrt{s}$ > 10TeV.

For $\sqrt{s}$ > E_freeze, the LO Boson multiplicity distribution obtained for $\sqrt{s}$ = E_freeze is used.

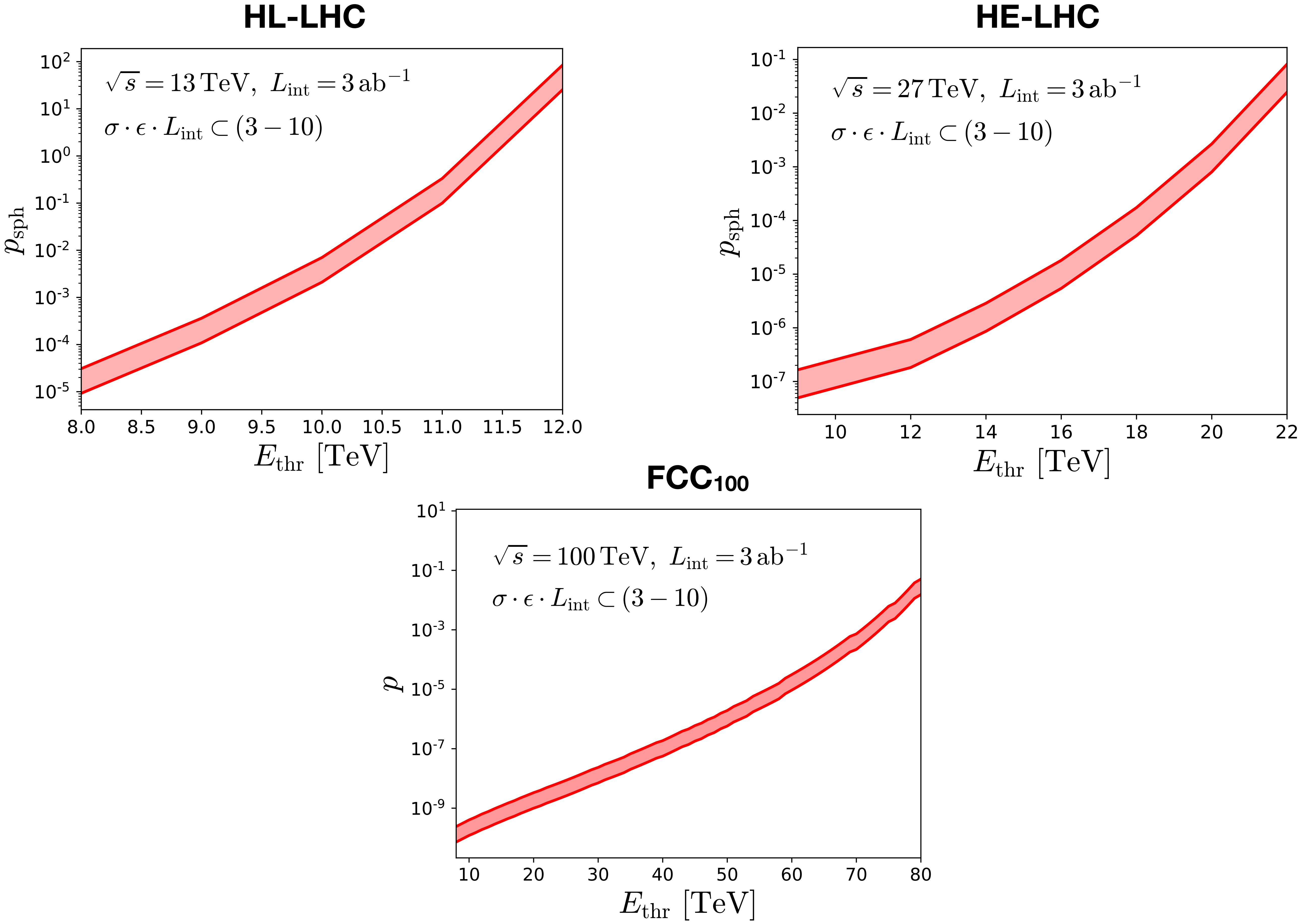
HL-LHC
$\sqrt{s} = 13\,\mathrm{TeV},\ L_{\mathrm{int}} = 3\,\mathrm{ab}^{-1}$
$\sigma \cdot \epsilon \cdot L_{\mathrm{int}} \subset (3-10)$
p_{sph}
10^{2}
10^{1}
10^{0}
10^{-1}
10^{-2}
10^{-3}
10^{-4}
10^{-5}
8.0
8.5
9.0
9.5
10.0
10.5
11.0
11.5
12.0
E_{thr} [TeV]
HE-LHC
$\sqrt{s} = 27\,\mathrm{TeV},\ L_{\mathrm{int}} = 3\,\mathrm{ab}^{-1}$
$\sigma \cdot \epsilon \cdot L_{\mathrm{int}} \subset (3-10)$
p_{sph}
10^{-1}
10^{-2}
10^{-3}
10^{-4}
10^{-5}
10^{-6}
10^{-7}
10
12
14
16
18
20
22
E_{thr} [TeV]
FCC$_{100}$
$\sqrt{s} = 100\,\mathrm{TeV},\ L_{\mathrm{int}} = 3\,\mathrm{ab}^{-1}$
$\sigma \cdot \epsilon \cdot L_{\mathrm{int}} \subset (3-10)$
p
10^{1}
10^{-1}
10^{-3}
10^{-5}
10^{-7}
10^{-9}
10
20
30
40
50
60
70
80
E_{thr} [TeV]

Summary 3

- Sphaleron